

# Dental and Medical Problems

QUARTERLY ISSN 1644-387X (PRINT) ISSN 2300-9020 (ONLINE)

[www.dmp.umed.wroc.pl](http://www.dmp.umed.wroc.pl)

2020, Vol. 57, No. 2 (April–June)

Ministry of Science and Higher Education – 20 pts.  
Index Copernicus (ICV) – 113.05 pts.



WROCLAW  
MEDICAL UNIVERSITY

# Dental and Medical Problems

ISSN 1644-387X (PRINT)

ISSN 2300-9020 (ONLINE)

www.dmp.umed.wroc.pl

**QUARTERLY**  
**2020, Vol. 57, No. 2**  
**(April–June)**

“Dental and Medical Problems” is a peer-reviewed open access journal published by Wrocław Medical University. Journal publishes articles from different fields of dentistry and other medical, biological, deontological and historical articles, which were deemed important to dentistry by the Editorial Board – original papers (clinical and experimental), reviews, clinical cases, and letters to the Editorial Board.

## Address of Editorial Office

Marcinkowskiego 2–6  
50-368 Wrocław, Poland  
Tel.: +48 71 784 11 33  
E-mail: dental@umed.wroc.pl

## Publisher

Wrocław Medical University  
Wybrzeże L. Pasteura 1  
50-367 Wrocław, Poland

© Copyright by Wrocław Medical University  
Wrocław 2020

Online edition is the original version of the journal.

## Editor-in-Chief

Tomasz Konopka

## Vice-Editor-in-Chief

Marcin Mikulewicz

## Thematic Editors

Anna Zalewska (Cariology)  
Mariusz Lipski (Endodontics)  
Urszula Kaczmarek (Pedodontics  
and Dental Prevention)  
Renata Górka (Oral Pathology)  
Korkud Demirel (Periodontology)  
Piotr Majewski (Implant Dentistry)

Andrzej Wojtowicz (Oral Surgery)  
Marcin Kozakiewicz (Maxillofacial Surgery)  
Teresa Sierpińska (Prosthodontics)  
Jolanta Kostrzewa-Janicka (Disorders  
of Masticatory System)  
Marcin Mikulewicz (Orthodontics)  
Ingrid Różyło-Kalinowska (Dental Radiology)

## International Advisory Board

Akira Aoki (Japan)  
Einar Berg (Norway)  
Ewa Czochrowska (Poland)  
Patrizia Defabianis (Italy)  
Korkud Demirel (Turkey)  
Marzena Dominiak (Poland)  
Barbara Dorocka-Bobkowska (Poland)  
Omar El-Mowafy (Canada)  
Katarzyna Emerich (Poland)  
Piotr Fudalej (Czech Republic, Switzerland)  
Thomas Gedrange (Germany)  
Hanna Gerber (Poland)  
Renata Górka (Poland)  
David Herrera (Spain)  
Michał Jeleń (Poland)  
Urszula Kaczmarek (Poland)  
Milan Kamínek (Czech Republic)  
Kazimierz Kobus (Poland)  
Krystyna Konopka (USA)  
Marcin Kos (Germany)  
Marcin Kozakiewicz (Poland)  
Tadeusz F. Krzemiński (Poland)  
Monika Łukomska-Szymańska (Poland)

Piotr Majewski (Poland)  
Agnieszka Mielczarek (Poland)  
Marcin Mikulewicz (Poland)  
Joseph Nissan (Israel)  
Raphaël Olszewski (Belgium)  
Hyo-Sang Park (South Korea)  
Alina Pūrienė (Lithuania)  
Małgorzata Radwan-Oczko (Poland)  
Monique-Marie Rousset-Caron (France)  
Ingrid Różyło-Kalinowska (Poland)  
Teresa Sierpińska (Poland)  
Franciszek Szatko (Poland)  
Jacek C. Szepietowski (Poland)  
Selena Toma (Belgium)  
János Vág (Hungary)  
Andreas Wielgosz (Canada)  
Mieszko Więckiewicz (Poland)  
Andrzej Wojtowicz (Poland)  
Dariusz Wołowicz (Poland)  
Grażyna Wyszyńska-Pawelec (Poland)  
Anna Zalewska (Poland)  
Marek Ziętek (Poland)

### **Statistical Editor**

Krzysztof Topolski

### **Technical Editorship**

Adam Barg

Joanna Gudarowska

Paulina Piątkowska

Marek Misiak

### **English Language Copy Editors**

Eric Hilton

Sherill Howard-Pociecha

Jason Schock

Marcin Tereszewski

### **Editorial Policy**

During the reviewing process, the Editorial Board conforms to the "Uniform Requirements for Manuscripts Submitted to Biomedical Journals: Writing and Editing for Biomedical Publication" approved by the International Committee of Medical Journal Editors (<http://www.icmje.org/>). Experimental studies must include a statement that the experimental protocol and informed consent procedure were in compliance with the Helsinki Convention and were approved by the ethics committee.

Indexed in: MEDLINE, Scopus, DOAJ, GFMER, Index Copernicus, Ministry of Science and Higher Education, CiteFactor, WorldCat, Directory of Research Journal Indexing.

This publication has been co-financed by the Ministry of Science and Higher Education.

Typographic design: Monika Kołęda, Piotr Gil

Cover: Monika Kołęda

DTP: Wrocław Medical University Press

Printing and binding: EXDRUK

## Contents

### Original papers

- 131 Dina Badawy Farag, Samah Sayed Mehanny  
**Histopathological alterations of the intrinsic tongue muscles following zoledronic acid treatment in a rat model**
- 137 Hirak Shubhra Bhattacharya, Shiva Shankar Gummaluri, Madhusudan Astekar, Ram Kumar Gummaluri  
**Novel method of determining the periodontal regenerative capacity of T-PRF and L-PRF: An immunohistochemical study**
- 145 Hamed Mortazavi, Azadeh Ghasemi, Mohammad Reza Vatankhah  
**Comparison of salivary total antioxidant levels in male smokers and non-smokers according to their personality types**
- 149 Numan Dedeoğlu, Suayip Burak Duman  
**Clinical significance of maxillary sinus hypoplasia in dentistry: A CBCT study**
- 157 Umair Shoukat Ali, Rashna Hoshang Sukhia, Mubassar Fida  
**Effect of class II extractions and functional appliance treatment on smile esthetics**
- 165 Wafaa Abdelbaky Khalil, Faisal Alghamdi, Esraa Aljahdali  
**Strengthening effect of bioceramic cement when used to repair simulated internal resorption cavities in endodontically treated teeth**
- 171 Ertuğrul Karataş, Ayhan Kul, Ebru Tepecik  
**Association of ankylosing spondylitis with radiographically and clinically diagnosed apical periodontitis: A cross-sectional study**
- 177 Maha Kareem Jabbar, Suha Fadhil Dulaimi  
**Effect of the combined zirconium dioxide surface treatment on the shear bond strength of a veneering ceramic to zirconium dioxide**
- 185 Qusay Khaznadar Nassif, Fendi Fendi Alshaarani  
**Influence of porcelain firing on changes in the marginal fit of metal-ceramic fixed partial dental prostheses fabricated with laser sintering: An in vivo study**
- 191 Tameem Khuder Jassim, Ali Ehsan Kareem, Mohamed Adnan Alloaibi  
**In vivo evaluation of the impact of various border molding materials and techniques on the retention of complete maxillary dentures**

### Reviews

- 197 Ahmed Aziz, Omar El-Mowafy, Saira Paredes  
**Clinical outcomes of lithium disilicate glass-ceramic crowns fabricated with CAD/CAM technology: A systematic review**

## Clinical cases

- 207 Damla Torul, Mehmet Melih Omezli  
**Mirror-image phenomenon in Turkish monozygotic twins: A report of 3 cases**
- 213 Krystyna Pietrzycka, Halina Pawlicka  
**Clinical aspects of pulp stones: A case report series**

## Spis treści

### Prace oryginalne

- 131 Dina Badawy Farag, Samah Sayed Mehanny  
**Zmiany histopatologiczne wewnętrznych mięśni języka szczura po zastosowaniu kwasu zoledronowego**
- 137 Hirak Shubhra Bhattacharya, Shiva Shankar Gummaluri, Madhusudan Astekar, Ram Kumar Gummaluri  
**Nowa metoda określania periodontologicznego potencjału regeneracyjnego T-PRF i L-PRF – badanie immunohistochemiczne**
- 145 Hamed Mortazavi, Azadeh Ghasemi, Mohammad Reza Vatankhah  
**Porównanie całkowitej zdolności antyoksydacyjnej śliny u palących i niepalących mężczyzn w odniesieniu do ich typów osobowości**
- 149 Numan Dedeoğlu, Suayip Burak Duman  
**Znaczenie kliniczne niedorozwoju zatoki szczękowej w stomatologii – badanie w tomografii stożkowej**
- 157 Umair Shoukat Ali, Rashna Hoshang Sukhia, Mubassar Fida  
**Wpływ ekstrakcji i leczenia czynnościowego wad zgryzu klasy II na estetykę uśmiechu**
- 165 Wafaa Abdelbaky Khalil, Faisal Alghamdi, Esraa Aljahdali  
**Wytrzymałość zębów leczonych endodontycznie po wypełnieniu symulowanych ubytków resorpcji wewnętrznej cementem bioceramicznym**
- 171 Ertuğrul Karataş, Ayhan Kul, Ebru Tepecik  
**Związek zeszytniającego zapalenia stawów kręgosłupa z zapaleniem tkanek okołowierzchołkowych rozpoznawanym radiologicznie i klinicznie – badanie przekrojowe**
- 177 Maha Kareem Jabbar, Suha Fadhil Dulaimi  
**Wpływ kondycjonowania powierzchni dwutlenku cyrkonu na zdolność wiązania ceramiki licowanej z dwutlenkiem cyrkonu**
- 185 Qusay Khaznadar Nassif, Fendi Fendi Alshaarani  
**Wpływ spiekania ceramiki na zmiany integracji brzeżnej mostów metalowo-ceramicznych wykonywanych laserową synteryzacją – badanie in vivo**
- 191 Tameem Khuder Jassim, Ali Ehsan Kareem, Mohamed Adnan Alloaibi  
**Ocena in vivo wpływu różnych materiałów i technik uszczelnienia brzeżnego na utrzymanie protez całkowitych w szczęce**

### Prace pogładowe

- 197 Ahmed Aziz, Omar El-Mowafy, Saira Paredes  
**Ocena kliniczna koron szklano-ceramicznych z dwukrzemianu litu wytwarzanych w technologii CAD/CAM – systematyczny przegląd piśmiennictwa**

## Prace kazuistyczne

- 207 Damla Torul, Mehmet Melih Omezli  
**Fenomen lustrzanych odbić u tureckich monozygotycznych bliźniąt – opis trzech przypadków**
- 213 Krystyna Pietrzycka, Halina Pawlicka  
**Aspekty kliniczne kamieni miazgi – seria przypadków**

# Histopathological alterations of the intrinsic tongue muscles following zoledronic acid treatment in a rat model

## Zmiany histopatologiczne wewnętrznych mięśni języka szczura po zastosowaniu kwasu zoledronowego

Dina Badawy Farag<sup>A-F</sup>, Samah Sayed Mehanny<sup>A-F</sup>

Department of Oral Biology, Faculty of Dentistry, Cairo University, Egypt

A – research concept and design; B – collection and/or assembly of data; C – data analysis and interpretation; D – writing the article; E – critical revision of the article; F – final approval of the article

Dental and Medical Problems, ISSN 1644-387X (print), ISSN 2300-9020 (online)

*Dent Med Probl.* 2020;57(2):131–136

### Address for correspondence

Dina Badawy Farag  
E-mail: dina.badawyf@gmail.com

### Funding sources

None declared

### Conflict of interest

None declared

Received on October 18, 2019  
Reviewed December 1, 2019  
Accepted on December 16, 2019

Published online on May 28, 2020

### Cite as

Farag DB, Mehanny SS. Histopathological alterations of the intrinsic tongue muscles following zoledronic acid treatment in a rat model. *Dent Med Probl.* 2020;57(2):131–136. doi:10.17219/dmp/115368

### DOI

10.17219/dmp/115368

### Copyright

© 2020 by Wrocław Medical University  
This is an article distributed under the terms of the Creative Commons Attribution 3.0 Unported License (CC BY 3.0) (<https://creativecommons.org/licenses/by/3.0/>).

## Abstract

**Background.** Bisphosphonates (BPs) are widely used as anti-bone-resorptive agents. Despite the great benefits of BPs, they may cause local and systemic adverse side effects.

**Objectives.** The aim of this study was to evaluate the histopathological effect zoledronic acid (ZA), which belongs to BPs, has on the intrinsic tongue muscles in a rat model.

**Material and methods.** A total of 30 adult male albino rats were divided into 3 groups (10 rats each): group I served as a control; group II was given an intraperitoneal (i.p.) injection of 0.2 mg/kg of ZA once per week for 3 weeks; and group III received the same dosage of ZA, but for 8 weeks. After the animals were euthanized, the tongue tissue was dissected and examined histologically, histochemically and immunohistochemically.

**Results.** Histologically, a normal architecture of the muscle fascicles was observed in the control group. Group II showed degenerated muscle fibers with an indistinct sarcolemma. In group III, the muscle fibers were degenerated with severe sarcoplasmic dissolution. The histochemical examination using Masson's trichrome (MT) demonstrated a significant increase in collagen fibers in groups II and III as compared to the control group. The immunohistochemical results revealed a statistically significantly higher expression of nuclear factor kappa B (NF-κB) in the ZA-treated groups (II and III) as compared to the control group, with the highest mean value recorded in group III.

**Conclusions.** Zoledronic acid induced histopathological changes to the intrinsic tongue muscles, and this effect was exaggerated with a longer duration of administration.

**Key words:** zoledronic acid, bisphosphonates, muscle fibers, collagen, rats

**Słowa kluczowe:** kwas zoledronowy, bisfosfoniany, włókna mięśniowe, kolagen, szczury



## Introduction

Bisphosphonates (BPs) are a class of drugs that are widely used in the treatment of osteoclast-mediated bone loss.<sup>1</sup> They are synthetic, stable analogs of inorganic pyrophosphates – naturally occurring polyphosphates found in urine and blood serum. The ability of BPs to bind divalent cations such as  $\text{Ca}^{2+}$  helps them bind to bone mineral surfaces, predominantly at sites of active bone remodeling.<sup>2,3</sup> Bisphosphonates are usually classified into 2 main groups with different mechanisms of action: non-nitrogen-containing bisphosphonates (non-N-BPs) and nitrogen-containing bisphosphonates (N-BPs).<sup>4</sup> Of all the anti-bone-resorptive BPs available nowadays, those containing nitrogen in the heterocyclic ring (zoledronic acid – ZA) are 10,000 times more potent than non-N-BPs.<sup>5</sup>

Zoledronic acid is well-established as a therapy for reducing skeletal-related events associated with bone metastases in several types of cancer, including prostate cancer.<sup>6</sup> Moreover, ZA has been shown to improve immune surveillance against tumors, opening up new possibilities for therapeutic applications.<sup>7</sup> However, several adverse effects have been demonstrated to be associated with ZA treatment. Bisphosphonate-associated osteonecrosis of the jaw<sup>8</sup> and altered oral mucosal epithelium leading to delayed soft tissue healing<sup>9</sup> are among the most significant side effects. An antiangiogenic effect of ZA has also been reported in many studies. It was observed that ZA could interfere with endothelial progenitor cell differentiation,<sup>10</sup> impair endothelial cell proliferation, induce endothelial cell apoptosis, and modulate their adhesion and migration.<sup>11</sup>

With this background in mind, the present study was performed to evaluate the possible effect of ZA treatment on the intrinsic tongue muscles in male albino rats using histological, histochemical and immunohistochemical analysis.

## Material and methods

### Ethical statement

This experimental study was carried out in the animal house of the Faculty of Medicine at Cairo University in Egypt, according to the recommendations and approval of the Institutional Animal Care and Use Committee of Cairo University (CU-IACUC) (approval No. CU/III/F/37/19).

### Experimental design

A total of 30 adult male albino Wistar rats weighing  $200 \pm 10$  g were included in the study. All animals were housed in a sterile environment, maintained at room temperature ( $21 \pm 2^\circ\text{C}$ ) and 50–55% humidity with a 12-hour

light cycle. The animals were fed with pelleted rat food and water ad libitum. The rats were randomly divided into 3 equal groups, with 10 rats in each group. The control group (group I) rats were given an intraperitoneal (i.p.) injection of saline solution. The group II rats received 0.2 mg/kg of ZA<sup>12</sup> (Zometa®; Novartis, Basel, Switzerland) i.p. once per week for 3 weeks. The rats in group III received 0.2 mg/kg of ZA<sup>12</sup> i.p. once per week for 8 weeks. All animals were euthanized by an i.p. injection of anesthetic overdose and the tongue was dissected.

### Light microscopic examination

All tongue specimens were fixed in 10% formaldehyde solution. After staying in a fixative material for 24 h, the samples were washed under running water, dehydrated in an ethanol series, then cleared in xylene, and embedded in liquid paraffin. The tissues were then cut into 4–6-micrometer-thick sections and subjected to examination.

### Histopathological examination

The sections were stained with hematoxylin and eosin (H&E).

### Histochemical examination

The sections were stained with Masson's trichrome (MT) for the detection of collagen fibers.

### Immunohistochemical examination

The sections were deparaffinized and hydrated, then washed in 0.1 M phosphate buffer saline (PBS). Endogenous peroxidases were blocked by treatment with  $\text{H}_2\text{O}_2$  in methanol. Non-specific background staining was inhibited through incubation at room temperature for 30 min in 0.3% bovine serum albumin. The sections were incubated with primary antibodies for nuclear factor kappa B (NF- $\kappa$ B) at room temperature for 60 min. Then, the sections were washed in buffer 3 times, each time for 5 min, and incubated for further 30 min with biotinylated secondary antibodies, followed by washing. Diaminobenzidine solution was used as a chromogen and Mayer's hematoxylin was used as a counterstain for 5 min. Phosphate buffer saline was used as a negative controller. The slides were then finally mounted. Positive immunoreactivity for NF- $\kappa$ B appeared in the form of brown coloration of the cytoplasm and/or nuclei of the immunoreactive cells.

### Image analysis

For the evaluation of staining affinity, the area percentage of collagen fibers in the sections stained with MT as well as NF- $\kappa$ B immunoreactivity were measured

by an image analyzer (Leica DM LB2 with QWin Plus image analysis software; Leica Camera, Wetzlar, Germany). The image analysis was done in different, non-overlapping fields of each specimen.

## Statistical analysis

The data obtained from the image analysis was statistically described in terms of mean  $\pm$  standard deviation ( $M \pm SD$ ). Student's *t*-test was used for multiple pairwise comparisons. A probability value (*p*-value) of  $<0.05$  was considered statistically significant. All statistical calculations were done using Microsoft Excel 2007 (Microsoft Corporation, Redmond, USA) and SPSS for Windows v. 15 (SPSS Inc., Chicago, USA).

## Results

### Histopathological results

Group I (the control group) showed a normal architecture of the muscle fascicles. The muscle fibers were arranged differently, with some being cut longitudinally while others were cut transversely. The fibers demonstrated homogenous acidophilic sarcoplasm with multiple peripheral elongated nuclei beneath a well-defined sarcolemma (Fig. 1A).

The muscle fascicles in group II were ill-defined as compared to the control group. Degenerated muscle fibers with an indistinct sarcolemma were also detected. Degeneration was in the form of serration, widely distributed sarcoplasmic dissolution and nuclear atypia (change in size and position). Chronic inflammatory cellular infiltrate was obvious (Fig. 1B).

Group III demonstrated the degeneration of most of the intrinsic muscle fibers of the tongue. Degenerated muscle fibers appeared swollen with severe sarcoplasmic dissolution. The remnants of eosinophilic muscle fibers were also observed within the coalesced fascicles. A thickened perimysium with marked inflammatory cell infiltration was noticed. Histiocytes appeared with different patterns: with homogenous basophilic cytoplasm, with a central basophilic body, or with a regular pattern of giant, deeply basophilic stained cells. The accumulation of fat droplets was also noted (Fig. 1C).

### Histochemical results

The histochemical examination using MT for the detection of collagen fiber bundles (the stains in blue) revealed that the tongue intrinsic muscles of the control group consisted of tightly packed, regularly arranged, parallel perimysial collagen bundles (Fig. 2A). The mean collagen area percentage was  $7.06 \pm 0.21$ .

Disorganized perimysial collagen fiber bundles were observed in group II. Some areas showed dense, wavy collagen bundles related to clumped muscle fascicles. However, other areas had a thin perimysium (Fig. 2B). The mean value of collagen area percentage was  $17.77 \pm 2.19$ ; statistical analysis revealed that it was significantly higher than that of group I ( $p = 0.015$ ).

Group III exhibited dense, curly, disorganized perimysial collagen bundles (Fig. 2C). The highest mean value of collagen area percentage was found in this group –  $23.55 \pm 1.11$ . Statistical analysis revealed that this mean value was statistically significantly higher as compared to group I ( $p = 0.004$ ), but it was not statistically significantly different from that of group II ( $p = 0.081$ ).

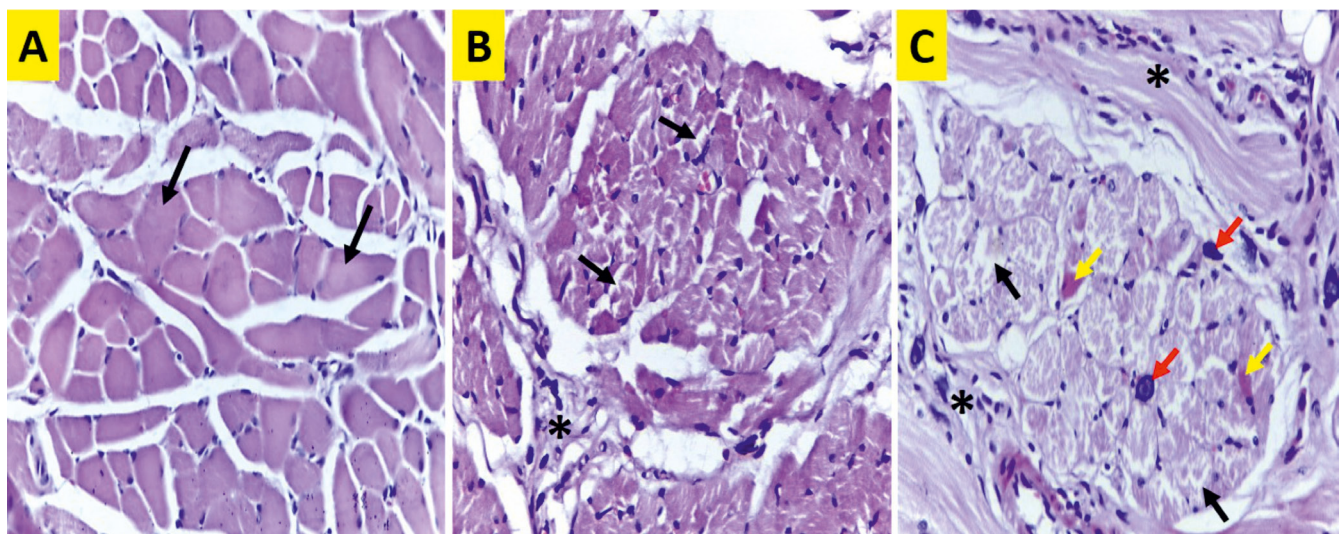


Fig. 1. Photomicrograph of the intrinsic tongue muscles (hematoxylin and eosin (H&E) staining)

A – control group with normally arranged muscle fibers (arrows) and a well-defined sarcolemma; B – group II with degenerated muscle fibers (arrows) and chronic inflammatory cell infiltration (asterisk); C – group III with severe muscle fiber degeneration (black arrows), eosinophilic coagulation (yellow arrows), a thickened perimysium with chronic inflammatory cells (asterisks), and histiocytes (red arrows); original magnification  $\times 400$ .

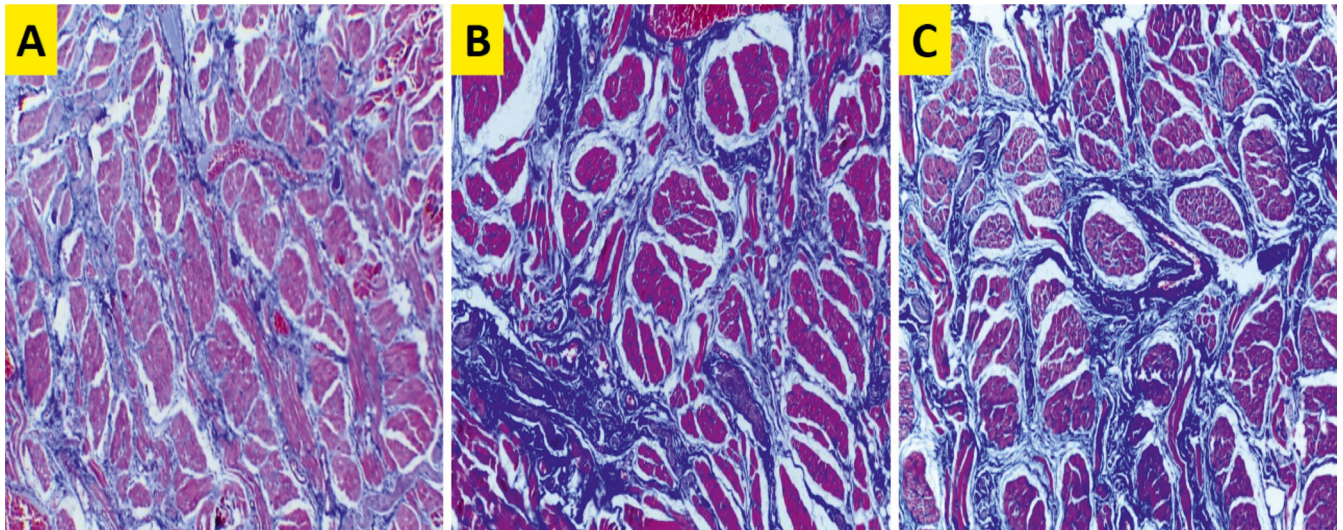


Fig. 2. Photomicrograph of the intrinsic tongue muscles (Masson's trichrome (MT) staining)

A – control group with regularly arranged collagen fibers in the perimysium; B – group II with disorganized, wavy perimysial collagen fibers; C – group III with disorganized, curly perimysial collagen fibers; original magnification  $\times 100$ .

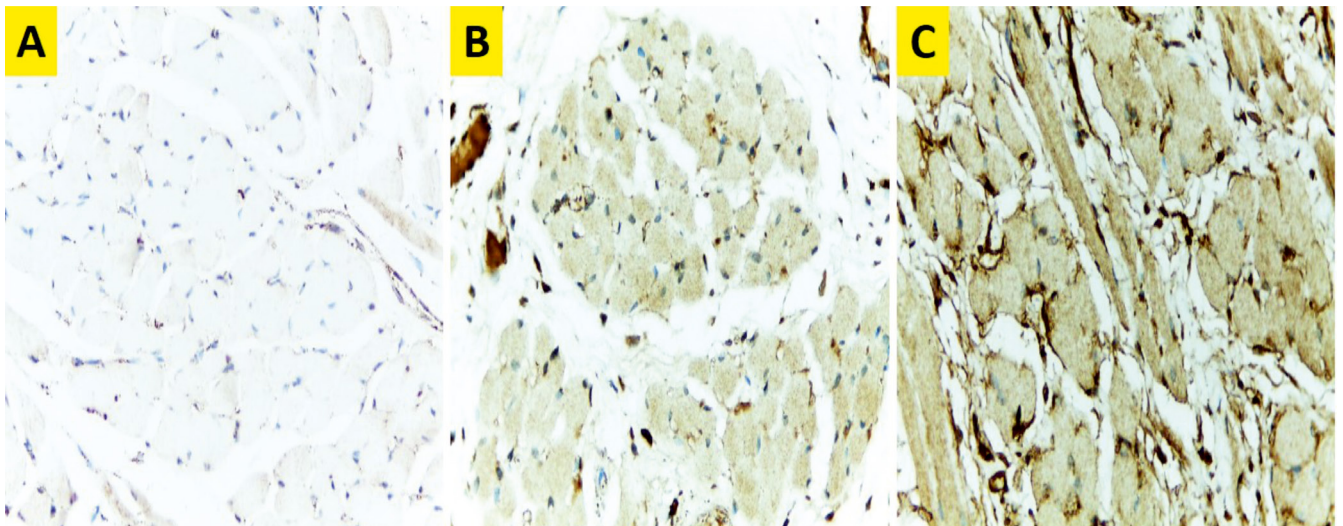


Fig. 3. Photomicrograph of the intrinsic tongue muscles showing (nuclear factor kappa B (NF- $\kappa$ B) staining)

A – negative immunoreactivity for activated NF- $\kappa$ B in the control group; B – moderate immunoreactivity for activated NF- $\kappa$ B in the cytoplasm and nucleus of the muscle fibers in group II; C – high immunoreactivity for activated NF- $\kappa$ B in the cytoplasm and nucleus of the muscle fibers in group III; original magnification  $\times 400$ .

### Immunohistochemical results

The NF- $\kappa$ B immunohistochemical staining of the intrinsic tongue muscle tissue from the control group showed no detectable cytoplasmic or nuclear immunoreactivity (Fig. 3A). The mean percentage of the area of NF- $\kappa$ B immunoreactivity in this group was  $0.06 \pm 0.03$ .

Moderate immunoreactivity for NF- $\kappa$ B was observed in the cytoplasm of the muscle fibers in group II. Some immunopositive muscle fibers showed positively stained nuclei (Fig. 3B). The mean percentage of the area of NF- $\kappa$ B immunoreactivity was  $22.74 \pm 4.18$ . Statistical analysis revealed that this mean value was significantly higher as compared to group I ( $p = 0.000$ ).

High cytoplasmic and nuclear immunoreactivity for activated NF- $\kappa$ B was noted in group III (Fig. 3C). The highest mean percentage of the area of NF- $\kappa$ B immunoreactivity was revealed in this group –  $36.32 \pm 2.56$ . Statistical analysis revealed that this value was statistically significantly different from that of both group I ( $p = 0.000$ ) and group II ( $p = 0.003$ ).

### Discussion

Zoledronic acid is a highly effective drug that inhibits osteoclast-mediated bone resorption.<sup>13</sup> Although ZA is well-tolerated, numerous short-term and long-term adverse reactions have been reported to be associated with

the administration of ZA.<sup>14</sup> Severe musculoskeletal pain is one of the side effects related to BP treatment. It has been reported to occur days or months (median time: 14 days) after starting a BP therapy and to resolve only if the therapy is stopped.<sup>15</sup> Based on this clinical observation, the skeletal muscle was the tissue of choice to be investigated in the current study.

The tongue is a unique skeletal muscle with differences in the muscle fiber composition when compared with limb, masticatory and orofacial muscles, most likely reflecting genotypic and phenotypic functional specialization in oral function. The prevalence of type II fibers, regional differences in the fiber composition and complex muscle structure generally suggest rapid and flexible actions in shaping and positioning the tongue while performing vital functions, such as speech, swallowing, mastication, and breathing.<sup>16</sup> These facts reinforce the decision to select the intrinsic tongue muscles to be the examined tissue in this study.

The histopathological examination in the present study revealed a normal architecture of the muscle fascicles in the control group. On the other hand, group II (3 weeks of ZA treatment) showed degenerated muscle fibers with an indistinct sarcolemma. Swollen muscle fibers with severe sarcoplasmic dissolution were observed after 8 weeks of ZA administration (group III). Inflammatory cellular infiltration was noticed in both ZA-treated groups. Interestingly, the muscle tissue in the group III rats was infiltrated by various patterns of histiocytes. Cells with central basophilic bodies was one of the patterns observed in the present study. Histologically, as explained by Gillett et al.,<sup>17</sup> this pattern is a result of defective phagolysosomal activity within macrophages; thus, it will contain partially digested bacteria. This leads to the deposition of calcium and iron, resulting in a basophilic inclusion structure (Michaelis–Gutmann bodies). Large macrophages which are present at sites of infection (von Hansemann cells) exhibit numerous secondary lysosomes containing partially digested organisms. The fusion and calcification of these lysosomes result in the formation of intracytoplasmic bodies called Michaelis–Gutmann bodies. It has been proposed that local bacterial antigen load, due to tissue necrosis, might lead to the accumulation of macrophages, which would facilitate the local production of Michaelis–Gutmann bodies.<sup>18</sup> Such an explanation could be supported by the current study, suggesting extensive muscle degeneration in group III. Another postulate could be that bacterial invasion may occur as a result of the negative effect of BPs on the adhesion and metabolism of oral mucosal cells.<sup>19</sup>

The degeneration and inflammatory cellular infiltration associated with ZA treatment observed in this study supports previous studies, which reported obvious histopathological changes following ZA administration. These changes included severe tubular degeneration, hyper eosinophilia, cell necrosis, and interstitial fibrosis in the

renal tissue.<sup>20,21</sup> Furthermore, necrotic zones and intense acute inflammatory infiltrate were observed in the alveolar bone tissue of rats receiving ZA.<sup>12</sup>

The NF- $\kappa$ B complex is activated in response to a variety of stimuli, including bacterial infection, exposure to pro-inflammatory cytokines and growth factors, and oxidative and biomechanical stress.<sup>22</sup> In this study, activated NF- $\kappa$ B was immunohistochemically located in the tongue muscle tissue as an indicator of an inflammatory response and oxidative stress. The results showed that NF- $\kappa$ B immun-expression was higher following ZA administration, with the greatest mean value recorded after 8 weeks (group III). This was in accordance with Muratsu et al., who revealed that ZA activated NF- $\kappa$ B expression in a cultured murine macrophage cell line.<sup>23</sup>

The correlation between the histopathological and immunohistochemical results observed in the present study could be explained by understanding the ZA molecular mechanism of action. Zoledronic acid has been reported to be the most potent N-BP in inhibiting the enzymes farnesyl diphosphate synthase (FPPS) and geranylgeranyl diphosphate synthase (GGPPS) in the mevalonate pathway.<sup>24</sup>

The inhibition of FPPS has been suggested to increase the intracellular levels of isopentyl pyrophosphate, which induces T-cell activation; this results in the release of inflammatory cytokines.<sup>15</sup> It has also been reported that the inactivation of GGPPS results in the stimulation of the proinflammatory mitogen-activated protein kinases and NF- $\kappa$ B signaling pathways.<sup>25</sup> Although NF- $\kappa$ B regulates the expression of proinflammatory cytokines, these cytokines are considered potent activators of NF- $\kappa$ B. This establishes a positive feedback loop, resulting in the overstimulation of NF- $\kappa$ B.<sup>22</sup> It has been suggested that the persistent stimulation of the skeletal muscle fibers through positive feedback loops may result in the overstimulation of NF- $\kappa$ B.<sup>26</sup> This hypothesis could explain the enhanced NF- $\kappa$ B immun-expression observed in the present study. Nuclear factor kappa B has been reported to be one of the most important signaling pathways related to the loss of the skeletal muscle mass. The activation of NF- $\kappa$ B in the skeletal muscle leads to the degradation of specific muscle proteins, induces inflammation and fibrosis, and blocks the regeneration of myofibers after injury/atrophy.<sup>27</sup>

The MT staining procedure was used in the present study to assess the extent of fibrosis<sup>28</sup> in the intrinsic tongue muscles. A progressive increase in the amount of collagen fibers was observed among the experimental groups. The lowest mean value was recorded in the control group, whereas the highest value was recorded in group III. An increase in fibrosis was concomitant with a degree of muscle injury.

According to Lańcut et al., an increase in the intrafascicular connective tissue usually represents a response to myofiber loss, wherein fibroblasts replace the damaged area, with the subsequent formation of collagen fibers.<sup>29</sup>

It has also been suggested that a persistent inflammatory response alters the extracellular environment and increases the secretion of various inflammatory cytokines, which contributes to muscle fibrosis.<sup>30</sup>

## Conclusions


It can be concluded that ZA induces histopathological changes in the intrinsic tongue muscles, and that this effect is exaggerated by a longer administration. These changes might predict a poorer functional outcome of these muscles.

## Recommendations

Since the intrinsic tongue muscles contribute substantially to chewing, swallowing, speaking, and respiration, it is recommended that clinicians be aware of the expected poor outcomes in these functions in patients under ZA treatment. Further studies need to be performed on other muscles of the aerodigestive tract involved in swallowing and mastication, as well as on females, using various investigatory tools.

### ORCID iDs

Dina Badawy Farag  <https://orcid.org/0000-0002-8856-8906>

Samah Sayed Mehanny  <https://orcid.org/0000-0002-8910-904X>

### References

- Shaw NJ, Bishop NJ. Bisphosphonate treatment of bone disease. *Arch Dis Child.* 2005;90(5):494–499.
- Rogers MJ. New insights into the molecular mechanisms of action of bisphosphonates. *Curr Pharm Des.* 2003;9(32):2643–2658.
- Masarachia P, Weinreb M, Balena R, Rodan GA. Comparison of the distribution of 3H-alendronate and 3H-etidronate in rat and mouse bones. *Bone.* 1996;19(3):281–290.
- Lehenkari PP, Kellinsalmi M, Näpänkangas JP, et al. Further insight into mechanism of action of clodronate: Inhibition of mitochondrial ADP/ATP translocase by a nonhydrolyzable, adenine-containing metabolite. *Mol Pharmacol.* 2002;61(5):1255–1262.
- Ballantyne E. Bisphosphonates: Possible modes of action and implications for dental implant treatment. A review of the literature. *J Gen Pract.* 2015;3:192.
- Valdespino V, Tsagozis P, Pisa P. Current perspectives in the treatment of advanced prostate cancer. *Med Oncol.* 2007;24(3):273–286.
- Coscia M, Quagliano E, Iezzi M, et al. Zoledronic acid repolarizes tumour-associated macrophages and inhibits mammary carcinogenesis by targeting the mevalonate pathway. *J Cell Mol Med.* 2010;14(12):2803–2815.
- Ruggiero SL. Bisphosphonate-related osteonecrosis of the jaw: An overview. *Ann NY Acad Sci.* 2011;1218:38–46.
- Allam E, Allen M, Chu TM, Ghoneima A, Jack Windsor L. In vivo effects of zoledronic acid on oral mucosal epithelial cells. *Oral Dis.* 2011;17(3):291–297.
- Yamada J, Tsuno NH, Kitayama J, et al. Anti-angiogenic property of zoledronic acid by inhibition of endothelial progenitor cell differentiation. *J Surg Res.* 2009;151(1):115–120.
- Wood J, Bonjean K, Ruetz S, et al. Novel antiangiogenic effects of the bisphosphonate compound zoledronic acid. *J Pharmacol Exp Ther.* 2002;302(3):1055–1061.
- Pacheco VN, Langie R, Benfica JRD, et al. Nitrogen-containing bisphosphonate therapy – Part II: Assessment of alveolar bone tissue inflammatory response in rats – a blind randomized controlled trial. *Int J Exp Pathol.* 2018;99(5):258–263.
- Berenson JR, Rosen LS, Howell A, et al. Zoledronic acid reduces skeletal-related events in patients with osteolytic metastases. *Cancer.* 2001;91(7):1191–1200.
- Kuchay MS, Farooqui KJ, Mithal A. Acute severe diarrhea and hyponatremia after zoledronic acid infusion: An acute phase reaction. *Clin Cases Miner Bone Metab.* 2017;14(1):101–104.
- Lim SY, Bolster MB. What can we do about musculoskeletal pain from bisphosphonates? *Cleve Clin J Med.* 2018;85(9):675–678.
- Stål P, Marklund S, Thornell LE, De Paul R, Eriksson PO. Fibre composition of human intrinsic tongue muscles. *Cells Tissues Organs.* 2003;173(3):147–161.
- Gillett MB, Pradeep KE, Mikhail M. Malacoplakia of the tongue. *J Clin Pathol.* 2006;59(1):112.
- Pesce C, Pate G, Valente S, Tanzi R. Focal malacoplakia in chronic periapical periodontitis. *Histopathology.* 1999;34(2):140–143.
- Basso FG, Pansani TN, Soares DG, Cardoso LM, Hebling J, de Souza Costa CA. Influence of bisphosphonates on the adherence and metabolism of epithelial cells and gingival fibroblasts to titanium surfaces. *Clin Oral Investig.* 2018;22(2):893–900.
- Markowitz GS, Fine PL, Stack JI, et al. Toxic acute tubular necrosis following treatment with zoledronate (Zometa). *Kidney Int.* 2003;64(1):281–289.
- Pfister T, Atzpödien E, Bauss F. The renal effects of minimally nephrotoxic doses of ibandronate and zoledronate following single and intermittent intravenous administration in rats. *Toxicology.* 2003;191(2–3):159–167.
- Kumar A, Takada Y, Boriek AM, Aggarwal BB. Nuclear factor-kappaB: Its role in health and disease. *J Mol Med (Berl).* 2004;82(7):434–448.
- Muratsu D, Yoshiga D, Taketomi T, et al. Zoledronic acid enhances lipopolysaccharide-stimulated proinflammatory reactions through controlled expression of SOCS1 in macrophages. *PLoS One.* 2013;8(7):e67906.
- Gong L, Altman RB, Klein TE. Bisphosphonates pathway. *Pharmacogenet Genomics.* 2011;21(1):50–53.
- Wang XX, Ying P, Diao F, et al. Altered protein prenylation in Sertoli cells is associated with adult infertility resulting from childhood mumps infection. *J Exp Med.* 2013;210(8):1559–1574.
- Kumar A, Boriek AM. Mechanical stress activates the nuclear factor-kappaB pathway in skeletal muscle fibers: A possible role in Duchenne muscular dystrophy. *FASEB J.* 2003;17(3):386–396.
- Thoma A, Lightfoot AP. NF-κB and inflammatory cytokine signaling: Role in skeletal muscle atrophy. *Adv Exp Med Biol.* 2018;1088:267–279.
- Meinen S, Barzaghi P, Lin S, Lochmüller H, Rugg MA. Linker molecules between laminins and dystroglycan ameliorate laminin-alpha2-deficient muscular dystrophy at all disease stages. *J Cell Biol.* 2007;176(7):979–993.
- Lańcut M, Jedrych B, Lis-Sochocka M, Czerny K. Histological and ultrastructural changes in cross-striation muscle cells, under the influence of atorvastatin-reductase HMG-CoA inhibitor. *Ann Univ Mariae Curie Skłodowska Med.* 2004;59(2):32–37.
- Gosselin LE, McCormick KM. Targeting the immune system to improve ventilatory function in muscular dystrophy. *Med Sci Sports Exerc.* 2004;36(1):44–51.

# Novel method of determining the periodontal regenerative capacity of T-PRF and L-PRF: An immunohistochemical study

## Nowa metoda określania periodontologicznego potencjału regeneracyjnego T-PRF i L-PRF – badanie immunohistochemiczne

Hirak Shubhra Bhattacharya<sup>1,D–F</sup>, Shiva Shankar Gummaluri<sup>1,A–F</sup>, Madhusudan Astekar<sup>2,C–F</sup>, Ram Kumar Gummaluri<sup>3,A–C</sup>

<sup>1</sup> Department of Periodontology and Implantology, Institute of Dental Sciences, Bareilly, India

<sup>2</sup> Department of Oral and Maxillofacial Pathology and Microbiology, Institute of Dental Sciences, Bareilly, India

<sup>3</sup> Department of Chemistry, MVGR College of Engineering, Chintalavalasa, India

A – research concept and design; B – collection and/or assembly of data; C – data analysis and interpretation; D – writing the article; E – critical revision of the article; F – final approval of the article

Dental and Medical Problems, ISSN 1644-387X (print), ISSN 2300-9020 (online)

*Dent Med Probl.* 2020;57(2):137–144

### Address for correspondence

Madhusudan Astekar  
E-mail: madhu.tanu@gmail.com

### Funding sources

None declared

### Conflict of interest

None declared

Received on November 1, 2019

Reviewed on January 25, 2020

Accepted on January 31, 2020

Published online on June 9, 2020

### Cite as

Bhattacharya HS, Gummaluri SS, Astekar M, Gummaluri RK. Novel method of determining the periodontal regenerative capacity of T-PRF and L-PRF: An immunohistochemical study. *Dent Med Probl.* 2020;57(2):137–144. doi:10.17219/dmp/117721

### DOI

10.17219/dmp/117721

### Copyright

© 2020 by Wrocław Medical University

This is an article distributed under the terms of the

Creative Commons Attribution 3.0 Unported License (CC BY 3.0)

(<https://creativecommons.org/licenses/by/3.0/>).

## Abstract

**Background.** Platelet-rich fibrin (PRF) plays an important role in the regeneration of the lost periodontal tissues. Immunohistochemistry (IHC) is the most sensitive staining technique for the identification and localization of specific cells. There are few studies in the available literature which use IHC to compare PRF prepared from titanium and silica glass tubes.

**Objectives.** The aim of the study was to use IHC to evaluate and compare cells present in the PRF membrane prepared from titanium and silica glass tubes.

**Material and methods.** Blood was drawn from 10 healthy volunteers and PRF was prepared from titanium and silica glass tubes. Immunohistochemical staining for the localization, distribution and pattern of cells present in PRF with the CD 3, CD 15, CD 20, CD 34, CD 61, and CD 163 antibodies was carried out. A statistical analysis including the  $\chi^2$  test, independent *t*-test and unpaired *t*-test was performed to determine significant differences.

**Results.** There were significantly more T cells, B-lymphocytes and platelets, with a strongly positive staining in terms of the cell distribution and the labeling index in the T-PRF group in comparison with the L-PRF group. However, in terms of localization, a stronger positive staining was obtained with platelets in the T-PRF group and stem cells in the L-PRF group. In terms of the cell pattern, a significantly stronger positive staining was obtained by neutrophils in the L-PRF group and B-lymphocytes in the T-PRF group.

**Conclusions.** Titanium PRF has the edge over PRF prepared from silica glass tubes, and emerged as a better alternative for use in the field of periodontal regeneration.

**Key words:** immunohistochemistry, platelet-rich fibrin, periodontal regeneration, histological techniques

**Słowa kluczowe:** immunohistochemia, fibryna bogatopłytkowa, regeneracja periodontologiczna, techniki histologiczne

## Introduction

The regeneration of the periodontium means restoring the lost form and function of tissues so that they resemble the previously existing ones.<sup>1</sup> Various researchers have conducted studies on achieving regeneration with the help of different biomaterials.<sup>2</sup> The use of autologous blood products started with fibrin glue as an alternative for sutures, followed by platelet-rich plasma (PRP), in which platelets, growth factors, fibrin, and leucocytes are gathered in a gel that resembles an engineered tissue, and added a new dimension to regenerative medicine.<sup>3</sup> Due to concerns about antigenicity, a lengthy protocol and the inability of these products to deliver steady amounts of growth factors, leucocyte- and platelet-rich fibrin (L-PRF) was introduced by Choukroun et al.<sup>4</sup> This preparation did not require anticoagulants and was easily prepared by taking 10 mL of blood and centrifuging it at 2,800 rpm for 12 min.<sup>5</sup> Studies such as those by Agarwal et al.<sup>6</sup> and Pradeep et al.<sup>7</sup> used L-PRF as an adjunct to other biomaterials, such as a demineralized freeze-dried bone allograft (DFDBA) and 1% metformin, in the treatment of intrabony defects; they reported improvements in clinical parameters, such as a decreased pocket depth, clinical attachment level gain and increased bone fill, thus contributing to periodontal regeneration. These results were supported by a systematic review conducted by Verma et al. in 2017, in which L-PRF used as an adjunct to biomaterials yielded promising results.<sup>8</sup>

Later, to increase the number and variety of cells that get entrapped within the fibrin meshwork, researchers developed a low-speed centrifugation concept (1,500 rpm for 14 min), which led to the development of advanced platelet-rich fibrin (A-PRF).<sup>9</sup> These PRF membranes release growth factors at a constant rate, act as a good scaffold for cellular attachment and resorb within 7–11 days.<sup>10</sup> Still, this duration is not long enough to stimulate osteoblast cells for alveolar bone formation. Due to the prevailing controversies regarding the contamination and adverse effects of silica in either the short or long term, as O'Connell speculated,<sup>11</sup> there was again a search for a better biomaterial. During this process, titanium has attracted researchers' attention due to its hemocompatibility, the platelet-activating nature similar to that of silica and its extensive use in the medical field. The drawbacks of L-PRF and the advantages of titanium have led to the introduction of titanium tube-prepared platelet-rich fibrin (T-PRF) by Tunali et al.<sup>12</sup> The preparation is similar to that of L-PRF, but medical-grade titanium tubes are used instead of glass tubes. The membranes are formed by centrifuging 10 mL of blood for a period of 15 min at 3,500 rpm.<sup>12</sup> In T-PRF, titanium dioxide (TiO<sub>2</sub>) that is present on the inner surface of the tubes helps to activate platelets, which results in the formation of T-PRF. The studies conducted on rabbits revealed that T-PRF stayed at the surgical site for a period of 21 days, which was the key to periodontal tissue regeneration.<sup>13</sup>

Due to some constraints, such as a lack of surgical re-entry, studying cellular distribution in the sections of the PRF membranes could play an important role in determining the activity of cells, leading to periodontal regeneration.<sup>14</sup> As PRF is prepared from human blood, it contains various types of cells: T- and B-lymphocytes, monocytes, neutrophils, platelets, and stem/progenitor cells.<sup>15</sup> An *in vitro* study by He et al. showed that rat osteoblasts could differentiate and proliferate when placed in PRF; these changes were investigated at different time points with regard to the release of transforming growth factor  $\beta$  (TGF- $\beta$ ) and platelet-derived growth factor AB (PDGF-AB) as well as the activity of alkaline phosphatase (ALP).<sup>16</sup> Other studies revealed the proliferation of gingival fibroblasts, pre-adipocytes, dental pulp stem cells, and osteoblasts in PRF.<sup>17</sup> In their clinical applicability study, Mazor et al. detected bone-forming potential at the implantation sites 6 months after using PRF as a grafting material.<sup>18</sup>

Immunohistochemistry (IHC) plays an important role in identifying cells with their distribution in tissue, and is widely used in various fields of medicine and dentistry for establishing the final diagnosis.<sup>19</sup> It utilizes antibody markers in the form of proteins for identifying various specific cells. The presence of various types of cells in the PRF membrane helps to stimulate macrophages present at the tissue site, which in turn encourages periodontal healing and regeneration.<sup>9</sup> To our knowledge, no study has been conducted to compare T-PRF and L-PRF using IHC staining. Hence, the present study was aimed to evaluate and compare the distribution, staining pattern and labeling index percentage of cells present in T-PRF and L-PRF with IHC markers.

## Material and methods

The study involved 10 systemically healthy volunteers (5 males and 5 females), ranging in age from 18 to 26 years, who had all given informed consent. None of them were smokers or taking any medications that would affect the functioning of platelets, other blood cells or their relative counts. Pregnant and lactating females, subjects who had any systemic diseases or who had undergone any sort of periodontal treatment within the previous 6 months were excluded. The study was performed after obtaining approval from the ethics committee of the Institute of Dental Sciences in Bareilly, India. The sample collection was carried out in the same Institute's Department of Periodontology and Implantology, whereas the histopathological and IHC analyses of the slides were done in the Department of Oral and Maxillofacial Pathology and Microbiology therein.

## Procedure

We drew 20 mL of whole blood from the antecubital vein; from this, 10 mL was transferred into sterile medical glass test tubes (Borosil Glass Works Ltd., New Delhi, India)

and 10 mL into medical-grade titanium tubes (Supra Alloys, Camarillo, USA). These tubes were immediately subjected to centrifugation in an R-8C centrifuge (Remi, New Delhi, India) using Choukroun's protocol<sup>4</sup> and Tunali's protocol<sup>12</sup> to obtain L-PRF from sterile medical glass test tubes and T-PRF from titanium tubes, respectively (Table 1). No adverse centrifugation rates were applied to any of the tubes. Later, the clots were placed in 10% formalin solution for fixation for up to 24 h to preserve the structure and prevent autolysis. Then, the samples were routinely processed as per the protocol of Bankroft et al.,<sup>20</sup> and were subjected to IHC staining with various monoclonal mouse/rabbit anti-human antibodies (Table 2) according to the protocol described by Ghanaati et al.<sup>9</sup>

### Immunohistochemical staining procedure

Initially, blocks of a 4-micrometer uniform thickness were sectioned using a microtome. The sections were then deparaffinized by heating at 55–65°C, followed by immersion in xylene for residual deparaffinization in order to prepare the sections for staining. Subsequently, each section was immersed in proteinase K solution for 15 min for antigen retrieval and washed in phosphate buffer saline (PBS) for 3 min. Then, 3% hydrogen peroxide was used in 2 incubations to block peroxidase, followed by washing in distilled water. A 2-hour protein block (0.05% bovine serum albumin (BSA) in PBS) application was carried out. The slides were then washed in distilled water, followed by PBS rinses for the application of the primary antibodies – CD-3, CD-15, CD-20, CD-34, and CD-61 from Dako Denmark A/S

(Glostrup, Denmark) and CD-163 from PathnSitu Biotechnologies Pvt Ltd. (Hyderabad, India). After 2 h, excessive antibodies were removed by repeated washing in PBS and diaminobenzidine (DAB) was applied for 15 min. Then, a horseradish peroxidase (HRP) conjugate was applied for 15 min, followed by washing in PBS and incubation for 10 min. Later, the slides were washed in distilled water and counter-staining was done with Mayer's hematoxylin for 10 min. This was followed by washing under running water, and dehydration using 95% alcohol for 10 s, absolute alcohol 3 times for 10 s, and finally 3 xylol dips (10 s each). Then, the slides were mounted with coverslips using a mounting medium and dried for a microscopic examination (Fig. 1,2).

Table 1. Protocols used for preparing leucocyte- and platelet-rich fibrin (L-PRF) and titanium platelet-rich fibrin (T-PRF)

Biomaterial	Speed [rpm]	Time [min]
L-PRF (Choukroun's protocol) <sup>4</sup>	2,800	12
T-PRF (Tunali's M protocol) <sup>12</sup>	3,500	15

Table 2. List of anti-human antibodies used in the study

Antibody	Identification
CD-3	T-lymphocytes
CD-15	neutrophils
CD-20	B-lymphocytes
CD-34	stem/progenitor cells
CD-61	platelets (platelet glycoprotein IIa)
CD-163	monocytes

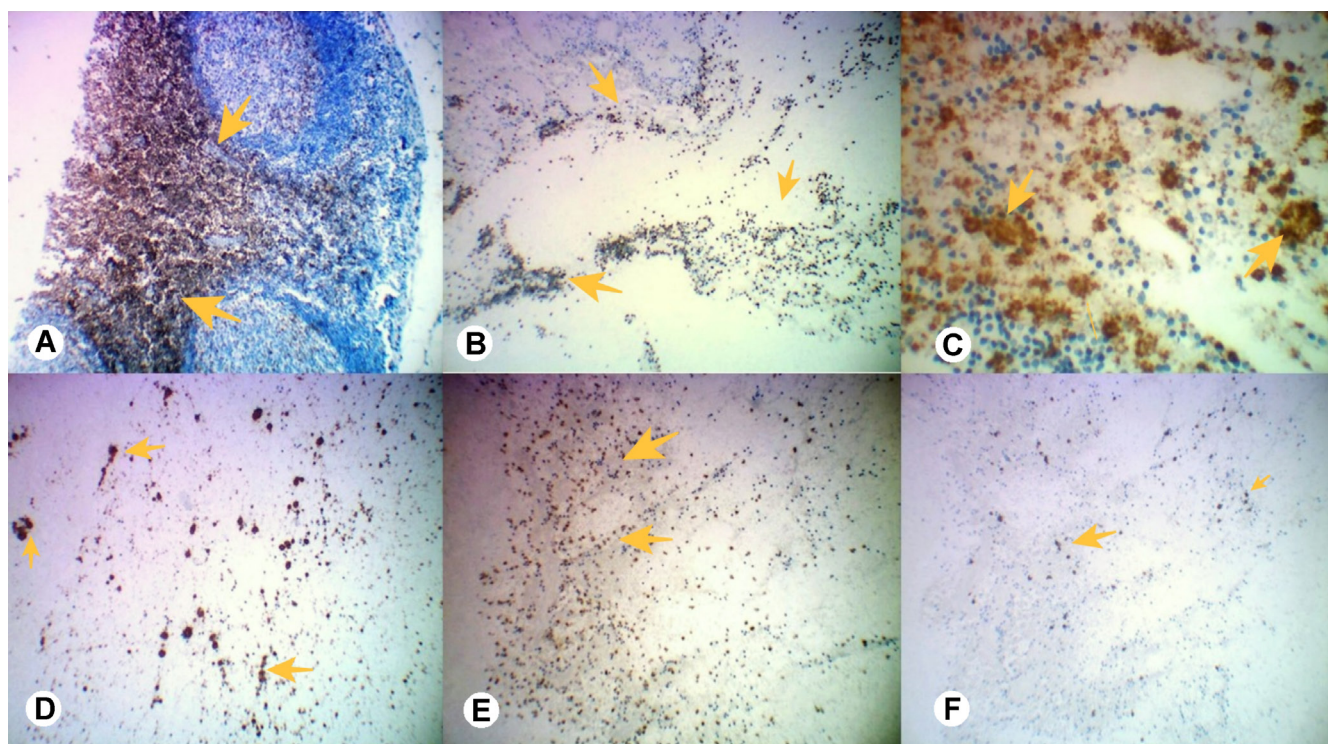


Fig. 1. Immunohistochemical images of the CD-3 (A,B), CD-15 (C,D) and CD-61 (E,F) antibody markers for both the T-PRF and L-PRF groups. Yellow arrows indicate the stained cells.



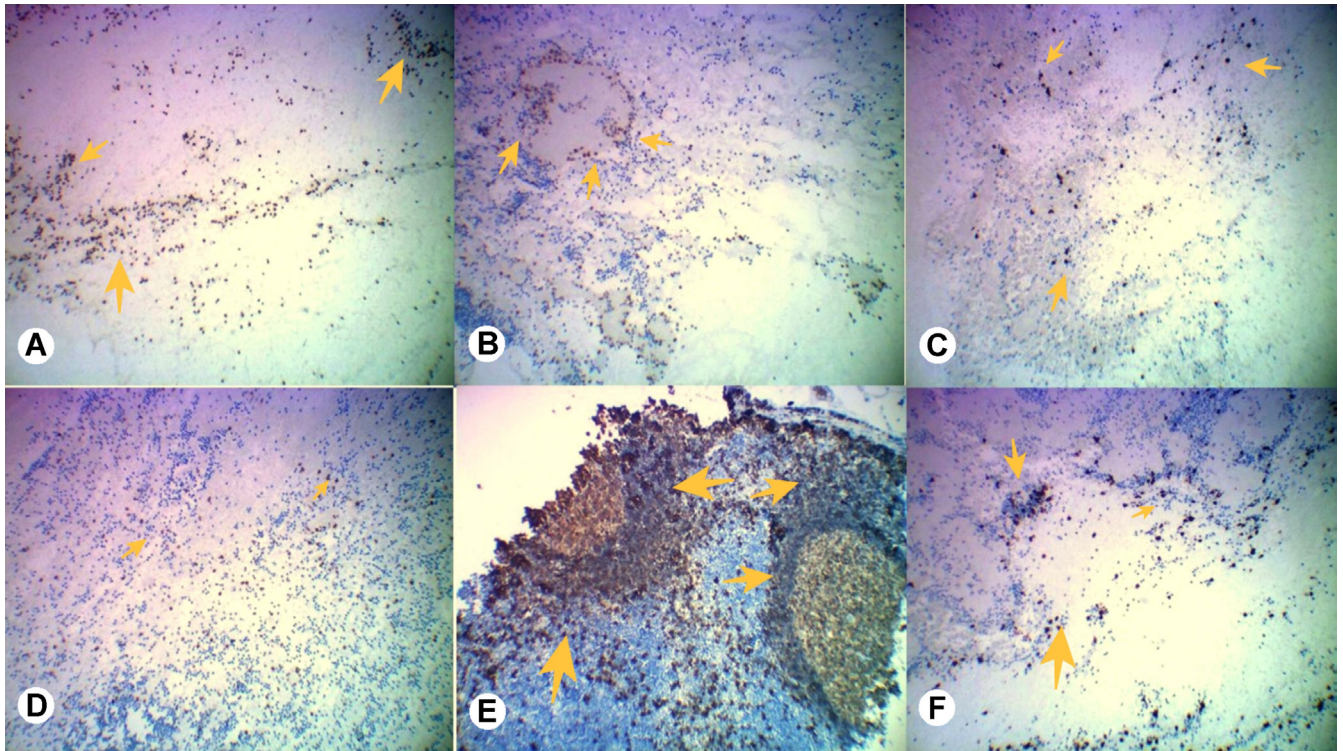


Fig. 2. Immunohistochemical images of the CD-163 (A,B), CD-34 (C,D) and CD-20 (E,F) antibody markers for both the T-PRF and L-PRF groups. Yellow arrows indicate the stained cells.

## Histological examination

In order to minimize inter-examiner variability, all slides were examined by 2 experienced pathologists until consensus was reached. The fields of interest were analyzed in terms of:

- the localization of staining – whether it was cytoplasmic and/or nucleus;
- cellular distribution, as mildly positive (0–25%), moderately positive (26–75%) or strongly positive (76–100%);

Table 3. Frequency distribution of the immunohistochemical (IHC) markers in terms of the localization of cell staining

IHC marker	Study group	Cytoplasm <i>n</i> (%)	Nucleus <i>n</i> (%)	<i>p</i> -value
CD-3 (T-lymphocytes)	L-PRF	8 (80)	2 (20)	0.075
	T-PRF	9 (90)	1 (10)	
CD-15 (neutrophils)	L-PRF	9 (90)	1 (10)	0.075
	T-PRF	8 (80)	2 (20)	
CD-20 (B-lymphocytes)	L-PRF	8 (80)	2 (20)	0.075
	T-PRF	9 (90)	1 (10)	
CD-34 (stem cells)	L-PRF	10 (100)	0 (0)	<0.001*
	T-PRF	6 (60)	4 (40)	
CD-61 (platelets)	L-PRF	6 (60)	4 (40)	0.003*
	T-PRF	8 (80)	2 (20)	
CD-163 (monocytes)	L-PRF	9 (90)	1 (10)	0.075
	T-PRF	8 (80)	2 (20)	

\* statistically significant.

- the cellular pattern – independent or clustered;
- the labeling index percentage,<sup>21</sup> calculated as the total number of stained cells / 500 × 100.

## Statistical analysis

All the data from the slides was tabulated using the Microsoft Excel<sup>®</sup> software (Microsoft Corporation, Redmond, USA), whereas the analysis was performed using the IBM SPSS Statistics for Windows v. 22 software (IBM Corp., Armonk, USA). The  $\chi^2$  test was performed to find any correlation between L-PRF and T-PRF in terms of localization, cellular distribution, the positivity of staining, and the cellular pattern. The independent *t*-test was performed for the evaluation of the positively stained cells and the labeling index percentage.

## Results

Regarding the localization of staining in both the L-PRF and T-PRF groups, all IHC markers showed predominant cytoplasmic staining when compared to the nucleus. The results were statistically significant for the CD-61 marker ( $p = 0.003$ ) for platelets in the T-PRF group and for the CD-34 marker ( $p < 0.001$ ) for stem cells in the L-PRF group. The rest of the markers showed nonsignificant results (Table 3).

In terms of cellular distribution, T-PRF showed a stronger positivity than L-PRF for the CD-3, CD-20 and CD-61 markers; the difference was statistically significant ( $p < 0.001$ ). The staining of the CD-15 and CD-163 markers was moderately positive, and CD-34 showed mildly positive cells in both the L-PRF and T-PRF groups, but the results were not statistically significant (Table 4).

Regarding the cellular patterns, all antibody markers in both the T-PRF and L-PRF groups showed predominantly clustered rather than independent patterns, but the values were statistically significant ( $p < 0.001$ )

**Table 4.** Cellular distribution shown with the IHC markers

IHC marker	Study group	Cell distribution <i>n</i> (%)			<i>p</i> -value
		mildly positive (0–25%)	moderately positive (26–75%)	strongly positive (76–100%)	
CD-3 (T-lymphocytes)	L-PRF	5 (50)	5 (50)	0 (0)	<0.001*
	T-PRF	0 (0)	0 (0)	10 (100)	
CD-15 (neutrophils)	L-PRF	0 (0)	10 (100)	0 (0)	0.0849
	T-PRF	0 (0)	10 (100)	0 (0)	
CD-20 (B-lymphocytes)	L-PRF	0 (0)	10 (100)	0 (0)	<0.001*
	T-PRF	0 (0)	0 (0)	10 (100)	
CD-34 (stem cells)	L-PRF	10 (100)	0 (0)	0 (0)	1.000
	T-PRF	10 (100)	0 (0)	0 (0)	
CD-61 (platelets)	L-PRF	0 (0)	10 (100)	0 (0)	<0.001*
	T-PRF	0 (0)	0 (0)	10 (100)	
CD-163 (monocytes)	L-PRF	0 (0)	10 (100)	0 (0)	0.611
	T-PRF	0 (0)	10 (100)	0 (0)	

\* statistically significant.

**Table 5.** Cell patterns shown with the IHC markers

IHC marker	Study group	Cell pattern <i>n</i> (%)		<i>p</i> -value
		independent	clustered	
CD-3 (T-lymphocytes)	L-PRF	2 (20)	8 (80)	0.862
	T-PRF	2 (20)	8 (80)	
CD-15 (neutrophils)	L-PRF	8 (80)	2 (20)	<0.001*
	T-PRF	3 (30)	7 (70)	
CD-20 (B-lymphocytes)	L-PRF	3 (30)	7 (70)	<0.001*
	T-PRF	1 (10)	9 (90)	
CD-34 (stem cells)	L-PRF	4 (40)	6 (60)	0.182
	T-PRF	3 (30)	7 (70)	
CD-61 (platelets)	L-PRF	4 (40)	6 (60)	0.182
	T-PRF	3 (30)	7 (70)	
CD-163 (monocytes)	L-PRF	3 (30)	7 (70)	0.142
	T-PRF	2 (20)	8 (80)	

\* statistically significant.

only for CD-15 (an independent pattern) in the L-PRF group and for CD-20 (a clustered pattern) in the T-PRF group (Table 5). The mean (*M*) and standard deviation (*SD*) values of the positively stained cells in the T-PRF and L-PRF groups were statistically significant ( $p = 0.000$ ) for the CD-3, CD-20 and CD-61 antibodies (Table 6). The mean labeling index percentage values for all markers were higher for the T-PRF group than for the L-PRF group, but the only statistically significant differences ( $p < 0.001$ ) were obtained for the CD-3, CD-20 and CD-61 markers (Table 7).

**Table 6.** Mean (*M*) and standard deviation (*SD*) values of the positively stained cells

IHC marker	Study group	Slides <i>N</i>	<i>M</i> ± <i>SD</i>	<i>p</i> -value
CD-3 (T-lymphocytes)	L-PRF	10	211.70 ± 69.32	0.075
	T-PRF	10	392.40 ± 8.69	
CD-15 (neutrophils)	L-PRF	10	234.50 ± 41.33	0.075
	T-PRF	10	272.00 ± 50.23	
CD-20 (B-lymphocytes)	L-PRF	10	231.00 ± 65.61	0.075
	T-PRF	10	392.30 ± 8.78	
CD-34 (stem cells)	L-PRF	10	99.90 ± 12.91	<0.001*
	T-PRF	10	96.30 ± 15.96	
CD-61 (platelets)	L-PRF	10	309.60 ± 31.17	0.003*
	T-PRF	10	390.40 ± 19.11	
CD-163 (monocytes)	L-PRF	10	251.50 ± 83.37	0.075
	T-PRF	10	292.50 ± 62.10	

\* statistically significant.

**Table 7.** Mean (*M*) and standard deviation (*SD*) values of the labeling index percentage of the positively stained cells

IHC marker	Study group	<i>N</i>	Labeling index percentage [%] <i>M</i> ± <i>SD</i>	<i>p</i> -value
CD-3 (T-lymphocytes)	L-PRF	10	44.38 ± 13.02	<0.001*
	T-PRF	10	78.48 ± 1.74	
CD-15 (neutrophils)	L-PRF	10	46.89 ± 8.77	0.102
	T-PRF	10	54.40 ± 10.05	
CD-20 (B-lymphocytes)	L-PRF	10	45.44 ± 13.68	<0.001*
	T-PRF	10	78.46 ± 1.76	
CD-34 (stem cells)	L-PRF	10	19.76 ± 2.63	0.718
	T-PRF	10	19.26 ± 3.19	
CD-61 (platelets)	L-PRF	10	60.80 ± 5.44	<0.001*
	T-PRF	10	78.08 ± 3.82	
CD-163 (monocytes)	L-PRF	10	47.89 ± 15.73	0.119
	T-PRF	10	58.50 ± 12.42	

\* statistically significant.

## Discussion

Tissue engineering plays an important role in predictable periodontal regeneration procedures.<sup>3</sup> The PRF membranes act as scaffolds for enmeshing various cells, including white blood cells, platelets, progenitor cells, and red blood cells, which release many growth factors and cytokines that create a transient inflammatory condition, inducing the formation of new periodontal tissues.<sup>22,23</sup> The PRF clots are autologous substances and do not require any additional anticoagulants for their preparation; they are easy to use and can be prepared at chairside in minimal time, so they can yield good results when used in combination with various biomaterials.<sup>3</sup> In the present study, as standard protocols were followed during the preparation of the L-PRF and T-PRF clots, the centrifugation rates were normal and the obtained clots had a mature fibrin meshwork.

In the present study, the maximum cell staining occurred in the cytoplasm rather than in the nucleus in both study groups. This was in accordance with the study conducted by Ghanaati et al.<sup>9</sup> It means a higher number of active cells, which could possibly lead to an increased release of growth factors and cytokines, resulting in the stimulation of cells to produce new periodontal tissues. In the present study, cellular distribution showed a significant 76–100% staining of T-lymphocytes, B-lymphocytes and platelets in the T-PRF group, whereas in both groups, a nonsignificant distribution of 26–75% staining was observed for neutrophils and monocytes, and 0–25% for stem cells. However, a study by Ghanaati et al. showed mixed cellular distribution, in which the maximum T-lymphocyte distribution was in the buffy coat, neutrophils covered 2/3 of the entire surface of the clot, platelets were distributed throughout the clot, and the rest of the cells covered <30% of the entire surface of the clot in both the A-PRF and L-PRF groups.<sup>9</sup> These variations in the localization of cell staining and in cellular distribution might be due to differences in the sedimentation rates, in the density, size and shape of the cells, and in centrifugation conditions.

In the present study, all cellular markers in both groups showed a predominantly clustered pattern, but the only statistically significant differences were noted among neutrophils and B-lymphocytes. This was in accordance with Tunalı et al., who stated that even though L-PRF and T-PRF shared a similar structure, a thicker fibrin mesh was found in T-PRF, which entrapped a greater number of cells in the fibrin clot.<sup>12</sup> This might be due to an increased centrifugation time and a better hemocompatibility of titanium, which led to the formation of a thicker fibrin mesh than in the L-PRF group and triggered more cells to accumulate in the fibrin mesh.

In the present study, platelets were significantly higher in the T-PRF group than in the L-PRF group in most respects, such as the localization of staining, cellular distri-

bution, the mean cell count, and the labeling index percentage, whereas the values regarding the cell pattern were nonsignificant in both groups; still, the platelets were distributed on the entire surface of the clot. This is in accordance with Ghanaati et al., where platelets were also distributed on the entire surface of the clot.<sup>9</sup> This might be due to a low centrifugation speed over an extended time. Still, in the present study, apart from an extended centrifugation time, an increased entrapment of platelets in the fibrin mesh might be due to a better activation of platelets by TiO<sub>2</sub> passivated within titanium tubes, as stated by Tunalı et al.<sup>12</sup> Platelets play an important role in the stimulation of the adjacent cells, such as neutrophils/monocytes and other cells, by altering the immune response, and releasing various cytokines, growth factors<sup>5</sup> and adhesion molecules (vitronectin, fibronectin, P-selectin and von Willebrand's factor<sup>24</sup>). These stimulate adjacent progenitor cells, thus releasing bone morphogenetic proteins and helping in new bone formation and healing.<sup>25</sup>

In their recent study, Choukroun and Ghanaati postulated that low-speed centrifugation increases the number of neutrophils, platelets and growth factors in injectable PRF.<sup>26</sup> While counting neutrophils and platelets, they observed higher counts of cells with a lower relative centrifugal force.<sup>26</sup> In contrast, the present study used a standard number of rotations per minute and an extended centrifugation time, but the results were better than those reported by Choukroun and Ghanaati, and showed nonsignificantly higher neutrophil counts for the mean cell count and the labeling index percentage in the T-PRF group than in the L-PRF group, whereas both groups showed similar cell distribution. The presence of neutrophils in PRF helps to prevent the clot contamination from bacteria and stimulates the adjacent cells at the surgical site by releasing cytokines, which are important in the regeneration of periodontal tissues.

Monocytes are cells that act as the second line of defense after neutrophils; they are chemotactically drawn to the site of inflammation and transform themselves into tissue histiocytes to regulate their phagocytic activity.<sup>27</sup> They secrete several growth factors, cause changes in angiogenesis, bone formation and tissue response, and guide regeneration and cell proliferation, necessary for rapid wound repair, healing and scar formation. They also contribute to the stimulation of lymphocytes, which help in periodontal regeneration.<sup>28–30</sup>

B-lymphocytes are the 2<sup>nd</sup> type of lymphocytes that act as powerful modulators of tissue regeneration. They also modulate the immune response by converting into plasma cells and presenting antigens to T cells. These help in regeneration by releasing pro- and anti-inflammatory cytokines.<sup>31</sup> Boyce et al. demonstrated that initially B-lymphocytes were not identified, as they accumulate gradually during the natural healing process, but with ongoing research they identified B-lymphocytes on the 5<sup>th</sup> day of the healing process.<sup>32</sup> Boyce et al. posited that

with increased B-lymphocyte counts there is an increased secretion of interleukin 6, promoting wound healing and periodontal regeneration.<sup>32</sup>

In the present study, significantly higher mean cell counts and labeling index percentage values were observed for T-lymphocytes, B-lymphocytes and platelets in the T-PRF group. This was in agreement with a previous histochemical study conducted by Chatterjee et al., who concluded that T-PRF had a better fibrin mesh, which contributed to a better cellular entrapment with higher cell counts.<sup>33</sup> The present study is also compatible with a study conducted by Mitra et al., who concluded that T-PRF had a denser fibrin mesh and cellularity than L-PRF.<sup>34</sup> On the other hand, contrasting results were reported by Yajamanya et al., who concluded that L-PRF had a thicker fibrin mesh with good cellular entrapment in young individuals as opposed to elderly subjects.<sup>35</sup>

In the present study, the cell distribution (mild positivity), mean cell count and labeling index of stem cells showed no significant differences between the L-PRF and T-PRF groups. This was in accordance with a study conducted by Ghanaati et al., in which stem cells covered no more than 30% of the clot surface.<sup>9</sup> In the present study, stem cells were obtained from the blood clot, and hence were thought to be of hematopoietic origin. Ogawa et al. stated that hematopoietic stem cells are pluripotent in nature and can differentiate into most types of cells.<sup>36</sup> Thus, they are unique assets of PRF, differentiating into various types of cells depending on requirements, such as the regeneration of bone, periodontal ligament or cementum at the site of interest, making them good candidates for therapeutic vehicles. They also have effects as immune modulators.<sup>37–39</sup>

## Conclusions

To our knowledge, this study was the first to compare the labeling index percentage of T-PRF and L-PRF using IHC markers.

The limitations of the study might be the small sample size, and the costs of titanium tubes and the antibody markers used. In addition, we did not assess the variations in centrifugation speed and duration. However, within the limitations of this study, it can be concluded that T-PRF has a significantly better cellular distribution for T-lymphocytes, B-lymphocytes, platelets, neutrophils, and monocytes than L-PRF. Due to this extra edge of T-PRF, it emerged as a novel entity, and can be used as a better alternative to L-PRF in the field of periodontal regeneration. However, progenitor cells, which are required for the formation of new periodontal tissues from differentiated cells, are present in very similar quantities in both T-PRF and L-PRF. Further interventional studies with long-term follow-ups are required to determine the extent of periodontal regeneration.

## ORCID iDs

Hirak Shubhra Bhattacharya  <https://orcid.org/0000-0001-8518-0597>  
 Shiva Shankar Gummaluri  <https://orcid.org/0000-0003-3892-7332>  
 Madhusudan Astekar  <https://orcid.org/0000-0002-6927-411X>  
 Ram Kumar Gummaluri  <https://orcid.org/0000-0002-8354-0349>

## References

- Chen FM, Jin Y. Periodontal tissue engineering and regeneration: Current approaches and expanding opportunities. *Tissue Eng Part B Rev.* 2010;16(2):219–255.
- Dzobo K, Thomford NE, Senthebane DA, et al. Advances in regenerative medicine and tissue engineering: Innovation and transformation of medicine. *Stem Cells Int.* 2018;2018:2495848.
- Agrawal AA. Evolution, current status and advances in application of platelet concentrate in periodontics and implantology. *World J Clin Cases.* 2017;5(5):159–171.
- Choukroun J, Adda F, Schoeffer C, Vervelle A. PRF: An opportunity in perio-implantology [in French]. *Implantodontie.* 2000;42:55–62.
- Dohan DM, Choukroun J, Diss A, et al. Platelet-rich fibrin (PRF): A second-generation platelet concentrate. Part I: Technological concepts and evolution. *Oral Surg Oral Med Oral Pathol Oral Radiol Endod.* 2006;101(3):e37–e44.
- Agarwal A, Gupta ND, Jain A. Platelet-rich fibrin combined with decalcified freeze-dried bone allograft for the treatment of human intrabony periodontal defects: A randomized split mouth clinical trial. *Acta Odontol Scand.* 2016;74(1):36–43.
- Pradeep AR, Nagpal K, Karvekar S, Patnaik K, Naik SB, Guruprasad CN. Platelet-rich fibrin with 1% metformin for the treatment of intrabony defects in chronic periodontitis: A randomized controlled clinical trial. *J Periodontol.* 2015;86(6):729–737.
- Verma UP, Yadav RK, Dixit M, Gupta A. Platelet-rich fibrin: A paradigm in periodontal therapy – a systematic review. *J Int Soc Prev Community Dent.* 2017;7(5):227–233.
- Ghanaati S, Booms P, Orłowska A, et al. Advanced platelet-rich fibrin: A new concept for cell-based tissue engineering by means of inflammatory cells. *J Oral Implantol.* 2014;40(6):679–689.
- Dohan Ehrenfest DM, de Peppo GM, Doglioli P, Sammartino G. Slow release of growth factors and thrombospondin-1 in Choukroun's platelet-rich fibrin (PRF): A gold standard to achieve for all surgical platelet concentrates technologies. *Growth Factors.* 2009;27(1):63–69.
- O'Connell SM. Safety issues associated with platelet-rich fibrin method. *Oral Surg Oral Med Oral Pathol Oral Radiol Endod.* 2007;103(5):587–593.
- Tunalı M, Özdemir H, Küçükodacı Z, Akman S, Fıratlı E. In vivo evaluation of titanium-prepared platelet-rich fibrin (T-PRF): A new platelet concentrate. *Brit J Oral Maxillofac Surg.* 2013;51(5):438–443.
- Tunalı M, Özdemir H, Küçükodacı Z, et al. A novel platelet concentrate for guided bone regeneration: Titanium-prepared platelet-rich fibrin. *Biomed Res Int.* 2014;2014:209548.
- Duan X, Lin Z, Lin X, et al. Study of platelet-rich fibrin combined with rat periodontal ligament stem cells in periodontal tissue regeneration. *J Cell Mol Med.* 2018;22(2):1047–1055.
- Di Liddo R, Bertalot T, Borean A, et al. Leucocyte and platelet-rich fibrin: A carrier of autologous multipotent cells for regenerative medicine. *J Cell Mol Med.* 2018;22(3):1840–1854.
- He L, Lin Y, Hu X, Zhang Y, Wu H. A comparative study of platelet-rich fibrin (PRF) and platelet-rich plasma (PRP) on the effect of proliferation and differentiation of rat osteoblasts in vitro. *Oral Surg Oral Med Oral Pathol Oral Radiol Endod.* 2009;108(5):707–713.
- Huang FM, Yang SF, Zhao JH, Chang YC. Platelet-rich fibrin increases proliferation and differentiation of human dental pulp cells. *J Endod.* 2010;36(10):1628–1632.
- Mazor Z, Horowitz RA, Del Corso M, Prasad HS, Rohrer MD, Dohan Ehrenfest DM. Sinus floor augmentation with simultaneous implant placement using Choukroun's platelet-rich fibrin as the sole grafting material: A radiologic and histologic study at 6 months. *J Periodontol.* 2009;80(12):2056–2064.
- Duraiyan J, Govindarajan R, Kaliyappan K, Palanisamy M. Applications of immunohistochemistry. *J Pharm Bioallied Sci.* 2012;4(Suppl 2): S307–S309.
- Bancroft JD, Cook H, Turner D. *Manual of Histological Techniques and Their Diagnostic Application.* 3<sup>rd</sup> ed. Philadelphia, USA: Churchill Livingstone/Elsevier Health Sciences; 1996:986–998.

21. Alrani D, Niranjana KC, Sarathy NA. Assessment of proliferative index between the tumor margin, center of tumor, and the invasive tumor front of oral squamous cell carcinoma with the help of Mcm-2: An immunohistochemical study. *Appl Immunohistochem Mol Morphol*. 2020;28(1):30–35.
22. Choukroun J, Diss A, Simonpieri A, et al. Platelet-rich fibrin (PRF): A second-generation platelet concentrate. Part IV: Clinical effects on tissue healing. *Oral Surg Oral Med Oral Pathol Oral Radiol Endod*. 2006;101(3):e56–e60.
23. Arora S, Agnihotri N. Platelet derived biomaterials for therapeutic use: Review of technical aspects. *Indian J Hematol Blood Transfus*. 2017;33(2):159–167.
24. Eppley BL, Pietrzak WS, Blanton M. Platelet-rich plasma: A review of biology and applications in plastic surgery. *Plast Reconstr Surg*. 2006;118(6):147e–159e.
25. Jenne CN, Urrutia R, Kuberski P. Platelets: Bridging hemostasis, inflammation, and immunity. *Int J Lab Hematol*. 2013;35(3):254–261.
26. Choukroun J, Ghanaati S. Reduction of relative centrifugation force within injectable platelet-rich-fibrin (PRF) concentrates advances patients' own inflammatory cells, platelets and growth factors: The first introduction to the low speed centrifugation concept. *Eur J Trauma Emerg Surg*. 2018;44(1):87–95.
27. Soltan M, Rohrer MD, Prasad HS. Monocytes: Super cells for bone regeneration. *Implant Dent*. 2012;21(1):13–20.
28. Tan KW, Chong SZ, Wong FH, et al. Neutrophils contribute to inflammatory lymphangiogenesis by increasing VEGF-A bioavailability and secreting VEGF-D. *Blood*. 2013;122(22):3666–3677.
29. Ekström K, Omar O, Granéli C, Wang X, Vazirisani F, Thomsen P. Monocyte exosomes stimulate the osteogenic gene expression of mesenchymal stem cells. *PLoS One*. 2013;8(9):e75227.
30. Maciel J, Oliveira MI, Colton E, et al. Adsorbed fibrinogen enhances production of bone- and angiogenic-related factors by monocytes/macrophages. *Tissue Eng Part A*. 2014;20(1–2):250–263.
31. Sîrbulescu RF, Boehm CK, Soon E, et al. Mature B cells accelerate wound healing after acute and chronic diabetic skin lesions. *Wound Repair Regen*. 2017;25(5):774–791.
32. Boyce DE, Jones WD, Ruge F, Harding KG, Moore K. The role of lymphocytes in human dermal wound healing. *Br J Dermatol*. 2000;143(1):59–65.
33. Chatterjee A, Debnath K, Ali MM, Babu C, Gowda PL. Comparative histologic evaluation of titanium platelet-rich fibrin and platelet-rich fibrin in hypertensive and smoker participants: A cell cytology study. *J Indian Soc Periodontol*. 2017;21(3):195–200.
34. Mitra DK, Potdar PN, Prithyani SS, Rodrigues SV, Shetty GP, Talati MA. Comparative study using autologous platelet-rich fibrin and titanium prepared platelet-rich fibrin in the treatment of infrabony defects: An in vitro and in vivo study. *J Indian Soc Periodontol*. 2019;23(6):554–561.
35. Yajamanya SR, Chatterjee A, Babu CN, Karunanithi D. Fibrin network pattern changes of platelet-rich fibrin in young versus old age group of individuals: A cell block cytology study. *J Indian Soc Periodontol*. 2016;20(2):151–156.
36. Ogawa M, LaRue AC, Mehrotra M. Hematopoietic stem cells are pluripotent and not just "hematopoietic". *Blood Cells Mol Dis*. 2013;51(1):3–8.
37. Lim WF, Inoue-Yokoo T, Tan KS, Lai MI, Sugiyama D. Hematopoietic cell differentiation from embryonic and induced pluripotent stem cells. *Stem Cell Res Ther*. 2013;4(3):71–82.
38. Nicolaidou V, Wong MM, Redpath AN, et al. Monocytes induce STAT3 activation in human mesenchymal stem cells to promote osteoblast formation. *PLoS One*. 2012;7(7):e39871.
39. Wang L, Zhao Y, Shi S. Interplay between mesenchymal stem cells and lymphocytes: Implications for immunotherapy and tissue regeneration. *J Dent Res*. 2012;91(11):1003–1010.

# Comparison of salivary total antioxidant levels in male smokers and non-smokers according to their personality types

## Porównanie całkowitej zdolności antyoksydacyjnej śliny u palących i niepalących mężczyzn w odniesieniu do ich typów osobowości

Hamed Mortazavi<sup>1,A,E,F</sup>, Azadeh Ghasemi<sup>2,B,C</sup>, Mohammad Reza Vatankhah<sup>3,C,D</sup>

<sup>1</sup> Department of Oral Medicine, School of Dentistry, Shahid Beheshti University of Medical Sciences, Tehran, Iran

<sup>2</sup> Dental private office, Tehran, Iran

<sup>3</sup> Students' Research Committee, School of Dentistry, Shahid Beheshti University of Medical Sciences, Tehran, Iran

A – research concept and design; B – collection and/or assembly of data; C – data analysis and interpretation; D – writing the article; E – critical revision of the article; F – final approval of the article

Dental and Medical Problems, ISSN 1644-387X (print), ISSN 2300-9020 (online)

*Dent Med Probl.* 2020;57(2):145–148

### Address for correspondence

Hamed Mortazavi

E-mail: hamedmortazavi2013@gmail.com

### Funding sources

None declared

### Conflict of interest

None declared

Received on August 30, 2019

Reviewed on September 27, 2019

Accepted on November 20, 2019

Published online on June 29, 2020

### Cite as

Mortazavi H, Ghasemi A, Vatankhah MR. Comparison of salivary total antioxidant levels in male smokers and non-smokers according to their personality types. *Dent Med Probl.* 2020;57(2):145–148. doi:10.17219/dmp/114440

### DOI

10.17219/dmp/114440

### Copyright

© 2020 by Wrocław Medical University

This is an article distributed under the terms of the

Creative Commons Attribution 3.0 Unported License (CC BY 3.0)

(<https://creativecommons.org/licenses/by/3.0/>).

## Abstract

**Background.** Cigarette smoking is a major global health problem, associated with various oral diseases, such as oral cancers. Salivary antioxidants may play an important role in fighting against radicals and the oxidative components of cigarettes, which can cause DNA damage. Furthermore, psychological stress, which occurs more often in individuals with type A personality, affects plasma antioxidant levels.

**Objectives.** The objective of this study was to compare the levels of salivary total antioxidant capacity (TAC) between smokers and non-smokers according to their personality types.

**Material and methods.** In this descriptive cross-sectional study, saliva samples were collected from 40 male smokers (with  $\geq 0.1$  pack-years) and 40 male non-smokers. After centrifugation, the samples were assessed using an enzyme-linked immunosorbent assay (ELISA) kit. Pearson's correlation, Welch's *t*-test and the one-way analysis of variance (ANOVA) test were used for statistical analyses.

**Results.** The TAC of saliva in smokers was significantly lower than in non-smokers ( $p = 0.019$ ). Type A and type B smokers showed no significant decrease in TAC ( $p > 0.05$  and  $p = 0.05$ , respectively) as compared to type A and type B non-smokers, respectively. Type A smokers reported a higher number of cigarettes smoked per day as compared to smokers with type B personality ( $p = 0.043$ ).

**Conclusions.** Smoking cigarettes was associated with a significant decrease in salivary TAC. However, the personality type did not affect salivary TAC in the present study.

**Key words:** personality, antioxidants, saliva, antioxidant, smoking tobacco

**Słowa kluczowe:** osobowość, antyoksydanty, ślina, antyoksydacyjny, palenie tytoniu

## Introduction

Smoking has various negative effects on oral health. Also, it is considered as a major risk factor for oral cancers.<sup>1,2</sup> Furthermore, smoking tobacco is positively associated with buccal cell mutations,<sup>3</sup> periodontal diseases<sup>4</sup> and premalignant lesions.<sup>5</sup>

Reactive oxygen species, reactive nitrogen species as well as radicals are amongst the numerous toxic components found in cigarette smoke.<sup>6</sup> These oxidants and radicals can lead to oxidative DNA damage, the damage of cellular components, the inhibition of apoptosis, and increased angiogenesis. Hence, they are related to oral cancer initiation, promotion and progression.<sup>7,8</sup>

The disproportion between the levels of oxidative components (e.g., reactive oxygen species and free radicals) and antioxidants may be associated with several oral pathologies.<sup>9</sup> As a biological fluid, saliva contains antioxidant molecules, such as glutathione and uric acid, and enzymes, such as superoxide dismutase (SOD), guaiacol peroxidase (GP) and glutathione peroxidase (GSH-PX).<sup>10</sup> Cigarette smoke may interfere with the antioxidants in saliva. A previous study showed that smoking a single cigarette induced a significant reduction in the concentration of glutathione in saliva.<sup>11</sup> Also, another study demonstrated that salivary TAC levels were significantly lower in smokers as compared to non-smokers.<sup>12</sup>

It has been shown that psychological stress can increase DNA oxidation and lipid peroxidation, and decrease the total antioxidant capacity (TAC) of plasma in university students.<sup>13</sup> Another study showed increased peroxidation levels and decreased TAC levels of plasma in patients with depression.<sup>14</sup> Both psychological stress and depression occur with a higher incidence in persons with type A personality. These individuals are more impatient, more competitive and more aggressive. Also, they tend to exhibit addictive behaviors, such as cigarette smoking.<sup>15</sup>

The current lack of evidence has led us to design this descriptive cross-sectional study to measure and compare the TAC levels of saliva in smokers and non-smokers according to their personality types.

## Material and methods

This descriptive cross-sectional study was conducted between 2016 and 2018. It was approved by the Ethics Committee of Shahid Beheshti University of Medical Sciences in Tehran, Iran (IR.SBMU.RIDS.REC.1395.350).

The sample size required to identify differences between the 2 groups, as stated in a previous similar study,<sup>10</sup> was 20 subjects in each group, assuming a nondirectional alpha risk of 0.05 and a power of 0.8. Forty male smokers and 40 male non-smokers were selected using a simple non-randomized sampling method. Each group had equally 20 individuals with type A or type B personality.

The groups consisted of patients attending the Department of Oral Medicine at the School of Dentistry of Shahid Beheshti University of Medical Sciences in Tehran, Iran.

Individuals with a history of  $\geq 0.1$  pack-years are considered as smokers.<sup>16</sup> The inclusion criteria contained the following: the ability to fill out the questionnaire; no consumption of alcohol; age under 60 years; the absence of pregnancy; no presence of oral lesions or systemic diseases, such as diabetes mellitus, leukemia, thalassemia, or rheumatoid arthritis; and not taking medications during the previous 6 months at least.

All individuals signed informed consent. The investigator requested the participants not to eat or drink 2 h before the collection of saliva. In addition, smokers were prohibited from smoking 1 h before the collection of saliva. After mouth washing with water and waiting for 2 min, 5 mL of saliva was sampled in an upright resting position between 9 am and 12 am. The samples were immediately placed in ice, and then moved to the laboratory. They were centrifuged at 1,000 g at 4°C for 10 min. After removing debris, the samples were preserved at a temperature of  $-80^{\circ}\text{C}$ . The exact duration of the saliva collection was also recorded to calculate the salivary flow.<sup>17</sup> A blinded technician measured the TAC levels using an enzyme-linked immunosorbent assay (ELISA) kit (ZellBio GmbH, Rostock, Germany). This kit was able to detect 0.1 mM of TAC, using ascorbic acid as a standard.<sup>18,19</sup> The DANA-3200<sup>®</sup> ELISA reader (Garni Medical Eng. Co., Tehran, Iran) was used to read the results.

To determine the type of personality, we used the self-administered 14-item Bortner questionnaire in the Persian language with total scores ranging from 0 to 140, assuming 70 as a borderline.<sup>18</sup> Results with scores less or more than 70 are considered as type B or type A personality, respectively. The reliability and validity of the Persian version of the Bortner questionnaire were assessed and confirmed in previous separate studies.<sup>19,20</sup>

The analyses were carried out using the IBM SPSS Statistics for Windows software, v. 21 (IBM Corp., Armonk, USA). The comparison of different brands of cigarettes was made using the  $\chi^2$  test. Welch's *t*-test was used to compare smoking years, the number of cigarettes smoked per day and age between the groups. To compare the levels of TAC between the groups, the one-way analysis of variance (ANOVA) test was implemented. The statistical significance level of the present study was set at 5%.

## Results

The mean age of the participants was  $39.6 \pm 7.32$  years. There was no significant difference in terms of age between the groups ( $p > 0.05$ ).

Table 1 shows that the levels of TAC in smokers were significantly lower than in non-smokers ( $p = 0.019$ ). There

was no significant difference in the levels of TAC between type A smokers and type A non-smokers ( $p > 0.05$ ), but this difference was at the borderline for the type B group ( $p = 0.05$ ). Furthermore, there was no significant difference in the TAC levels between smokers with regard to their personality types ( $p > 0.05$ ). According to Table 2, the number of cigarettes smoked per day for the type A group was significantly greater than for the type B group ( $p = 0.043$ ). However, the difference in smoking years between the 2 groups was not significant ( $p > 0.05$ ).

The salivary flow of smokers was lower than that of non-smokers, but the difference was not statistically significant ( $p > 0.05$ ).

**Table 1.** Comparison of the total antioxidant capacity (TAC) levels between the groups

Group	Sample size (n)	TAC [U/L]	p-value
Type A smokers	20	0.34 ± 0.19	0.840
Type A non-smokers	20	0.39 ± 0.19	
Type B smokers	20	0.24 ± 0.15	0.050**
Type B non-smokers	20	0.39 ± 0.17	
Type A and type B smokers	40	0.29 ± 0.17	0.019*
Type A and type B non-smokers	40	0.39 ± 0.18	
Type A smokers	20	0.34 ± 0.19	0.323
Type B smokers	20	0.24 ± 0.15	

Data presented as mean ± standard deviation ( $M \pm SD$ ).

\* statistically significant; \*\* at the borderline of statistical significance.

**Table 2.** Factors associated with cigarette smoking in each smoker group

Factor	Type A smokers (n = 20)	Type B smokers (n = 20)	p-value
Mean duration of cigarette smoking [years]	18.35	18.00	0.897
Mean number of cigarettes smoked per day	12.40	8.65	0.043*

\* statistically significant.

## Discussion

The maximum prevalence of cigarette smoking is seen between the age of 30 and 49.<sup>21,22</sup> Similarly to previous studies,<sup>2,10</sup> the mean age of participants in this study was in the aforesaid range.

It has been shown that the levels of TAC are significantly higher in males.<sup>23</sup> For this reason and to eliminate the possible effect of sex, we only included male participants in the present study.

The measurement of TAC is better than the measurement of all known antioxidants separately, as it requires less time, and takes into account the activity of unknown antioxidants as well as the positive or negative interactions between different antioxidants.<sup>11</sup>

In the present study, salivary TAC in smokers was significantly lower than in non-smokers. This outcome was similar to those of some previous studies, reporting lower

levels of TAC or SOD, GP and GSH-PX separately.<sup>2,10</sup> Nevertheless, some other studies showed no significant difference in salivary TAC between smokers and non-smokers.<sup>24</sup> Conversely, previous research showed significantly higher levels of TAC in smokers as compared to non-smokers.<sup>25</sup> These controversies may be related to the differences in the study design, inclusion and exclusion criteria, sample size, saliva sampling methods, intensity and duration of the smoking habit, and antioxidant measurement methods.

Although some studies reported a significantly lower salivary flow for smokers, our results showed no significant difference in the salivary flow between the 2 groups, confirming the outcomes of previous research.<sup>24</sup>

Individuals with type A or type B personality exhibit different psychological states; however, our findings showed no significant difference between the 2 types in the duration of cigarette smoking, although participants with type A personality reported a significantly higher number of cigarettes smoked per day as compared to participants with type B personality. These findings are parallel to prior evidence and can indicate that smoking is more common among people with type A personality than in the case of type B personality.<sup>26</sup>

Individuals with type A personality were smoking more cigarettes per day as compared to type B individuals, but they did not have lower levels of TAC. This result is similar to that of a previous study, which showed no significant difference in nicotine intake between the 2 different personality types. However, that study reported similar smoking behaviors in type A and type B smokers.<sup>27</sup> Our findings with different smoking behaviors (more cigarettes per day in the type A personality group) are in line with the findings of the aforementioned study with similar smoking behaviors in the 2 groups. Maybe other factors, such as the number of puffs per cigarette or the duration of each puff, influence this controversy.

Another study demonstrated that the administration of nicotine caused a significant change in the plasma lipid profile, promoting lipid peroxidation in plasma. This increase in peroxidation decreases the levels of SOD, catalase and GSH-PX in plasma.<sup>28</sup>

What can be regarded as a limitation of this study is the fact that we did not measure some of the known smoking behavior indicators, such as the number of puffs per cigarette and the duration of each puff.

The personality type affects more than a single smoking behavior that can lead to an alteration in salivary TAC levels; therefore, assessing other factors, such as differences in the diet, working conditions and socioeconomic situation, is recommended for further studies.

This study lays an important foundation for future research; more studies on the possible relation between personality types and the TAC levels are needed with a higher sample size and different methods used. Due to a large number of people involved, even if the effect of personality



types on the TAC levels is generally small, such studies may provide important information that can be used to modify prevention policies and cessation programs.


The smoker's personality profile is considered as an important obstacle to cessation.<sup>29</sup> In addition, smoking tobacco is an important risk factor for oral cancers. Therefore, properly planned prevention policies and cessation programs, in order to be efficacious, should take into account the aspect of personality.<sup>1</sup>


## Conclusions

The results of this study suggest that smoking cigarettes is associated with a significant decrease in salivary TAC. However, there was no significant difference in salivary TAC levels between type A and type B smokers.

### ORCID iDs

Hamed Mortazavi  <https://orcid.org/0000-0002-0778-5299>

Azadeh Ghasemi  <https://orcid.org/0000-0002-9550-5436>

Mohammad Reza Vatankhah  <https://orcid.org/0000-0001-9988-6005>

### References

- Warnakulasuriya S. Causes of oral cancer – an appraisal of controversies. *Br Dent J*. 2009;207(10):471–475.
- Abdolsamadi HR, Goodarzi MT, Mortazavi H, Robati M, Ahmadi-Motemaye F. Comparison of salivary antioxidants in healthy smoking and non-smoking men. *Chang Gung Med J*. 2011;34(6):607–611.
- Proia NK, Paszkiewicz GM, Sullivan Nasca MA, Franke GE, Pauly JL. Smoking and smokeless tobacco-associated human buccal cell mutations and their association with oral cancer – a review. *Cancer Epidemiol Biomarkers Prev*. 2006;15(6):1061–1077.
- Johnson GK, Guthmiller JM. The impact of cigarette smoking on periodontal disease and treatment. *Periodontol* 2000. 2007;44:178–194.
- Jahanbani J. Prevalence of oral leukoplakia and lichen planus in 1,167 Iranian textile workers. *Oral Dis*. 2003;9(6):302–304.
- Pryor WA, Stone K. Oxidants in cigarette smoke. Radicals, hydrogen peroxide, peroxyxynitrate, and peroxyxynitrite. *Ann N Y Acad Sci*. 1993;686:12–27.
- Pfeifer GP, Denissenko MF, Olivier M, Tretyakova N, Hecht SS, Hainaut P. Tobacco smoke carcinogens, DNA damage and p53 mutations in smoking-associated cancers. *Oncogene*. 2002;21(48):7435–7451.
- Choudhari SK, Chaudhary M, Gadabail AR, Sharma A, Tekade S. Oxidative and antioxidative mechanisms in oral cancer and precancer: A review. *Oral Oncol*. 2014;50(1):10–18.
- Battino M, Ferreiro MS, Gallardo I, Newman HN, Bullon P. The antioxidant capacity of saliva. *J Clin Periodontol*. 2002;29(3):189–194.
- Bakhtiari S, Azimi S, Mehdipour M, Amini S, Elmi Z, Namazi Z. Effect of cigarette smoke on salivary total antioxidant capacity. *J Dent Res Dent Clin Dent Prospects*. 2015;9(4):281–284.
- Bakhtiari S, Taheri JB, Bakhshi M, et al. Effect of vitamin C on salivary total antioxidant capacity in smokers. *Iran J Pharm Res*. 2012;11(4):1045–1049.
- Zappacosta B, Persichilli S, De Sole P, Mordente A, Giardina B. Effect of smoking one cigarette on antioxidant metabolites in the saliva of healthy smokers. *Arch Oral Biol*. 1999;44(6):485–488.
- Kusano C, Ferrari CKB. Total antioxidant capacity: A biomarker in biomedical and nutritional studies. *J Cell Mol Biol*. 2008;7(1):1–15.
- Yanik M, Erel O, Kati M. The relationship between potency of oxidative stress and severity of depression. *Acta Neuropsychiatr*. 2004;16(4):200–203.
- Moriana JA, Herruzo J. Type A behavior pattern as a predictor of psychiatric sick-leaves of Spanish teachers. *Psychol Rep*. 2005;96(1):77–82.
- Lee YH, Shin MH, Kweon SS, et al. Cumulative smoking exposure, duration of smoking cessation, and peripheral arterial disease in middle-aged and older Korean men. *BMC Public Health*. 2011;11:94.
- Navazesh M, Kumar SKS. Measuring salivary flow: Challenges and opportunities. *J Am Dent Assoc*. 2008;139(Suppl):355–405.
- Walsh JJ, Wilding JM, Eysenck MW. Stress responsivity: The role of individual differences. *Pers Individ Differ*. 1994;16(3):385–394.
- Farnodi F, Amiri H, Jalali R. The association of personality type A and B to type 2 diabetes mellitus in patients referring to diabetes center, Kermanshah, 2014. *J Clin Res Paramed Sci*. 2015;4(3):188–194.
- Roushan CR, Modaresi F. Personality types and mental health impact of systemic lupus erythematosus and rheumatoid arthritis. *Hakim Res J*. 2003;5(4):255–261.
- Jha P, Ranson MK, Nguyen SN, Yach D. Estimates of global and regional smoking prevalence in 1995, by age and sex. *Am J Public Health*. 2002;92(6):1002–1006.
- Ebadi M, Vahdaninia M, Azin A, et al. Prevalence of tobacco consumption: Iranian health perception survey. *Payesh*. 2011;10(3):365–372.
- Lettrichová I, Tóthová L, Hodosy J, Behuliak M, Celec P. Variability of salivary markers of oxidative stress and antioxidant status in young healthy individuals. *Redox Rep*. 2016;21(1):24–30.
- Charalabopoulos K, Assimakopoulos D, Karkabounas S, Danielidis V, Kiortsis D, Evangelou A. Effects of cigarette smoking on the antioxidant defence in young healthy male volunteers. *Int J Clin Pract*. 2005;59(1):25–30.
- Nagler RM. Altered salivary profile in heavy smokers and its possible connection to oral cancer. *Int J Biol Marker*. 2007;22(4):274–280.
- Oyefeso AO, Odeyale MA. Smoking and type A behaviour. *Scand J Psychol*. 1991;32(1):79–81.
- Hughes JR, Pickens RW, Gust SW, Hatsukami DK, Svikis DS. Smoking behavior of type A and type B smokers. *Addict Behav*. 1986;11(2):115–118.
- Chattopadhyay K, Chattopadhyay BD. Effect of nicotine on lipid profile, peroxidation & antioxidant enzymes in female rats with restricted dietary protein. *Indian J Med Res*. 2008;127(6):571–576.
- de Cássia Rondina R, Gorayeb R, Botelho C. Psychological characteristics associated with tobacco smoking behavior. *J Bras Pneumol*. 2007;33(5):592–601.

# Clinical significance of maxillary sinus hypoplasia in dentistry: A CBCT study

## Znaczenie kliniczne niedorozwoju zatoki szczękowej w stomatologii – badanie w tomografii stożkowej

Numan Dedeoğlu<sup>A,B,D,E</sup>, Suayip Burak Duman<sup>B,D–F</sup>

Department of Oral and Maxillofacial Radiology, Faculty of Dentistry, İnönü University, Malatya, Turkey

A – research concept and design; B – collection and/or assembly of data; C – data analysis and interpretation;  
D – writing the article; E – critical revision of the article; F – final approval of the article

Dental and Medical Problems, ISSN 1644-387X (print), ISSN 2300-9020 (online)

*Dent Med Probl.* 2020;57(2):149–156

### Address for correspondence

Suayip Burak Duman  
E-mail: suayipburakduman@gmail.com

### Funding sources

None declared

### Conflict of interest

None declared

Received on July 31, 2019

Reviewed on October 21, 2019

Accepted on December 2, 2019

Published online on June 29, 2020

### Cite as

Dedeoğlu N, Duman SB. Clinical significance of maxillary sinus hypoplasia in dentistry: A CBCT study. *Dent Med Probl.* 2020;57(2):149–156. doi:10.17219/dmp/114982

### DOI

10.17219/dmp/114982

### Copyright

© 2020 by Wrocław Medical University

This is an article distributed under the terms of the

Creative Commons Attribution 3.0 Unported License (CC BY 3.0)

(<https://creativecommons.org/licenses/by/3.0/>).

## Abstract

**Background.** The anatomy of the maxillary sinus is especially important for dentists due to the close proximity of the sinus to the maxillary posterior teeth.

**Objectives.** The aim of the present study was to investigate the frequency of maxillary sinus pathology, anatomical variations, and the relationship between the tooth roots and the maxillary sinus by comparing a group with maxillary sinus hypoplasia (MSH) and a control group using cone-beam computed tomography (CBCT).

**Material and methods.** In the study, 69 CBCT images of 50 patients with MSH and 84 CBCT images of 49 patients without MSH were evaluated for pathology, and the presence of an accessory ostium, a septum and Haller cells in each maxillary sinus.

**Results.** The coincidence of pathology with MSH was 29%, and with non-hypoplastic maxillary sinuses it was 44% ( $p = 0.055$ ). An accessory ostium was found in 14.5% of scans with MSH and in 39.3% of those without MSH ( $p = 0.001$ ). Haller cells were found in 2.9% of the MSH cases, whereas their incidence in the control group was 23.8% ( $p = 0.000$ ). The occurrence of a sinus septum was at the level of 4.3% in the group with MSH and 23.8% in the group without MSH ( $p = 0.001$ ).

**Conclusions.** The incidence of the relationship between the sinus wall and the posterior root apices was found smaller in the dentulous MSH patients. Also, the distance between the root apices and the sinus wall was longer in the dentulous MSH patients, and the vertical and horizontal alveolar bone was larger in the posteriorly edentulous MSH patients.

**Key words:** dental implant, endodontic treatment, alveolar crest, maxillary sinus hypoplasia

**Słowa kluczowe:** implant stomatologiczny, leczenie endodontyczne, grzebień zębodołowy, niedorozwój zatoki szczękowej

## Introduction

The anatomy of the maxillary sinus is especially important for dentists because of the close proximity of the sinus to the maxillary posterior teeth. In some cases, maxillary sinusitis may have an odontogenic cause due to the close relationship between the sinus wall and the root apices of the maxillary posterior teeth, which can lead to some impairment, such as periodontal and periapical lesions and tooth extractions.<sup>1</sup>

The maxillary sinus, the largest paranasal sinus, begins to develop in the 10<sup>th</sup>–12<sup>th</sup> week of gestation and the cavity becomes identifiable at 16 weeks of gestation. At birth, the volume of the maxillary sinus is 6–8 mm<sup>3</sup>, and it increases with the growth of the nasal cavity, the infraorbital wall, the alveolar process, and the zygomatic process. The volume of the maxillary antrum increases vertically and laterally by 2 mm per year and by 3 mm per year anteroposteriorly. The final pneumatization of the maxillary sinus occurs principally in an inferior direction after the eruption of the maxillary teeth. The adult size is reached at the age of 15–18.<sup>2,3</sup>

Maxillary sinus hypoplasia (MSH) is a relatively rare clinical condition,<sup>2</sup> not particularly well-known among dentists and oral surgeons. Maxillary sinus hypoplasia can be congenital or acquired (due to surgery or trauma).<sup>4</sup> Most cases of MSH do not cause any symptoms in patients, who are unaware of their condition, and it is generally diagnosed incidentally.<sup>2</sup>

Currently, cone-beam computed tomography (CBCT) is widely used in the diagnostic imaging of the head and neck region, although it is a relatively new radiological technique.<sup>5</sup> Cone-beam computed tomography enables three-dimensional (3D) data acquisition, followed by image reconstruction, display, and interpretation. The CBCT scanning is rapid and delivers only low doses of radiation; its modality is ideal for imaging children and claustrophobic adults.<sup>6</sup> Cone-beam computed tomography has been shown to be at least as good as computed tomography (CT) when used to examine bone structures (e.g., the skull base, the paranasal sinuses and the temporal bone) and pathologies in the oral and maxillofacial regions.<sup>7,8</sup> Even though CBCT is commonly used by dentists, otolaryngologists also favor this technique because of the good image quality it provides.<sup>9</sup>

The aim of this study was to investigate the frequency of maxillary sinus pathology, anatomical variations, and the relationship between the tooth roots and the maxillary sinus by comparing the CBCT records of patients from the group with MSH and from the group without MSH.

## Material and methods

In the study, 69 CBCT images of 50 patients with MSH and 84 CBCT images of 49 patients without MSH were used. In total, 153 maxillary sinuses of 99 patients

were evaluated, of which 88 had teeth in the neighboring dental arch, whereas 65 dental arches adjacent to the maxillary sinuses were edentulous. Forty-five of the 88 sinuses with the posterior maxillary teeth were hypoplastic sinuses, whereas of the 65 posteriorly edentulous maxillary sinuses, 24 were hypoplastic. The CBCT records of the posteriorly edentulous patients belonged to people who had been scanned for pre-surgical implant evaluation. The age of the patients who participated in the study was between 20 and 90 years.

All the walls of the maxillary sinus and the teeth near the base of the sinus wall were determined as the work area of each half-jaw. A maxillary sinus with half or less of the maximum horizontal or vertical linear dimension of the orbit on the same side was defined as hypoplastic (Fig. 1).<sup>10</sup>

The exclusion criteria were the following: dental loss and deficiency in the process area; an implant or a bone graft; large pathologies disrupting the anatomy of the process area; planned surgery in the maxillary sinus; bone metabolism diseases; or third molars with no apical foramina.

The CBCT images obtained from the Department of Oral and Maxillofacial Radiology at the Faculty of Dentistry of İnönü University in Malatya, Turkey, were evaluated retrospectively by an experienced oral radiologist (N.D.). This study was approved by the İnönü University Scientific Research and Publication Ethics Committee (approval No. 2019/2-1 as of January 22, 2019).

The images evaluated in the study were performed using the NewTom 5G CBCT device (NewTom, Verona, Italy) (standard 110 kVp, 20 mA maximum). The scanning time was 18 s, and a display area of 18 cm × 16 cm or 15 cm × 12 cm (field of view – FOV) was used. The voxel values of the images were 0.3 mm, 0.25 mm and 0.2 mm.

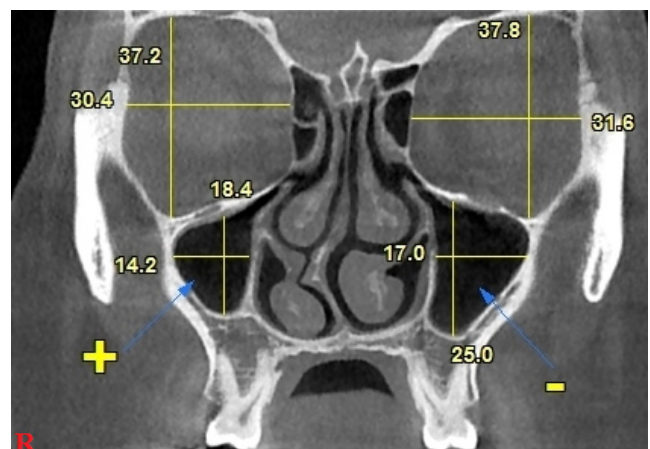


Fig. 1. The right maxillary sinus is considered hypoplastic, since the maximum maxillary dimension is less than half the maximum orbital dimension – 18.4 < 18.6 (37.2 / 2); the left maxillary sinus is not regarded as hypoplastic, as the maximum maxillary dimension is more than half the maximum orbital dimension – 25 > 18.9 (37.8 / 2)

The CBCT images were evaluated using the NNT (New NewTom) software. All images reviewing coronal sections, pathology and the presence of accessory ostia, septa and Haller cells in each maxillary sinus were evaluated and recorded with regard to the groups with and without MSH (Fig. 2). We also evaluated whether the tooth root apices were associated with the maxillary sinus (Fig. 3A,3B).

In the maxillary sinuses with the posterior teeth, the distance between the closest tooth root to the maxillary sinus wall and the sinus was measured linearly along the tooth root–sinus floor in the groups with and without hypoplasia, respectively (Fig. 3C,3D). When the tooth root penetrated the sinus wall, the distance from the sinus wall to the root apices was accepted as 0 (Fig. 3E).

In the maxillary sinuses without the posterior teeth, the narrowest alveolar crest width, along with the vertical length where the distance between the alveolar crest and the maxillary sinus was the smallest, was measured linearly (Fig. 4).

The data obtained in this study were analyzed with the IBM SPSS Statistics for Windows software, v. 22 (IBM Corp., Armonk, USA). When investigating the normal distribution of variables, the Shapiro–Wilk test was

utilized due to the number of units. When examining the differences between the groups, the Mann–Whitney  $U$ -test was chosen, as the variables were not normally distributed. The  $\chi^2$  test was used when examining the relationships between the groups with nominal variables. When interpreting the results, the level of significance was set at 0.05. The kappa value for the inter-observer agreement was calculated.

## Results

In this study, the mean age of the population of 99 patients – 43 men (43.3%) and 56 women (56.7%) – was found to be  $42.25 \pm 14.27$  years (*min*: 20; *max*: 90). The mean age of the patients with MSH was 41.1 years (*min*: 20; *max*: 90) and the mean age of the patients without MSH was 43.53 years (*min*: 21; *max*: 74). There were 50 patients with MSH, including 22 men (44%) and 28 women (56%). There were 49 people without MSH – 21 men (42.9%) and 28 women (57.1%). In the study, 153 maxillary sinuses of 99 patients were evaluated. Eighty-four of these 153 sinuses belonged to female patients, whereas 69 belonged to male patients.

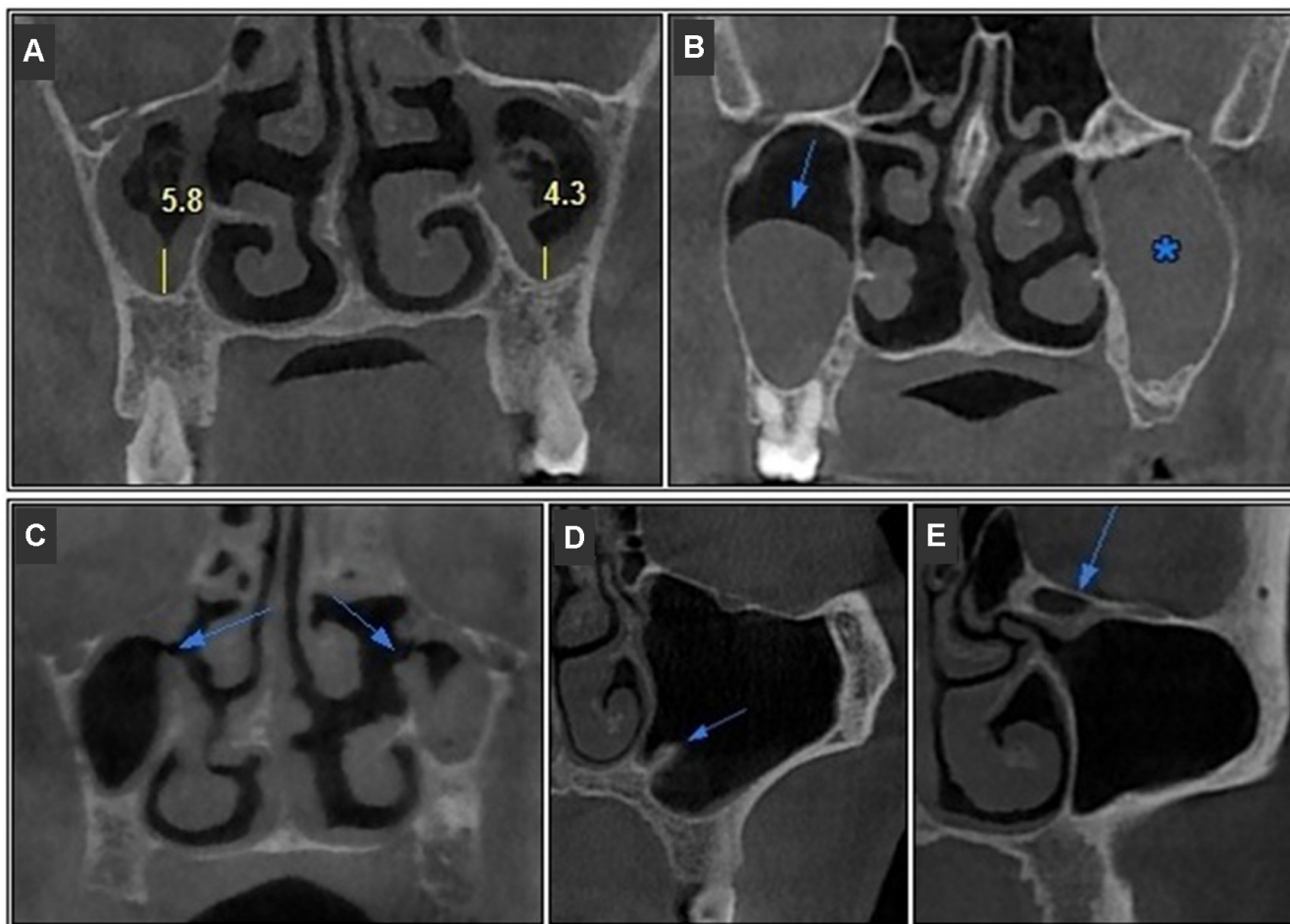


Fig. 2. A – mucosal thickening (>3 mm); B – mucosal retention cyst (arrow) and polypoid lesion (asterisk); C – accessory ostium; D – septum; E – Haller cells

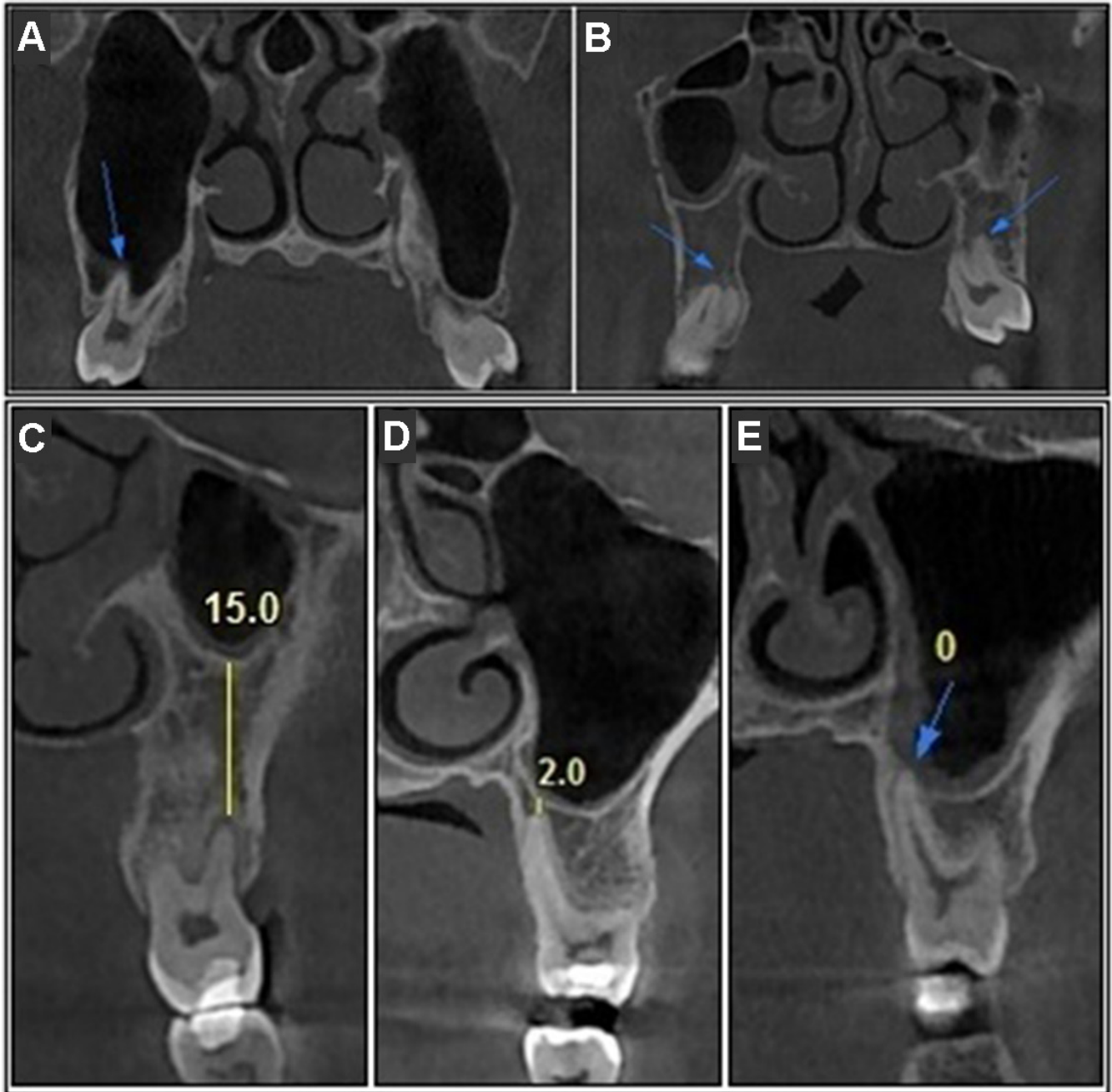


Fig. 3. A – tooth roots associated with the maxillary sinus; B – unbound; C,D – distance between the tooth root apices and the sinus wall; E – tooth root penetrating the sinus wall

A total of 88 maxillary sinuses (45 hypoplastic and 43 non-hypoplastic) belonging to 56 patients with the posterior teeth (31 women and 25 men) were evaluated. Twenty-three of the 45 hypoplastic maxillary sinuses with the posterior teeth belonged to female patients, whereas 22 of them belonged to male patients. Twenty-five of the 43 non-hypoplastic maxillary sinuses with the posterior teeth belonged to female patients and 18 of them to male patients (Table 1).

A total of 65 maxillary sinuses (24 hypoplastic and 41 non-hypoplastic) belonging to 43 posteriorly edentulous patients (25 women and 18 men) were evaluated. Thirteen of the 24 hypoplastic maxillary sinuses with

Table 1. Prevalence of maxillary sinus hypoplasia (MSH) by gender

Study group	Gender	Patients n (%)	Maxillary sinuses n (%)
Dentulous hypoplastic sinus	female	17 (17.17)	23 (15.03)
	male	15 (15.15)	22 (14.38)
Dentulous non-hypoplastic sinus	female	14 (14.14)	25 (16.34)
	male	10 (10.10)	18 (11.76)
Edentulous hypoplastic sinus	female	11 (11.11)	13 (8.50)
	male	7 (7.07)	11 (7.19)
Edentulous non-hypoplastic sinus	female	14 (14.14)	23 (15.03)
	male	11 (11.11)	18 (11.76)
Total N		99	153

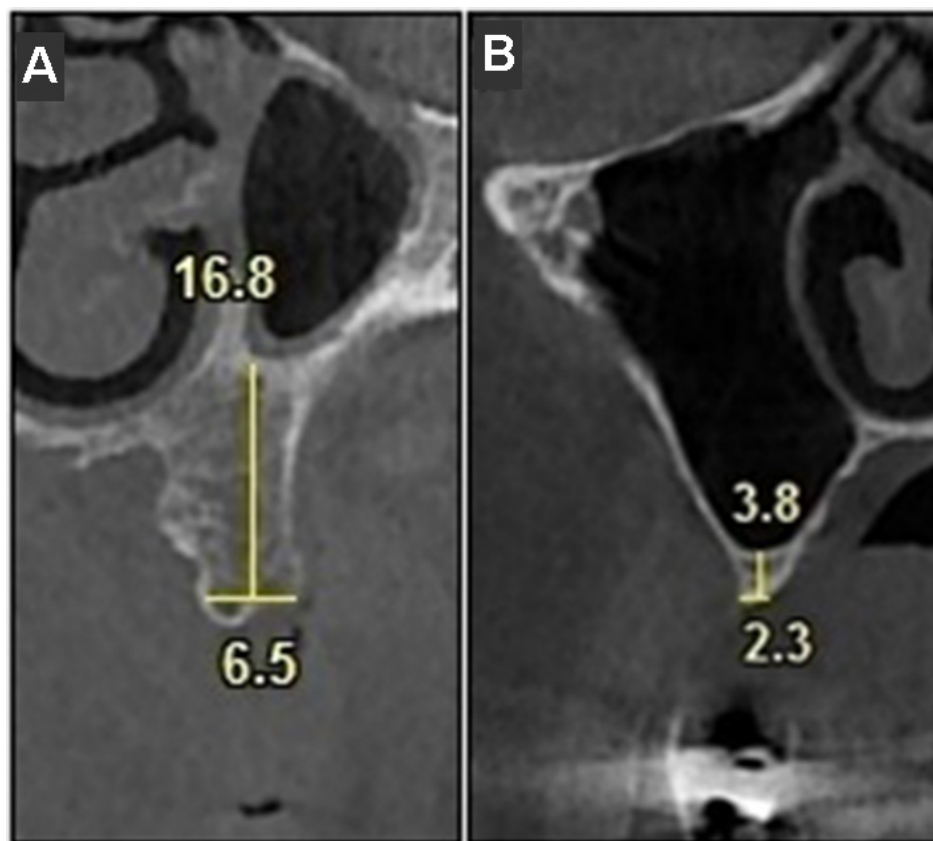


Fig. 4. Horizontal and vertical alveolar crest dimensions

A – hypoplastic sinus;

B – non-hypoplastic sinus.

posteriorly edentulous jaws belonged to female patients, whereas 11 of them belonged to male patients. Twenty-three of the 41 non-hypoplastic maxillary sinuses with posteriorly edentulous jaws belonged to female patients and 18 of them to male patients (Table 1).

### Comparison of the group with maxillary sinus hypoplasia and the group without maxillary sinus hypoplasia in terms of anatomic variations

The incidence of pathology in the group with MSH was 29%, whereas it was 44% in the group with non-hypoplastic maxillary sinuses. No statistically significant difference was found when comparing these 2 groups (Table 2).

In the group with MSH, the incidence of an accessory ostium was 14.5%, whereas 39.3% of the group without MSH had an accessory ostium. A statistically significant difference was found when comparing these 2 groups (Table 2).

Haller cells were found in 2.9% of the group with MSH, whereas 23.8% of the scans without MSH displayed Haller cells. This difference was statistically significant (Table 2).

The presence of a maxillary sinus septum was observed in 4.3% of the group with MSH, whereas it was 23.8% in the group without MSH. When these 2 groups were compared, a statistically significant difference was found (Table 2).

Table 2. Statistical comparison of pathology, anatomic variations and the tooth root–sinus relationship in hypoplastic and non-hypoplastic maxillary sinuses

Pathology, anatomical variations, root–sinus relationship	Hypoplastic maxillary sinuses <i>n</i> (%)	Non-hypoplastic maxillary sinuses <i>n</i> (%)	<i>p</i> -value
Pathology <sup>a</sup>	20 (29)	37 (44)	0.055
Accessory ostium <sup>a</sup>	10 (14.5)	33 (39.3)	0.001*
Haller cells <sup>a</sup>	2 (2.9)	20 (23.8)	0.000*
Septum <sup>a</sup>	3 (4.3)	20 (23.8)	0.001*
Root–sinus relationship <sup>b</sup>	1 (2.2)	14 (32.6)	0.000*

<sup>a</sup> comparison between all maxillary sinuses; <sup>b</sup> comparison between edentulous maxillary sinuses; \* statistically significant;  $\chi^2$  test.

### Comparison of the group with maxillary sinus hypoplasia with the posterior teeth and the group without maxillary sinus hypoplasia with the posterior teeth

The incidence of the root–sinus relationship in the group with MSH was 2.2%, whereas it was 32.6% in the group without MSH. A statistically significant difference was found between these 2 groups (Table 2).

In the patients with MSH and the posterior teeth, the minimum distance of the root apex to the sinus base was found to be 5.98 mm on average. This value was 0.62 mm in the group without MSH, but with the posterior teeth. The difference between these 2 values was statistically significant ( $p = 0.000$ ) (Table 3).

**Table 3.** Statistical comparison of the average minimum distance between the root apices and the sinus, and the average minimum horizontal and vertical alveolar crest dimensions in hypoplastic and non-hypoplastic maxillary sinuses

Measurement	Hypoplastic maxillary sinuses				Non-hypoplastic maxillary sinuses				p-value
	n	min	max	M ±SD	n	min	max	M ±SD	
Minimum distance between the root apex and the maxillary sinus floor <sup>a</sup> [mm]	45	0	15.0	5.98 ±3.83	43	0	7.5	0.62 ±1.42	0.000*
Minimum horizontal alveolar crest dimension <sup>b</sup> [mm]	24	2.8	8.5	5.17 ±1.87	41	1.3	13.4	3.83 ±2.10	0.002*
Minimum vertical alveolar crest dimension <sup>b</sup> [mm]	24	4.0	19.5	12.47 ±3.94	41	0.5	13.3	5.03 ±3.08	0.000*

M – mean; SD – standard deviation; <sup>a</sup> comparison between dentulous maxillary sinuses; <sup>b</sup> comparison between edentulous maxillary sinuses; \* statistically significant; Mann–Whitney U-test.

The kappa value (inter-observer agreement) was 0.92 for the closest distance between the root apex and the sinus base.

### Comparison of the group with maxillary sinus hypoplasia without the posterior teeth and the group without maxillary sinus hypoplasia without the posterior teeth

In the group with MSH without the posterior teeth, the minimum horizontal dimension of the alveolar crest was 5.17 mm on average. This value was found to be 3.83 mm in the group without MSH and without the posterior teeth. There was a statistically significant difference between these 2 values ( $p = 0.002$ ) (Table 3). The kappa value (inter-observer agreement) was 0.87 for the minimum horizontal alveolar crest dimension.

In the patients with MSH without the posterior teeth, the minimum vertical dimension of the alveolar crest was found to be 12.47 mm on average. This value was 5.03 mm in the group without MSH and without the posterior teeth. There was a significant difference between these 2 values ( $p = 0.000$ ) (Table 3). The kappa value (inter-observer agreement) was 0.87 for the minimum vertical alveolar crest dimension.

## Discussion

The maxillary sinus is located between the nasal and oral cavities, so maxillary sinus diseases are most often caused by bacterial invasion.<sup>11</sup> Root canal treatment, a tooth extraction or trauma may cause the bacteria of the dental area to pass into the maxillary sinus. When looking at the bacterial pathways leading to acute sinusitis,<sup>12</sup> pathogenic bacteria have been observed in the oral cavity (*Streptococcus pneumoniae*, *Haemophilus influenzae* and *Moraxella catarrhalis*). In the present study, the relationship between MSH and the root apices was compared with regard to normal sinuses, which has not been done before. The relationship between the maxillary sinus

floor and the maxillary tooth root tips was greater in the patients without MSH than in the MSH patients. Moreover, the minimum distance between the root apex and the sinus floor was compared between the MSH group and the group without MSH. The minimum distance between the maxillary sinus floor and the maxillary tooth root tip was shorter in the patients without MSH than in the MSH patients. In other words, the sinuses in the MSH patients were farther away from the dental area. There have been studies reporting that chronic inflammation in the maxillary sinus has a dental origin in 14–24% of cases.<sup>13,14</sup> Although not confirmed by other studies, the risk of sinus infections of dental origin was predicted to be lower in the case of MSH. The present study revealed that fewer complications are to be expected in posterior maxilla endodontic and surgical treatment of MSH patients due to a longer distance from the root apex to the sinus floor. Also, due to the sufficient amount of bone, this area might be regarded as a suitable autograft area.

Researchers have reported similar results of sinus infections in patients with MSH. Erdem et al. revealed a relationship between MSH and chronic maxillary sinusitis.<sup>15</sup> They suggested that hypoplasia or an absent uncinat process may be the cause of sinusitis.<sup>15</sup> Similarly, Milczuk et al. mentioned a relationship between MSH and chronic maxillary sinusitis in children.<sup>16</sup> In our study, there was a lower prevalence of sinus pathology in the patients with MSH than in the control group, although the difference was not statistically significant.

Haller cells were first described by Albrecht von Haller in 1765 and alternatively named infraorbital ethmoid cells. These cells are mostly encountered as incidental findings during the CT examination of the paranasal sinuses. Haller cells develop into the floor of the orbit (the medial portion) and above the maxillary sinus ostium (the lateral portion). Although unilateral Haller cells are encountered frequently, bilateral Haller cells are rare.<sup>17,18</sup> The presence of Haller cells is thought to be a basic factor in recurrent maxillary sinusitis,<sup>18,19</sup> especially because various retrospective studies have shown a crucial correlation between the size of Haller cells (greater than 3 mm)

and maxillary sinusitis.<sup>16,20</sup> In the present study, Haller cells were found considerably less often in the patients with MSH than in those with normal sinuses. According to our study, a low occurrence of Haller cells in the patients with MSH may be considered as a factor that reduces the likelihood of maxillary sinusitis as compared to the patients without MSH.

Although there are no studies in the literature investigating the direct effect of a sinus septum on maxillary sinus infections, the perforation of the maxillary sinus mucosa, which is one of the complications especially in implant surgery, is a highly serious situation. Studies have shown that the risk of perforation increases in the presence of a sinus septum and that the placement of graft material in the region is difficult.<sup>21</sup> In our study, the incidence of a sinus septum in the patients with MSH was found to be statistically lower than in the patients without sinus hypoplasia, so it could be interpreted that it was safer in terms of perforation risk.

It is still controversial in the literature whether an elliptically shaped accessory ostium,<sup>22</sup> which can be easily diagnosed during routine endoscopic nasal examinations, is congenital or acquired following acute maxillary sinusitis.<sup>23</sup> This anatomic variation has been thought to play a role in the development of maxillary sinusitis.<sup>24</sup> Some researchers have suggested that an accessory maxillary ostium develops as a result of maxillary sinusitis, since they have reported that the prevalence of an accessory maxillary ostium is higher in patients with infundibular narrowing or a maxillary sinus infection.<sup>25,26</sup> In our study, the prevalence of an accessory ostium was significantly lower in the patients with MSH, which supports the idea that the risk of a sinus infection from an accessory ostium is lower than in non-MSH patients.


The required alveolar bone height for long-term implant prognosis should be a minimum of 10–12 mm. Unfortunately, the alveolar bone height in posteriorly edentulous maxillae below the maxillary sinuses is often less than 10 mm.<sup>27</sup> Although there is no precise ratio provided, it has been observed that as the vertical height increases, the cumulative success rate of a dental implant increases in the long term (10–12 years).<sup>28</sup> Some alternative methods are available to solve this problem, such as augmenting the maxillary bone, using zygomatic implants or using short implants (4–8-millimeter long).<sup>29</sup> In our study, the mean minimum vertical alveolar bone height in the posterior maxillae with MSH was found to be 12.47 mm, which was statistically significantly higher than in the patients without sinus hypoplasia. Additionally, the mean minimum horizontal alveolar bone dimension in the posterior maxillae with MSH was found to be statistically greater than in the patients without sinus hypoplasia. Clinically speaking, implant surgery can be safe in patients with posteriorly edentulous maxillae and MSH due to the vertical and horizontal bone dimensions, according to our study.

## Conclusions

This study differs in some aspects from others in the literature. The results show that in the case of MSH, endodontic and surgical treatment is less likely to cause complications due to a larger distance between the tooth apex and the sinus floor. Anatomical variations that can cause sinusitis, such as accessory ostia and Haller cells, were found to be less frequent in the MSH patients. Other anatomical variations, such as sinus septa, were found to be less frequent in MSH. For implant surgery, the bone mass was found to be higher in the posteriorly edentulous maxillae of the MSH patients, as the dimensions of the posterior alveolar vertical and horizontal bone proved to be greater in the case of MSH. Before a surgical procedure, clinicians should at least be aware of this anatomical change.

### ORCID iDs

Numan Dedeoğlu  <https://orcid.org/0000-0003-0892-3654>

Suayip Burak Duman  <https://orcid.org/0000-0003-2552-0187>

### References

1. Peyneau PD, Oliveira LGT, Carneiro PMR, Manzi FR. Maxillary sinus disease of odontogenic origin. *Dent Press Endod.* 2013;3(2):80–83.
2. Thiagarajan B, Narashiman S. Hypoplasia of all paranasal sinuses: A case series and literature review. *Otolaryngol Online J.* 2012;2(2):20–25.
3. Kosko JR, Hall BE, Tunkel DE. Acquired maxillary sinus hypoplasia: A consequence of endoscopic sinus surgery? *Laryngoscope.* 1996;106(10):1210–1213.
4. Bassiouny A, Newlands WJ, Ali H, Zaki Y. Maxillary sinus hypoplasia and superior orbital fissure asymmetry. *Laryngoscope.* 1982;92(4):441–448.
5. Altun O, Duman SB, Bayraktar IS, Yasa Y, Duman S, Yılmaz SG. Cone beam computed tomography imaging of superior semicircular canal morphology: A retrospective comparison of cleft lip/palate patients and normal controls. *Acta Odontol Scand.* 2018;76(4):247–252.
6. Demirel O, Kaya E, Üçok CÖ. Evaluation of mastoid pneumatization using cone-beam computed tomography. *Oral Radiol.* 2014;30:92–97.
7. Hanzelka T, Dusek J, Ocacek F, et al. Movement of the patient and the cone beam computed tomography scanner: Objectives and possible solutions. *Oral Surg Oral Med Oral Pathol Oral Radiol.* 2013;116(6):769–773.
8. Teymoortash A, Hamzei S, Murthum T, Eivazi B, Kureck I, Werner JA. Temporal bone imaging using digital volume tomography and computed tomography: A comparative cadaveric radiological study. *Surg Radiol Anat.* 2011;33(2):123–128.
9. Fakhran S, Alhilali L, Sreedher G, et al. Comparison of simulated cone beam computed tomography to conventional helical computed tomography for imaging of rhinosinusitis. *Laryngoscope.* 2014;124(9):2002–2006.
10. Sirikçi A, Bayazit Y, Gümüşburun E, Bayram M, Kanlikana M. A new approach to the classification of maxillary sinus hypoplasia with relevant clinical implications. *Surg Radiol Anat.* 2000;22(5–6):243–247.
11. Brook I. Sinusitis of odontogenic origin. *Otolaryngol Head Neck Surg.* 2006;135(3):349–355.
12. Nash D, Wald E. Sinusitis. *Pediatr Rev.* 2001;22:111–117.
13. Uvarov VM. *Odontogenic Maxillary Sinusitis* [in Russian]. Leningrad, Russia: Medgiz; 1962:34–39.
14. Shargorodsky AG. *Inflammatory Diseases of the Maxillofacial Region and the Neck* [in Russian]. Moscow, Russia: Medgiz; 1985:15–24.
15. Erdem T, Aktas D, Erdem G, Miman MC, Ozturan O. Maxillary sinus hypoplasia. *Rhinology.* 2002;40(3):150–153.
16. Milczuk HA, Dalley RW, Wessbacher FW, Richardson MA. Nasal and paranasal sinus anomalies in children with chronic sinusitis. *Laryngoscope.* 1993;103(3):247–252.



17. Ahmad M, Khurana N, Jaber J, Sampair C, Kuba RK. Prevalence of infra-orbital ethmoid (Haller's) cells on panoramic radiographs. *Oral Surg Oral Med Oral Pathol Oral Radiol Endod.* 2006;101(5):658–661.
18. Kantarci M, Karasen RM, Alper F, Onbas O, Okur A, Karaman A. Remarkable anatomic variations in paranasal sinus region and their clinical importance. *Eur J Radiol.* 2004;50(3):296–302.
19. Stammberger H, Wolf G. Headaches and sinus disease: The endoscopic approach. *Ann Otol Rhinol Laryngol Suppl.* 1988;134:3–23.
20. Bolger WE, Butzin CA, Parsons DS. Paranasal sinus bony anatomic variations and mucosal abnormalities: CT analysis for endoscopic sinus surgery. *Laryngoscope.* 1991;101(1 Pt 1):56–64.
21. Ulm CW, Solar P, Krennmair G, Matejka M, Watzek G. Incidence and suggested surgical management of septa in sinus-lift procedures. *Int J Oral Maxillofac Implants.* 1995;10(4):462–465.
22. Thiagarajan B. Advanced anatomy of lateral nasal wall: For the endoscopic sinus surgeon [Internet]. Version 12. *Ent Scholar.* 2012 Sep 19. <https://entscholar.wordpress.com/article/advanced-anatomy-of-lateral-nasal-wall/>. Accessed on September 19, 2012.
23. Genc S, Ozcan M, Titiz A, Unal A. Development of maxillary accessory ostium following sinusitis in rabbits. *Rhinology.* 2008;46(2):121–124.
24. Yenigun A, Fazliogullari Z, Gun C, Uysal II, Nayman A, Karabulut AK. The effect of the presence of the accessory maxillary ostium on the maxillary sinus. *Eur Arch Otorhinolaryngol.* 2016;273(12):4315–4319.
25. Mladina R, Vuković K, Poje G. The two holes syndrome. *Am J Rhinol Allergy.* 2009;23(6):602–604.
26. Gutman M, Houser S. Iatrogenic maxillary sinus recirculation and beyond. *Ear Nose Throat J.* 2003;82(1):61–63.
27. das Neves FD, Fones D, Bernardes SR, do Prado CJ, Neto AJ. Short implants – an analysis of longitudinal studies. *Int J Oral Maxillofac Implants.* 2006;21(1):86–93.
28. Ferrigno N, Laureti M, Fanali S. Dental implants placement in conjunction with osteotome sinus floor elevation: A 12-year life-table analysis from a prospective study on 588 ITI implants. *Clin Oral Implants Res.* 2006;17(2):194–205.
29. Esposito M, Barausse C, Pistilli R, Sammartino G, Grandi G, Felice P. Short implants versus bone augmentation for placing longer implants in atrophic maxillae: One-year post-loading results of a pilot randomised controlled trial. *Eur J Oral Implantol.* 2015;8(3):257–268.

# Effect of class II extractions and functional appliance treatment on smile esthetics

## Wpływ ekstrakcji i leczenia czynnościowego wad zgryzu klasy II na estetykę uśmiechu

Umair Shoukat Ali<sup>A,B,D</sup>, Rashna Hoshang Sukhia<sup>C,E,F</sup>, Mubassar Fida<sup>A,F</sup>

Aga Khan University and Hospital, Karachi, Pakistan

A – research concept and design; B – collection and/or assembly of data; C – data analysis and interpretation; D – writing the article; E – critical revision of the article; F – final approval of the article

Dental and Medical Problems, ISSN 1644-387X (print), ISSN 2300-9020 (online)

Dent Med Probl. 2020;57(2):157–163

### Address for correspondence

Rashna Hoshang Sukhia  
E-mail: rashna\_aga@yahoo.com

### Funding sources

None declared

### Conflict of interest

None declared

Received on July 12, 2019

Reviewed on November 5, 2019

Accepted on December 9, 2019

Published online on June 30, 2020

### Cite as

Ali US, Sukhia RH, Fida M. Effect of class II extractions and functional appliance treatment on smile esthetics. *Dent Med Probl.* 2020;57(2):157–163. doi:10.17219/dmp/115169

### DOI

10.17219/dmp/115169

### Copyright

© 2020 by Wrocław Medical University

This is an article distributed under the terms of the

Creative Commons Attribution 3.0 Unported License (CC BY 3.0)

(<https://creativecommons.org/licenses/by/3.0/>).

## Abstract

**Background.** Class II malocclusion is routinely observed in orthodontics. Its treatment usually revolves around the growth modification or the extractions of the teeth. Identifying treatment that leads to the greatest improvement can aid clinicians in providing the desired smile esthetics.

**Objectives.** The aim of the study was to compare smile esthetics between treatment groups by measuring various smile variables and the esthetic perceptions of 3 panels of raters.

**Material and methods.** A cross-sectional study was performed on 66 patients equally divided into the functional appliance (FA) and upper first premolar extraction (UPE) groups. Eight smile variables were measured on post-treatment photographs using the Adobe Photoshop® software. Ten orthodontic residents, general dentists and laypersons performed the subjective evaluations of smiles using the visual analog scale (VAS). The Mann–Whitney *U*-test was applied to compare smile variables between the groups. The Kruskal–Wallis test was used to compare esthetic scores (ES) among the raters. The simple linear regression analysis, followed by the multiple linear regression analysis was applied to determine the smile variables associated with the ES values.

**Results.** Statistically significant differences were found between the FA and UPE groups for the buccal corridor ratio (BCR) ( $p = 0.046$ ), the visible dentition width ratio (VDWR) ( $p = 0.019$ ) and the arch form index (AFI) ( $p < 0.001$ ). The Kruskal–Wallis test showed significant differences in ES among the raters for the FA ( $p < 0.001$ ) and UPE ( $p = 0.004$ ) groups. The simple linear regression analysis showed significant associations between ES and the patient's age ( $p = 0.002$ ), BCR ( $p = 0.020$ ) and VDWR ( $p = 0.006$ ). The multiple linear regression analysis showed that age ( $p = 0.008$ ) and VDWR ( $p = 0.021$ ) were significantly associated with the ES values.

**Conclusions.** The FA group had narrower buccal corridor spaces, a greater visible dentition width and a wider arch form in their smiles. The UPE group showed an increase in the buccal corridor width. Each panel rated the FA appliance group as superior.

**Key words:** orthodontic appliances, malocclusion, Angle class II, smile

**Słowa kluczowe:** aparaty ortodontyczne, nieprawidłowy zgryz, wada zgryzu klasy II Angle'a, uśmiech

## Introduction

Smile esthetics is the primary focus of orthodontic treatment in the contemporary age. An esthetic smile can boost a person's confidence, and improve social interaction and quality of life.<sup>1,2</sup> It is crucial for an orthodontist to be able to assess smile esthetics and meet the patient's expectations.<sup>3</sup> According to Goldstein, the smile is one of the most fundamental features of facial attractiveness.<sup>4</sup> Ackerman and Ackerman suggested that even with successfully treated orthodontic patients, obtaining ideal smile esthetics is challenging for experienced practitioners.<sup>5</sup>

Class II malocclusion occurs at rates of approx. 24.5% in Asians, 33% in Caucasians and 15% in the US population.<sup>6–8</sup> In most cases, mandibular retrognathism is the culprit of skeletal class II malocclusion, giving patients a characteristic convex profile.<sup>8,9</sup> Hence, enhancing the mandibular growth in pre-adolescent patients is indicated to improve mandibular deficiency.<sup>10</sup> The growth modification of the mandible depends on the skeletal maturational age of the patient as assessed by the cervical maturation index proposed by Baccetti et al.<sup>11</sup> Functional appliances improve skeletal disharmony during the growth period (CS (cervical stage)-3) by posturing the mandible forward and stimulating the mandibular growth.<sup>12</sup> An example of a commonly used functional appliance is Clark's twin block (CTB).<sup>13</sup> However, once the desired results of functional appliance treatment are achieved, a brief course of fixed mechanotherapy is required to finish the process.

If, on the other hand, the patient has surpassed their growth potential (CS-5–CS-6), class II correction is confined to either orthodontic camouflage or orthognathic surgery.<sup>14</sup> Orthodontic camouflage is defined as masking the skeletal discrepancies of the face without correcting the underlying jaw disharmony.<sup>14,15</sup> A majority of orthodontic patients prefer to avoid orthognathic surgery, as it is invasive, and instead opt for camouflage.<sup>16</sup> Orthodontic camouflage is suitable for patients with average or short facial patterns, mild anteroposterior jaw discrepancies, crowding <4–6 mm, and normal soft tissues.<sup>17</sup> Class II camouflage is most commonly achieved with the extraction of the upper first premolars.<sup>18</sup>

The evaluation of smile esthetics at the end of orthodontic treatment can provide useful information on how different modalities affect the perception of smile esthetics. Therefore, the identification of treatment that leads to the greatest improvement of facial esthetics can aid clinicians in selecting appropriate treatment modalities. The objectives of this study were to compare smile esthetics in patients who underwent functional appliance therapy followed by fixed mechanotherapy and those who underwent fixed appliance therapy with upper first premolar extraction, and to evaluate the esthetic perceptions of 3 panels of raters, including orthodontic residents, general dentists and laypersons. The null hypothesis was that there would be no difference between the 2 treatment groups in terms of smile esthetics as perceived by the raters.

## Material and methods

A cross-sectional study that included 66 participants was performed after obtaining approval from the Aga Khan University ethics review board (2018-0295-161), Karachi, Pakistan. Data was obtained from the post-treatment follow-up frontal smiling photographs of subjects treated for skeletal class II malocclusion. These patients had been treated consecutively over a period of 4 years (2013–2017) at the Orthodontic Clinic, with post-treatment follow-ups advised every 6 months.

The sample size was calculated using the OpenEpi<sup>®</sup> software v. 3.01 ([www.openepi.com](http://www.openepi.com)), taking into account the findings of Johnson and Smith, who reported a mean inter-canine–visible dentition width of  $0.77 \pm 0.032$  mm for non-extraction treatment and  $0.80 \pm 0.050$  mm for extraction treatment.<sup>19</sup> Keeping  $\alpha = 0.05$  and a power of 80%, a total of 31 subjects were required in each group. Since we had 2 groups, a total sample of 62 was required. This value was inflated to include 33 subjects per group. The samples were divided into the functional appliance (FA) group (CTB) and the upper first premolar extraction (UPE) group. The mean age of our sample groups at the post-treatment follow-up was  $20.3 \pm 1.2$  years for the FA group and  $23.3 \pm 2.8$  years for the UPE group. The gender distribution for the FA group was 15 males and 18 females; for the UPE group, it was 14 males and 19 females.

## Inclusion criteria

### Functional appliance group

The inclusion criteria for the FA group were as follows: skeletal class II patients with  $ANB > 6^\circ$ , a normal or low vertical facial growth pattern, proclined upper incisors ( $UI-SN > 107^\circ$ ), and normal or retro-lined lower incisors ( $IMPA < 90^\circ$ ) with a procumbent lower lip due to mandibular deficiency. The patients in this group had existent growth potential (CS-3) on lateral cephalograms according to the classification by Baccetti et al.<sup>11</sup> The CTB bite registration for advancing the mandible was obtained as recommended by Proffit et al. (4–6 mm of sagittal advancement and 3–4 mm of vertical opening).<sup>8</sup> Two-phase therapy was performed, starting with phase I – the growth modification with a removable CTB for a mean duration of  $11.0 \pm 1.3$  months; phase II – the final finishing and detailing – was performed in this group with fixed appliances (Roth prescription 0.022-inch slots) for a mean duration of  $12.2 \pm 2.1$  months.

### Upper first premolar extraction group

The patients in the UPE group had comparable cephalometric characteristics to the FA group, except that they had mild mandibular deficiency ( $4^\circ < ANB < 6^\circ$ ) with minimal or no growth potential left (CS-5 or CS-6) to plan for the growth modification. The selected patients had dental

class II molar relationships (end-on, 3/4 or full cusp). No extractions were done in the lower arch, since no discrepancies or crowding were present.<sup>20</sup> Single-phase treatment with comprehensive fixed appliance therapy was performed (Roth prescription 0.022-inch slots) for a mean duration of  $27.4 \pm 1.1$  months. After upper first premolar extraction, the patients underwent the retraction of the canines on 0.018-inch stainless steel (SS) wires followed by the retraction of the incisor segments via looped mechanics on 0.017-inch  $\times$  0.025-inch SS wires.

## Exclusion criteria

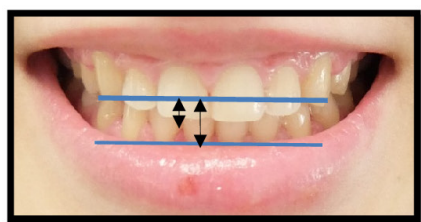
The exclusion criteria were any previous history of orthodontic or orthopedic treatment, any craniofacial/dental anomaly or syndrome, a history of trauma or surgery involving facial structures, or any skeletal discrepancy in which camouflage was not indicated.

## Procedures

Post-treatment follow-up frontal smiling photographs were taken for each participant using a Sony<sup>®</sup> DSC-WX200 digital camera (maximum resolution

4896  $\times$  3672, approx. 18.2 megapixels) (Sony Corp., Tokyo, Japan); the pictures were stored in the JPEG format. To standardize the images, we followed the guidelines published by Desai et al.<sup>21</sup> and Chetan et al.<sup>22</sup> The camera was affixed to a tripod approx. 4 ft from the standing subject. While taking the photographs, the patients were asked to look straight into an imaginary mirror, holding their head in a natural position. The camera was adjusted to the position parallel to the apparent occlusal plane. The grid ruler option was used in the camera, so that the capture area was situated in the center of the frame. Both ears of the patient were equally visible to ensure there was no error of orientation in the transverse plane. While the frontal smiling photographs were being taken, the patients were asked to say 'seven' or 'cheese'. The continuous shooting mode (burst mode) was used to take multiple images and the best picture, in which all the necessary anatomical landmarks were captured, was selected for each patient. Evaluations were made using the Adobe Photoshop<sup>®</sup> software (Adobe, San Jose, USA).

The perioral area was cropped and 8 smile variables were measured as ratios to limit the bias and compensate for the magnification differences among the pictures (Fig. 1).<sup>23</sup>



smile arc ratio (SAR) – distance from the maxillary incisal edge to the inter-canine connecting line divided by the distance from the lower lip to the inter-canine connecting line



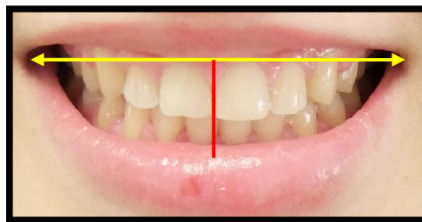
maxillary incisor display (MID) – distance from the maxillary incisal edge to the upper lip divided by the maxillary incisor width



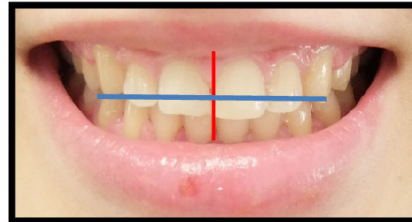
mandibular teeth exposure (MTE) – visible mandibular incisor length divided by the mandibular incisor width



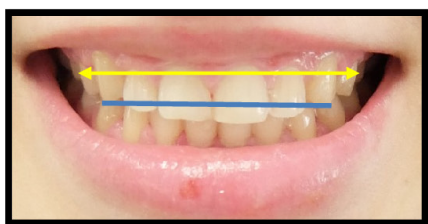
buccal corridor ratio (BCR) – inter-commissure width divided by the inter-canine width



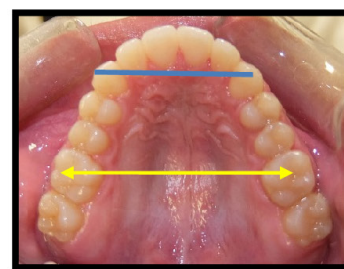
smile index (SI) – inter-commissure width divided by the interlabial gap



interlabial gap ratio (ILGR) – lip separation during a smile divided by the inter-canine width



visible dentition width ratio (VDWR) – maxillary inter-canine width divided by the visible dentition width



arch form index (AFI) – inter-canine width divided by the inter-molar width

Fig. 1. Smile variables

The measured smile variables were as follows: the smile arc ratio (SAR) – the distance from the maxillary incisal edge to the inter-canine connecting line divided by the distance from the lower lip to the inter-canine connecting line; maxillary incisor display (MID) – the distance from the maxillary incisal edge to the upper lip divided by the maxillary incisor width; mandibular teeth exposure (MTE) – the visible mandibular incisor length divided by the mandibular incisor width; the buccal corridor ratio (BCR) – the inter-commissure width divided by the inter-canine width; the smile index (SI) – the inter-commissure width divided by the interlabial gap; the interlabial gap ratio (ILGR) – lip separation during a smile divided by the inter-canine width; the visible dentition width ratio (VDWR) – the maxillary inter-canine width divided by the visible dentition width; and the arch form index (AFI) – the inter-canine width divided by the inter-molar width.

Subjective assessments were made by different panels of raters, which included 10 orthodontic residents, 10 general dentists and 10 laypersons. Each participant's frontal smiling photograph was analyzed and scored on a visual analog scale (VAS). It was created on a 100-millimeter uninterrupted line, anchored at 0 on the left (very unattractive) and at 10 on the right (very attractive).<sup>23</sup>

The panel of orthodontic residents consisted of 6 females and 4 males of a mean age of  $28.6 \pm 2.1$  years. In the general dentist panel, there were 6 females and 4 males of a mean age of  $27.5 \pm 2.3$  years. In the layperson panel, we had 4 females and 6 males of a mean age of  $22.8 \pm 1.4$  years.

To test the intra-examiner reliability, 10 frontal smiles were randomly selected and re-measured by the principal investigator. The intra-class correlation coefficient (ICC) showed values ranging from 0.85 to 1.0 between the 2 sets of measurements, indicating excellent agreement.

The data was analyzed by means of the IBM SPSS Statistics for Windows software, v. 20.0 (IBM Corp., Armonk, USA). Descriptive statistics were applied to calculate the mean age and distribution by gender. The Shapiro–Wilk test yielded a non-normal distribution of the sample. The Mann–Whitney *U*-test was used for the comparison of smile variables in the FA and UPE treatment groups. The one-way analysis of variance (ANOVA) was used to compare smile esthetic scores (ES) among the 3 panels of raters. The simple and multiple linear regression analyses were used to evaluate the variables which affected the subjective smile ES for both treatment groups. A *p*-value  $\leq 0.05$  was considered statistically significant.

## Results

The comparisons of smile variables between the 2 treatment groups showed BCR ( $p = 0.046$ ), VDWR ( $p = 0.019$ ) and AFI ( $p < 0.001$ ) to be significantly higher in the UPE group (Table 1).

Table 1. Comparison of smile variables between the functional appliance (FA) and upper first premolar extraction (UPE) treatment groups

Variable (ratio)	Treatment group		<i>p</i> -value
	FA (n = 33)	UPE (n = 33)	
SAR	0.50 (0.40, 0.65)	0.50 (0.40, 0.64)	0.831
MID	0.95 (0.80, 0.95)	0.97 (0.77, 1.14)	0.681
MTE	0.66 (0.56, 0.78)	0.60 (0.00, 0.85)	0.535
BCR	1.52 (1.40, 1.60)	1.62 (1.50, 1.70)	0.046*
SI	4.80 (4.40, 4.80)	5.10 (4.50, 6.00)	0.534
ILGR	0.31 (0.25, 0.36)	0.31 (0.26, 0.36)	0.724
VDWR	1.29 (1.21, 1.34)	1.39 (1.26, 1.43)	0.019*
AFI	0.78 (0.74, 0.79)	0.84 (0.81, 0.87)	<0.001**

Data presented as median (interquartile range) (Me (IQR)).

SAR – smile arc ratio; MID – maxillary incisor display; MTE – mandibular teeth exposure; BCR – buccal corridor ratio; SI – smile index; ILGR – interlabial gap ratio; VDWR – visible dentition width ratio; AFI – arch form index; \*  $p \leq 0.05$ ; \*\*  $p < 0.001$ ; Mann–Whitney *U*-test.

The comparisons of the ES provided by the different panels of raters showed statistically significant differences among the raters for the FA group ( $p < 0.001$ ) and the UPE group ( $p = 0.004$ ). Among the raters, orthodontic residents and laypersons gave higher scores to both the treatment groups than general dentists did. However, while comparing the treatment groups, all 3 panels of raters preferred the FA group over the UPE group (Table 2).

Table 2. Comparison of smile perceptions using the esthetic scores (ES) of 3 groups of raters

Treatment group	Orthodontic residents (n = 10)	General dentists (n = 10)	Laypersons (n = 10)	<i>p</i> -value
FA	56 (47, 65)	43 (35, 46)	58 (50, 63.5)	<0.001**
UPE	51 (41, 60)	41 (36, 52)	48 (38, 61)	0.004*

Data presented as Me (IQR).

\*  $p \leq 0.05$ ; \*\*  $p < 0.001$ ; Kruskal–Wallis test.

The simple linear regression analysis showed that age ( $p = 0.002$ ), BCR ( $p = 0.020$ ) and VDWR ( $p = 0.006$ ) were negatively correlated with the mean ES of the raters (Table 3); the correlations were statistically significant. Age ( $R^2 = 0.13$ ) explained 13% of the variability in the mean ES values, whereas BCR ( $R^2 = 0.07$ ) and VDWR ( $R^2 = 0.11$ ) accounted for 7% and 11% of the variability, respectively.

The multiple linear regression was applied to the variables which were found to be significant in the simple linear regression analysis. Age ( $p = 0.008$ ) and VDRW ( $p = 0.021$ ) were again found to be statistically significant. Age and VDWR ( $R^2 = 0.181$ ) each explained 18% of the variability in the mean ES values (Table 4).

Table 3. Effect of smile variables on ES

Variable	Crude beta coefficient (M ±SD)	95% CI	R <sup>2</sup>	p-value
Treatment modality	2.49 ±2.70	(-2.90, 7.88)	0.013	0.350
Gender	-0.35 ±2.80	(-6.00, 5.28)	<0.001	0.900
Age [years]	-0.63 ±0.20	(-1.03, -0.23)	0.130	0.002*
SAR	0.29 ±1.40	(-2.60, 3.20)	<0.001	0.840
MID	-3.80 ±4.80	(-13.40, 5.86)	0.009	0.430
MTE	-0.24 ±1.99	(-4.23, 3.70)	<0.001	0.900
BCR	-19.40 ±8.33	(-36.12, 2.81)	0.070	0.020*
SI	1.16 ±1.07	(-0.97, 3.30)	0.018	0.280
ILGR	-9.60 ±7.79	(-25.18, 5.97)	0.020	0.220
VDWR	-31.60 ±11.11	(-53.80, -9.42)	0.110	0.006*
AFI	1.70 ±7.80	(-13.91, 17.43)	<0.001	0.820

N = 66; M – mean; SD – standard deviation; CI – confidence interval; \* p ≤ 0.05; simple linear regression analysis.

Table 4. Multiple regression analysis of the smile variables affecting ES

Treatment group	Crude beta coefficient (M ±SD)	95% CI	p-value	R <sup>2</sup> adjusted
Age [years]	-0.53 ±0.19	(-0.93, -0.14)	0.008*	0.181
VDWR	-25.66 ±10.82	(-47.28, -4.03)	0.021*	

N = 66; \* p ≤ 0.05; multiple linear regression analysis.

## Discussion

This study was conducted to evaluate the effects of functional appliances and upper first premolar extraction therapy on smile esthetics. Various studies have been conducted to evaluate and compare the smile esthetics achieved with different treatment modalities.<sup>20,21–25</sup> In this study, we calculated the ratios to minimize the magnification errors and the measurement bias. However, since a ratio is affected by both its numerator and its denominator, it would be interesting to shed light on the factors that lead to changes in those ratios, and ultimately in smile esthetics. To our knowledge, this is the first study to evaluate the effects of removable functional appliances (CTB) and upper first premolar extraction on smile esthetics. According to our results, we rejected the null hypothesis in favor of the FA group, as the ES values given by the different panels of raters were higher for the FA group.

A review of the literature shows that numerous studies have found no differences between extraction and non-extraction treatment in terms of the eventual esthetic outcome.<sup>20,24</sup> In our study, we found statistically significant differences in BCR, VDWR and AFI between patients who underwent FA and UPE treatment. The extractions of teeth cause a reduction in the inter-molar width, leading to the constriction of the dental arches at the posterior dental segments. This reflects the mesial movement

of the posterior teeth into narrower parts of the arch.<sup>25</sup> Similarly, we found that the extraction of the upper first premolars produced the constriction of the upper arch. A reduction in the inter-molar width in the UPE group resulted in a greater AFI value, implying that UPE resulted in a narrower upper arch. This is in concordance with the findings of Cheng and Wang.<sup>23</sup> However, Johnson and Smith argued against the constriction of the dental arch after premolar extractions and pointed out deficiencies in the interpretation of these measurements.<sup>19</sup> We routinely perform maxillary expansion in conjunction with functional appliance treatment to facilitate class II correction, and this had an impact on the inter-molar width in this treatment group, leading to better and wider smiles.

Maxillary incisor display and the smile arc are among the most crucial aspects of smile esthetics. Improving MID and the smile arc either by increasing or decreasing incisal display can enhance smile esthetics. The MID value highlights the amount of incisal and gingival display while smiling. A higher MID ratio would suggest an increased incisal and gingival display during a smile. We found the UPE group to have a greater MID ratio owing to the retraction of the upper teeth, which is in agreement with a recent study by Cheng and Wang.<sup>23</sup> Similarly, Cheng and Wang also reported that their FA (non-extraction) group relied upon the expansion of the upper arch to gain space. This in turn resulted in a reduced incisal display and flattened smile arcs.<sup>23</sup> We also measured SAR, which is the depth of the arcs of curvature for the lower lip and the upper incisor teeth; a ratio of 1.0 would suggest a consonant and esthetic smile.<sup>26</sup> However, in both our treatment groups, SAR was below 1.0, which concurs with a study conducted by Prasad et al.<sup>27</sup> Despite all these differences between the 2 treatment groups, both MID and SAR were found to be statistically insignificant in our study. This can be attributed to the precise finishing and detailing received by both treatment groups via fixed labial brackets.

In contrast to MID, MTE during a smile is considered to be a sign of aging.<sup>28</sup> We found increased MTE and lower lip exposure in the FA group, but this difference was statistically insignificant. Functional appliance treatment might have improved the elasticity of the lower lip musculature, leading to a greater exposure of the lower incisors during a smile, hence the greater ratio. However, MTE had a negative association with ES, which concurs with a study conducted by Cheng and Wang.<sup>23</sup> Conversely, a study conducted by Prasad et al. found no association between MTE and ES.<sup>27</sup>

To visualize and quantify the frontal smile, Ackerman and Ackerman developed a ratio called the smile index: the inter-commissure width / the interlabial gap.<sup>5</sup> A high SI value indicates a large outer commissural width and/or a small interlabial gap; in other words, a limited smile area.<sup>29</sup> Since the interlabial gap is the denominator in the equation, a reduction of this denominator increases the ratio.

We found a reduction in the interlabial gap in the UPE group due to the retraction of the upper and lower lips. The smile index showed a positive association with ES, but it was statistically insignificant, implying that a limited smile area can also be considered acceptable. Our result is in agreement with Ahrari et al., who found that SI had no significant impact on ES.<sup>30</sup>

For a normal vertical growth pattern, Bhavsar et al. reported a mean ILGR of  $0.46 \pm 0.09$  in a pre-treatment group.<sup>31</sup> We found considerably reduced ILGRs in both our post-treatment groups as compared to their pre-treatment status, but no statistically significant differences were found between the 2 treatment modalities in terms of ILGR. A rationale for this could be that reduced interlabial gap, due to the retraction of the lips, and inter-canine width in the UPE group might have balanced ILGR, leading to similar median scores as in the FA group.

In both genders, minimal buccal corridors are considered attractive.<sup>24</sup> Narrower dental arches can cause wider buccal corridor spaces, which can be unesthetic. In our sample, we found that the UPE patients had wider buccal corridor spaces due to a reduced maxillary inter-canine width. A reduced maxillary inter-canine width led to an increased BCR in the UPE group. Gianelly found a slightly increased inter-canine width in non-extraction treatment as compared to the extraction of all premolars, which is in agreement with our results.<sup>32</sup> On the other hand, Yang et al. reported that neither extraction nor non-extraction treatment had any effect on the buccal corridor width.<sup>33</sup> It has been observed that after the 2<sup>nd</sup> decade of life, a reduction in the facial muscular tonicity and functionality can decrease the inter-commissure width of the lips during a smile; therefore, the corners of the lips are not stretched apart to the same extent as in the younger age group during a social smile.<sup>21</sup> Considering these age-related changes, wider buccal corridor spaces apparent in the UPE group at an early age might not be unesthetic in later years. Due to the constriction of the arch, the UPE group also suffered from less visible dentition during a smile, leading to a higher VDWR, implying fewer teeth visible during a smile. Contrary to our findings, Ghaffar and Fida found no significant difference in the visible dentition width while evaluating the impact of the extraction of all first premolars on smile esthetics.<sup>34</sup> In our study, variables such as SAR, MID, MTE, SI, and ILGR were not significantly different between the treatment groups; this is compatible with the results of other studies.<sup>23,33</sup>

The subjective assessments of smile esthetics made by 3 different panels of raters revealed that orthodontic residents, general dentists and laypersons all preferred the esthetic outcome of the FA group over the UPE group. However, a study conducted by Peck et al. reported that dental professionals' opinions might differ from laypersons' while evaluating the esthetics of frontal close-up smiles.<sup>35</sup> In contrast, we found no significant differences between the ES values given by laypersons and dental

professionals, and our results are in concordance with a study conducted by Ghaffar and Fida.<sup>34</sup> Although the general dentist group perceived the best esthetic outcomes with FA treatment, their overall ES values were much lower than those of the other raters. This could be due to the presence of white spot lesions or gingival inflammation induced by orthodontic treatment. In comparison, we believe that orthodontic residents scored the finished smile esthetics on the basis of alignment, the inclination of the teeth, coincident dental midlines, and the overall symmetry of the smile. White spot lesions and gingival conditions seemed to have little effect on their ES.

Among the variables we measured, age, BCR and VDWR were found to be statistically significant when compared to the mean ES values using simple linear regression. Age was negatively correlated with the mean ES values; this shows a strong association with better esthetic outcomes of the FA group, in which the patients started treatment at an earlier age. We found that BCR and VDWR were negatively associated with the mean ES values as well. In a computer-based survey, Roden-Johnson et al. reported that the buccal corridors had no influence on the ES values given by orthodontists, dentists and laypersons.<sup>36</sup> The multiple regression analysis revealed that both age and VDWR were significant factors affecting the ES values given by the raters. However, our multiple regression model can only explain 18% of the variability in the ES values. We recommend the evaluation of other factors of mini-esthetics and micro-esthetics to better explain the rest of the variability in the ES values.

## Conclusions

Our study compared the esthetic outcomes between functional appliance treatment and premolar extractions in skeletal class II malocclusion. The FA group had narrower buccal corridor spaces, a greater visible dentition width and a wider arch form while smiling. These variables are considered imperative in finishing orthodontic treatment, and providing patients with an attractive and youthful smile. The UPE group showed an increase in the buccal corridor width, a decreased visible dentition width and a narrower arch form during a smile. In the subjective assessments of smile esthetics, each panel preferred the FA group.

## Limitations

A smile is best judged in relation to the whole face, as perceived in the natural world. Moreover, a smile is a dynamic process, which means that capturing the ideal smile in each patient is difficult. While making measurements on the photographs, the lip thickness had some influence on a smile – younger participants had fuller and thicker lips on average, and that had an impact on the measurement of such variables as the inter-commissure width and the interlabial gap.

## ORCID iDs

Umair Shoukat Ali  <https://orcid.org/0000-0001-9252-8934>  
 Rashna Hoshang Sukhia  <https://orcid.org/0000-0001-9210-6432>  
 Mubassar Fida  <https://orcid.org/0000-0003-4842-9896>

## References

- Davis LG, Ashworth PD, Spriggs LS. Psychological effects of aesthetic dental treatment. *J Dent*. 1998;26(7):547–554.
- Işiksal E, Hazar S, Akyalçın S. Smile esthetics: Perception and comparison of treated and untreated smiles. *Am J Orthod Dentofacial Orthop*. 2006;129(1):8–16.
- Kiyak HA. Does orthodontic treatment affect patients' quality of life? *J Dent Educ*. 2008;72(8):886–894.
- Goldstein RE. Study of need for esthetics in dentistry. *J Prosthet Dent*. 1969;21(6):589–598.
- Ackerman MB, Ackerman JL. Smile analysis and design in the digital era. *J Clin Orthod*. 2002;36(4):221–236.
- Chew MT. Spectrum and management of dentofacial deformities in a multiethnic Asian population. *Angle Orthod*. 2006;76(5):806–809.
- Helm S. Malocclusion in Danish children with adolescent dentition: An epidemiologic study. *Am J Orthod*. 1968;54(5):352–366.
- Proffit WR, Fields HW Jr, Moray LJ. Prevalence of malocclusion and orthodontic treatment need in the United States: Estimates from the NHANES III survey. *Int J Adult Orthodon Orthognath Surg*. 1998;13(2):97–106.
- Rothstein T, Yoon-Tarlie C. Dental and facial skeletal characteristics and growth of males and females with class II, division 1 malocclusion between the ages of 10 and 14 (revisited) – part I: Characteristics of size, form, and position. *Am J Orthod Dentofacial Orthop*. 2000;117(3):320–332.
- Baccetti T, Franchi L, McNamara JA Jr, Tollaro I. Early dentofacial features of Class II malocclusion: A longitudinal study from the deciduous through the mixed dentition. *Am J Orthod Dentofacial Orthop*. 1997;111(5):502–509.
- Baccetti T, Franchi L, McNamara JA Jr. An improved version of the cervical vertebral maturation (CVM) method for the assessment of mandibular growth. *Angle Orthod*. 2002;72(4):316–323.
- Cozza P, Baccetti T, Franchi L, De Toffol L, McNamara JA Jr. Mandibular changes produced by functional appliances in Class II malocclusion: A systematic review. *Am J Orthod Dentofacial Orthop*. 2006;129(5):599.e1–e12;discussion e1–e6.
- Clark WJ. The twin block technique: A functional orthopedic appliance system. *Am J Orthod Dentofacial Orthop*. 1988;93(1):1–18.
- Tucker MR. Orthognathic surgery versus orthodontic camouflage in the treatment of mandibular deficiency. *J Oral Maxillofac Surg*. 1995;53(5):572–578.
- Proffit WR, Phillips C, Douvartzidis N. A comparison of outcomes of orthodontic and surgical-orthodontic treatment of Class II malocclusion in adults. *Am J Orthod Dentofacial Orthop*. 1992;101(6):556–565.
- Stirling J, Latchford G, Morris DO, Kindelan J, Spencer RJ, Bekker HL. Elective orthognathic treatment decision making: A survey of patient reasons and experiences. *J Orthod*. 2007;34(2):113–127; discussion 111.
- Guo Y, Han X, Xu H, Ai D, Zeng H, Bai D. Morphological characteristics influencing the orthodontic extraction strategies for Angle's class II division 1 malocclusions. *Prog Orthod*. 2014;15(1):44.
- Nangia A, Darendeliler M. Finishing occlusion in Class II or Class III molar relation: Therapeutic Class II and III. *Aust Orthod J*. 2001;17(2):89–94.
- Johnson DK, Smith RJ. Smile esthetics after orthodontic treatment with and without extraction of four first premolars. *Am J Orthod Dentofacial Orthop*. 1995;108(2):162–167.
- Bishara SE, Cummins DM, Jakobsen JR, Zaher AR. Dentofacial and soft tissue changes in Class II, division 1 cases treated with and without extractions. *Am J Orthod Dentofacial Orthop*. 1995;107(1):28–37.
- Desai S, Upadhyay M, Nanda R. Dynamic smile analysis: Changes with age. *Am J Orthod Dentofacial Orthop*. 2009;136(3):310.e1–e10; discussion 310–311.
- Chetan P, Tandon P, Singh GK, Nagar A, Prasad V, Chugh VK. Dynamics of a smile in different age groups. *Angle Orthod*. 2012;83(1):90–96.
- Cheng HC, Wang YC. Effect of nonextraction and extraction orthodontic treatments on smile esthetics for different malocclusions. *Am J Orthod Dentofacial Orthop*. 2018;153(1):81–86.
- Moore T, Southard KA, Casco JS, Qian F, Southard TE. Buccal corridors and smile esthetics. *Am J Orthod Dentofacial Orthop*. 2005;127(2):208–213.
- Kim E, Gianelly AA. Extraction vs nonextraction: Arch widths and smile esthetics. *Angle Orthod*. 2003;73(4):354–358.
- Hulsey CM. An esthetic evaluation of lip–teeth relationships present in the smile. *Am J Orthod*. 1970;57(2):132–144.
- Prasad V, Tandon P, Singh GK, Nagar A, Maurya RP. Comparison of smile esthetics after extraction and non-extraction orthodontic treatment. *IJODR*. 2018;4(4):182–189.
- Van Der Geld P, Oosterveld P, Kuijpers-Jagtman AM. Age-related changes of the dental aesthetic zone at rest and during spontaneous smiling and speech. *Eur J Orthod*. 2008;30(4):366–373.
- Sarver DM, Ackerman MB. Dynamic smile visualization and quantification: Part 2. Smile analysis and treatment strategies. *Am J Orthod Dentofacial Orthop*. 2003;124(2):116–127.
- Ahrari F, Heravi F, Rashed R, Zarrabi MJ, Setayesh Y. Which factors affect dental esthetics and smile attractiveness in orthodontically treated patients? *J Dent (Tehran)*. 2015;12(7):491–503.
- Bhavsar A, Nehete AL, Gulve ND, Shah KA, Aher S. Factors affecting smile esthetics in adults with different types of growth patterns. *IOSR-JDMS*. 2018;17(8):44–50.
- Gianelly AA. Arch width after extraction and nonextraction treatment. *Am J Orthod Dentofacial Orthop*. 2003;123(1):25–28.
- Yang IH, Nahm DS, Baek SH. Which hard and soft tissue factors relate with the amount of buccal corridor space during smiling? *Angle Orthod*. 2008;78(1):5–11.
- Ghaffar F, Fida M. Effect of extraction of first four premolars on smile aesthetics. *Eur J Orthod*. 2011;33(6):679–683.
- Peck S, Peck L, Kataja M. The gingival smile line. *Angle Orthod*. 1992;62(2):91–100;discussion 101–102.
- Roden-Johnson D, Gallerano R, English J. The effects of buccal corridor spaces and arch form on smile esthetics. *Am J Orthod Dentofacial Orthop*. 2005;127(3):343–350.





# Strengthening effect of bioceramic cement when used to repair simulated internal resorption cavities in endodontically treated teeth

## Wytrzymałość zębów leczonych endodontycznie po wypełnieniu symulowanych ubytków resorpcji wewnętrznej cementem bioceramicznym

Wafaa Abdelbaky Khalil<sup>1,A–F</sup>, Faisal Alghamdi<sup>2,A–F</sup>, Esraa Aljahdali<sup>3,B,C,F</sup>

<sup>1</sup> Department of Endodontics, Faculty of Dentistry, King Abdulaziz University, Jeddah, Saudi Arabia

<sup>2</sup> Department of Oral Biology, Faculty of Dentistry, King Abdulaziz University, Jeddah, Saudi Arabia

<sup>3</sup> Intern, Faculty of Dentistry, King Abdulaziz University, Jeddah, Saudi Arabia

A – research concept and design; B – collection and/or assembly of data; C – data analysis and interpretation; D – writing the article; E – critical revision of the article; F – final approval of the article

Dental and Medical Problems, ISSN 1644-387X (print), ISSN 2300-9020 (online)

Dent Med Probl. 2020;57(2):165–169

### Address for correspondence

Wafaa Abdelbaky Khalil  
Email: dr.wafa\_endo@hotmail.com

### Funding sources

None declared

### Conflict of interest

None declared

Received on November 11, 2019

Reviewed on December 20, 2019

Accepted on January 20, 2020

Published online on June 19, 2020

### Cite as

Khalil WA, Alghamdi F, Aljahdali E. Strengthening effect of bioceramic cement when used to repair simulated internal resorption cavities in endodontically treated teeth. *Dent Med Probl.* 2020;57(2):165–169. doi:10.17219/dmp/116743

### DOI

10.17219/dmp/116743

### Copyright

© 2020 by Wrocław Medical University

This is an article distributed under the terms of the

Creative Commons Attribution 3.0 Unported License (CC BY 3.0)

(<https://creativecommons.org/licenses/by/3.0/>).

## Abstract

**Background.** The reinforcement of teeth with internal root resorption is essential to prevent their fracture.

**Objectives.** The aim of this study was to assess the fracture resistance of the premolar teeth with internal root resorption cavities (IRCs), repaired with glass-ionomer cement (GIC), gutta-percha (GP) or EndoSequence<sup>®</sup> Root Repair Material<sup>™</sup> (RRM).

**Material and methods.** Forty lower premolars, instrumented to size 50, were used. Ten teeth were assigned to the control group, which received the full obturation of the root canals. In the remaining 30, IRCs were prepared with Gates–Glidden burs. The apical 8 mm was obturated to the level of IRC using the single-cone technique. Then, the teeth were divided into 3 groups according to the material used for repairing the cavities ( $n = 10$ ): GIC; GP; and RRM. The canals were filled with respective materials and backfilled with GP. All of the specimens were scanned at the level of IRC with a micro-computed tomography (micro-CT) system, and the volume of the IRCs and the percentages of voids in the filling materials were measured. The specimens were subjected to fracture testing. The force recorded at the time of fracture was analyzed with the Kruskal–Wallis test and the independent  $t$ -test.

**Results.** The control group showed a significantly higher mean value of fracture resistance as compared to the groups with IRCs ( $p < 0.05$ ). No significant difference was found between GIC and RRM, whereas the GP group had a significantly lower fracture resistance than other tested IRC groups ( $p < 0.05$ ). The percentage of voids was significantly higher in the GIC group as compared to the GP and RRM groups ( $p < 0.05$ ).

**Conclusions.** EndoSequence Root Repair Material provides more strength to the teeth than the GP/sealer technique when both are used to fill a resorption cavity. The fracture resistance of the teeth filled with RRM was close to that obtained with GIC.

**Key words:** glass-ionomer cement, EndoSequence Root Repair Material, root resorption, gutta-percha, tooth fracture

**Słowa kluczowe:** cement szkło-jonomerowy, materiał do naprawy korzenia zęba EndoSequence, resorpcja korzenia zęba, gutaperka, złamanie zęba

## Introduction

Internal root resorption is a progressive loss of the intraradicular dentin, without any repair and with the hard structure becoming replaced with granulation tissue. This resorption is associated with chronic inflammatory conditions and might be associated with bacteria.<sup>1-3</sup>

Internal root resorption is asymptomatic and can be discovered by a routine X-ray examination. It may appear as an oval circumscribed radiolucent area with ill-defined borders and asymmetrical variations in radiolucency. This can potentially extend to root perforation.<sup>4</sup> Extensive internal root resorption, combined with root perforation, could complicate the prognosis of endodontic treatment, as it causes the weakening of the remaining tooth structures.<sup>5</sup>

The management of internal root resorption presents a unique difficulty in preparation and obturation. The resorbed defect inside the root canal is inaccessible to direct mechanical instrumentation. Therefore, the primary goal of root canal treatment is to disinfect the root canal system and fill it with appropriate materials to prevent reinfection. The filling material should be dimensionally stable and biologically compatible<sup>6</sup>; it should also strengthen the treated teeth.<sup>7</sup>

The obturation materials used after internal root resorption should flow into the resorption space and fill it totally. Thermoplasticized gutta-percha (GP) is the most commonly used filling material in the treatment of internal root resorption. The Obtura<sup>®</sup> II system (Obtura Spartan, Fenton, USA) obturates resorptive defects better than cold lateral compaction or other techniques.<sup>8</sup>

Glass-ionomer cement (GIC) is used to fill root resorptive defects and root perforations due to its biocompatibility and antibacterial effects. It provides a satisfactory clinical performance when used as a root canal sealer or as an orthograde filling material because of its good adhesion and strength, which increases the resistance of the teeth to vertical fractures.<sup>9</sup>

In cases involving extensive perforation, there is a need for a reparative biocompatible material that seals perforations and does not irritate the adjacent tissues. For a long time, mineral trioxide aggregate (MTA) has been the material of choice for repairing perforations. The advantages of using MTA include its superior sealing properties and biocompatibility.<sup>10</sup> Other calcium silicate materials are effective in sealing resorptive defects and providing strength to the tooth structures.<sup>10</sup>

The latest calcium silicate cements, such as Endo-Sequence<sup>®</sup> Root Repair Material<sup>™</sup> (RRM) (Brasseler USA, Savannah, USA), have been introduced into the endodontic field. Root Repair Material has a pre-mixed, ready-to-use putty or injectable form and is used as a root repair material as well as for endodontic indications, similar as in case of other calcium silicate materials.<sup>11</sup>

According to the manufacturer, the main composition of both RRM formulations comprises the same calcium silicate, zirconium oxide, tantalum pentoxide, calcium phosphate monobasic, and filler agents, differing only in particle size. The material is biocompatible and bioactive; it also has good sealing properties.<sup>12,13</sup> The Endo-Sequence<sup>®</sup> Bioceramic (BC) sealer increases the resistance to fractures in the premolar teeth to a greater degree than MTA.<sup>14</sup> Moreover, it has a greater push-out bond strength than Biodentine<sup>®</sup> and NeoMTA<sup>®</sup> when used as a perforation repair material after the exposure of the teeth to sodium hypochlorite at the early setting stage.<sup>11,15,16</sup>

In the literature, no study has evaluated the fracture resistance of the premolars after filling the internally resorbed root canals with RRM. The aim of this study was to assess the fracture resistance of the premolar teeth with internal root resorption cavities (IRCs), repaired with GIC, GP or RRM.

## Material and methods

### Sample selection

Forty lower premolar teeth with single and wide root canals, confirmed to be radiographically free from open apices, caries, cracks, or fractures, were included for this study. The mesiodistal and buccolingual diameters of these teeth were measured at the cemento-enamel junction with a digital caliper, and the teeth included in the study had a width range of  $\pm 3$  mm. The teeth were cleaned and stored in a 10% formalin solution at room temperature.

### Preparation of the root canals

The access cavities were prepared using diamond burs, and then the Endo-Z<sup>®</sup> bur (Dentsply Maillefer, Ballaigues, Switzerland). The working length was established using a K-file 1 mm short of the apex. The preparation of the root canal was completed with the Pro Taper Next<sup>®</sup> file size X5 (Dentsply Maillefer), combined with intermittent irrigation with 2.5% sodium hypochlorite.

### Preparation of simulated internal root resorption cavities

Internal root resorption cavities were prepared not in the middle of the root, but a bit more coronal, at the level of 8 mm short of the apex using No. 1 and No. 2 Gates-Glidden drills (MANI, Inc., Takanezawa, Japan) with lateral pressure from the mesiodistal and buccolingual directions. The cavities were verified with mesiodistal and buccolingual radiographs.<sup>6</sup> The IRCs were prepared from 30 samples, and the other 10 samples were left intact and considered as a control group.

## Obturation of the root canals

The apical 8 mm of the samples with IRCs was obturated with the Pro Taper Next master cone, matched with gutta-percha points size X5 (Dentsply Maillefer) and the AH Plus® sealer (Dentsply DeTrey, Konstanz, Germany). At the same time, the control group received a full root canal obturation.

## Sample grouping

The samples were randomly distributed among 3 groups (10 teeth each) according to the filling materials used for repairing the IRCs:

- the GIC group received glass-ionomer cement (Fuji IX GP®, GC America Inc., Alsip, USA). The conditioner was applied to the cavity for 10 s; next, GIC was injected using a GIC applicator directly to the cavity, and then condensed with a No. 2 hand plugger (Dentsply Maillefer). After setting, the coronal part was added until the complete sealing of the access cavity;
- the GP group received thermoplasticized gutta-percha using the Obtura II gun (Obtura Spartan) and the AH Plus sealer. It was condensed vertically with a No. 2 hand plugger (Dentsply Maillefer);
- the RRM group received EndoSequence Root Repair Material, delivered by means of a Messing gun (Integra Life-Sciences Corp., Plainsboro, USA), and then compacted vertically with a No. 2 hand plugger (Dentsply Maillefer).

The samples were stored in an incubator at 37°C with 100% humidity for 24 h. Then, the root canals were backfilled with GP, and the coronal access cavities in all samples were sealed with a glass ionomer and stored for 1 week until the fracture resistance test.

## Micro-computed tomography analysis

The samples were scanned at the level of IRC with the micro-computed tomography (micro-CT) SkyScan® 1173 scanner system (Bruker Micro-CT, Kontich, Belgium). The system was operated at 90 kV with 88 mA and at a resolution of 7.4 µm using a 1-millimeter aluminum filter. Projection images were recorded in steps of 0.4°, from 0° to 360°. The collected raw data was reconstructed from the acquired images using the CTAn® software, v. 1.17.2 (Bruker Micro-CT). The CTVol® software, v. 2.2.3 (Bruker Micro-CT) was used to measure the volume of the IRCs in cubic millimeters and the volume of micro-voids in the IRC filling materials.

## Fracture resistance testing

The roots of the samples were covered with a thin layer of polyether impression material, 2 mm below the cervical line, simulating the periodontal membrane.<sup>17</sup> Then, the teeth were mounted vertically in self-cured acrylic resin

blocks, exposing 8 mm of the coronal length. The teeth embedded in the acrylic blocks were placed in a universal testing machine (LR 300K; Lloyd Instruments Ltd., Bognor Regis, UK) and a compressive load was applied at a speed of 1 mm/min with the spherical tips at the center of the cusps (Fig. 1). The force needed to fracture each sample was recorded in newtons.<sup>10</sup> The IBM SPSS Statistics for Windows software, v. 22 (IBM Corp., Armonk, USA) was used to analyze the data. The data was statistically analyzed using the Kruskal–Wallis test and the independent *t*-test with a *p*-value of 0.05 considered as statistically significant.

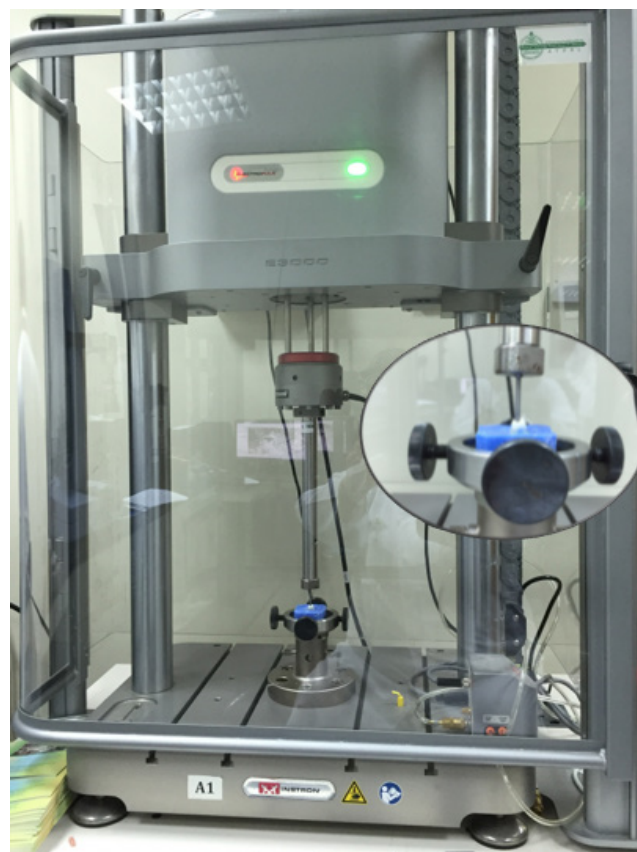


Fig. 1. Specimens placed in a universal testing machine

## Results

The mean (*M*) and standard deviation (*SD*) values of the IRC volume, the percentages of voids and the results of the fracture resistance test are shown in Table 1. There were no significant differences between the 3 tested groups regarding the IRC volume ( $p = 0.224$ ), whereas the percentage of voids was significantly higher in the GIC group as compared to the GP and RRM groups ( $p = 0.032$ ) (Fig. 2). The control group showed the highest mean value of fracture resistance as compared to the groups with IRCs ( $p = 0.027$ ). No significant difference was found between GIC and RRM ( $p = 0.104$ ), whereas the GP group had the fracture resistance value significantly lower than other tested groups ( $p = 0.048$ ).

**Table 1.** Fracture resistance values for the control and experimental groups

Group	n (N = 40)	IRC volume [MPa] M ±SD	Filling voids [%]	Force at fracture [N] M ±SD	max [N]	min [N]
Control	10	–	–	773.34 ±133.86 <sup>a</sup>	998.00	510.88
GIC	10	20.34 ±4.46 <sup>a</sup>	8.0 <sup>a</sup>	516.18 ±84.17 <sup>b</sup>	631.08	401.90
GP	10	21.69 ±5.77 <sup>a</sup>	2.1 <sup>b</sup>	494.30 ±102.88 <sup>c</sup>	635.44	370.33
RRM	10	23.49 ±3.92 <sup>a</sup>	1.7 <sup>b</sup>	514.05 ±87.77 <sup>b</sup>	599.65	388.23

Group GIC – glass-ionomer cement; group GP – gutta-percha; group RRM – EndoSequence Root Repair Material; IRC – internal root resorption cavity; M – mean; SD – standard deviation; different superscript letters indicate statistically significant differences ( $p < 0.05$ ).

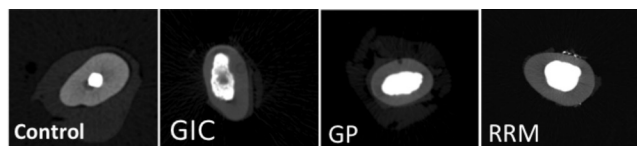


**Fig. 2.** Cross-sectional view of the representative three-dimensional (3D) reconstruction in the middle of the IRCs filled with respective materials – GIC, GP and RRM. It shows the adaptation of GP and RRM, whereas voids appear within GIC and at the material–dentin interface

## Discussion

Internal root resorption weakens the tooth structures and increases the chance for fractures,<sup>1</sup> which requires selecting a filling material that can strengthen the weakened tooth.<sup>18</sup> The effect of internal root resorption was proven in the current study, in which teeth with root canal fillings without IRCs proved to be more resistant to fractures.

In the present study, IRCs were performed through an access cavity, without either decoronation or root perforation, and this simulates the clinical situation.<sup>6</sup> By contrast, other studies used root perforation and decoronated the samples, which does not occur in the actual clinical situations and may affect the obtained results.<sup>10,18</sup> The research design based on the standardized smooth defects, combined with tooth decoronation, did not replicate the irregular ill-defined IRCs.<sup>10</sup>

In the current study, the total volume of the IRCs was measured using micro-CT.<sup>19</sup> Then, the IRCs were subjected to statistical analysis, which did not reveal significant differences between the groups; that means there was a degree of standardization.

Glass-ionomer cement has a higher compressive strength as compared to RRM.<sup>13,20</sup> Nevertheless, GIC did not reinforce the teeth, because GIC has a long setting reaction time, which can continue for more than 1 year.<sup>9</sup> Such a length of time affects its mechanical properties. Moreover, GIC is sensitive to hydration, unlike RRM, and this could induce more voids as compared to RRM. Both the GIC- and RRM-filled teeth had a significantly higher resistance to fracture than the GP-filled teeth. This could be related to the chemical bonding between the GIC or RRM and the dentin.<sup>21,22</sup> The warm GP technique has been reported as filling resorptive defects better than

other GP techniques.<sup>8</sup> Yet, it still has the lowest value of fracture resistance. These results are in agreement with other studies, which concluded that the GP/sealer combination provided less strength to the tooth structures than calcium silicate cements.<sup>10</sup>

In the current study, the authors tried to simulate the actual clinical situation of using natural teeth, and preparing IRCs without splitting the samples and without any decoronation. However, using these natural premolar teeth, stored at the Department of Surgery, may represent a limitation, as we were unaware of the age and lifestyle of the patients. Furthermore, testing teeth in vitro may differ from testing them in vivo.

## Conclusions

Within these limitations, it can be concluded that the filling of internal root resorption with RRM provided more strength to the tooth structures than the GP/sealer technique. The RRM-filled teeth had the value of fracture resistance close to that obtained with GIC, taking into consideration the biological effect and biocompatibility of RRM for clinical use.

### ORCID iDs

Wafaa Abdelbaky Khalil <https://orcid.org/0000-0002-2924-141X>

Faisal Alghamdi <https://orcid.org/0000-0003-2086-0772>

Esraa Aljahdali <https://orcid.org/0000-0002-2530-3054>

### References

- Patel S, Ford TP. Is the resorption external or internal? *Dent Update*. 2007;34(4):218–220.
- Wedenberg C, Lindskog S. Experimental internal resorption in monkey teeth. *Endod Dent Traumatol*. 1985;1(6):221–227.
- Patel S, Ricucci D, Durak C, Tay F. Internal root resorption: A review. *J Endod*. 2010;36(7):1107–1121.
- Gabor C, Tam E, Shen Y, Haapasalo M. Prevalence of internal inflammatory root resorption. *J Endod*. 2012;38(1):24–27.
- Silveira FF, Nunes E, Soares JA, Ferreira CL, Rotstein I. Double 'pink tooth' associated with extensive internal root resorption after orthodontic treatment: A case report. *Dent Traumatol*. 2009;25(3):e43–e47.
- Patel MH, Yagnik KN, Patel NK, Bhavsar BA. Obturating the pink tooth: An in vitro comparative evaluation of different materials. *Endodontology*. 2018;30(2):119–124.
- Teixeira FB, Teixeira ECN, Thompson JY, Trope M. Fracture resistance of roots endodontically treated with a new resin filling material. *J Am Dent Assoc*. 2004;135(5):646–652.

8. Gencoglu N, Yildirim T, Garip Y, Karagenc B, Yilmaz H. Effectiveness of different gutta-percha techniques when filling experimental internal resorptive cavities. *Int Endod J*. 2008;41(10):836–842.
9. De Bruyne MA, De Moor RJ. The use of glass ionomer cements in both conventional and surgical endodontics. *Int Endod J*. 2004;37(2):91–104.
10. Aktemur Türker S, Uzunoğlu E, Deniz Sungur D, Tek V. Fracture resistance of teeth with simulated perforating internal resorption cavities repaired with different calcium silicate-based cements and backfilling materials. *J Endod*. 2018;44(5):860–863.
11. Sultana N, Singh M, Nawal RR, et al. Evaluation of biocompatibility and osteogenic potential of tricalcium silicate-based cements using human bone marrow-derived mesenchymal stem cells. *J Endod*. 2018;44(3):446–451.
12. Khalil WA, Abunasef SK. Can mineral trioxide aggregate and nanoparticulate EndoSequence Root Repair Material produce injurious effects to rat subcutaneous tissues? *J Endod*. 2015;41(7):1151–1156.
13. Chen S, Öhman C, Jefferies SR, Gray H, Xia W, Engqvist H. Compressive fatigue limit of four types of dental restorative materials. *J Mech Behav Biomed Mater*. 2016;61:283–289.
14. Topçuoğlu HS, Tuncay Ö, Karataş E, Arslan H, Yeter K. In vitro fracture resistance of roots obturated with epoxy resin-based, mineral trioxide aggregate-based, and bioceramic root canal sealers. *J Endod*. 2013;39(12):1630–1633.
15. Alsubait SA. Effect of sodium hypochlorite on push-out bond strength of four calcium silicate-based endodontic materials when used for repairing perforations on human dentin: An in vitro evaluation. *J Contemp Dent Pract*. 2017;18(4):289–294.
16. Chen I, Karabucak B, Wang C, et al. Healing after root-end microsurgery by using mineral trioxide aggregate and a new calcium silicate-based bioceramic material as root-end filling materials in dogs. *J Endod*. 2015;41(3):389–399.
17. Soares CJ, Gava Pizi EC, Fonseca RB, Marcondes Martins LR. Influence of root embedment material and periodontal ligament simulation on fracture resistance tests. *Braz Oral Res*. 2005;19(1):11–16.
18. Ulusoy ÖI, Paltun YN. Fracture resistance of roots with simulated internal resorption defects and obturated using different hybrid techniques. *J Dent Sci*. 2017;12(2):121–125.
19. Keleş A, Alcin H, Kamalak A, Versiani MA. Micro-CT evaluation of root filling quality in oval-shaped canals. *Int Endod J*. 2014;47(12):1177–1184.
20. Guo YJ, Du TF, Li HB, et al. Physical properties and hydration behavior of a fast-setting bioceramic endodontic material. *BMC Oral Health*. 2016;16:23.
21. Han L, Okiji T. Bioactivity evaluation of three calcium silicate-based endodontic materials. *Int Endod J*. 2013;46(9):808–814.
22. Lalh MS, Titley K, Torneck CD, Friedman S. The shear bond strength of glass ionomer cement sealers to bovine dentine conditioned with common endodontic irrigants. *Int Endod J*. 1999;32(6):430–435.



# Association of ankylosing spondylitis with radiographically and clinically diagnosed apical periodontitis: A cross-sectional study

## Związek zeszywniającego zapalenia stawów kręgosłupa z zapaleniem tkanek okołowierzchołkowych rozpoznawanym radiologicznie i klinicznie – badanie przekrojowe

Ertuğrul Karataş<sup>1,A–D,F</sup>, Ayhan Kul<sup>2,A,B</sup>, Ebru Tepecik<sup>1,B</sup>

<sup>1</sup> Department of Endodontics, Faculty of Dentistry, Atatürk University, Erzurum, Turkey

<sup>2</sup> Department of Physical Medicine and Rehabilitation, Faculty of Medicine, Atatürk University, Erzurum, Turkey

A – research concept and design; B – collection and/or assembly of data; C – data analysis and interpretation; D – writing the article; E – critical revision of the article; F – final approval of the article

Dental and Medical Problems, ISSN 1644-387X (print), ISSN 2300-9020 (online)

*Dent Med Probl.* 2020;57(2):171–175

### Address for correspondence

Ertuğrul Karataş  
E-mail: dtertu@windowslive.com

### Funding sources

None declared

### Conflict of interest

None declared

Received on July 3, 2019

Reviewed on August 27, 2019

Accepted on November 21, 2019

Published online on February 27, 2020

### Cite as

Karataş E, Kul A, Tepecik E. Association of ankylosing spondylitis with radiographically and clinically diagnosed apical periodontitis: A cross-sectional study. *Dent Med Probl.* 2020;57(2):171–175. doi:10.17219/dmp/114463

### DOI

10.17219/dmp/114463

### Copyright

© 2020 by Wrocław Medical University

This is an article distributed under the terms of the

Creative Commons Attribution 3.0 Unported License (CC BY 3.0)

(<https://creativecommons.org/licenses/by/3.0/>).

## Abstract

**Background.** There are no studies evaluating the possible association between ankylosing spondylitis (AS) and apical periodontitis (AP).

**Objectives.** The aim of the present cross-sectional study was to investigate the possible association between AS and AP.

**Material and methods.** Fifty patients diagnosed with AS, receiving treatment at the Rheumatology Clinic in Erzurum, Turkey, were included in the experimental group. Another 50 age- and gender-matched individuals without any history of systemic disease were included in the study as the control group. All patients were examined radiographically and clinically to diagnose the presence of AP. The following data was recorded for all patients: the smoking habit, the number of teeth present, the number of teeth with AP, the number of root canal-treated (RCT) teeth, and the number of RCT teeth with AP.

**Results.** There were 1,283 teeth in the AS group and 1,305 in the control group. There was a significant association between teeth with AP and AS, as the prevalence of teeth with AP was significantly lower in the control group (1.3%) than in the AS group (2.9%) (*OR* (odds ratio) = 2.250; *p* = 0.005). There was no statistically significant difference between the groups in terms of the number of RCT teeth and RCT teeth with AP (*p* > 0.05).

**Conclusions.** Ankylosing spondylitis is significantly associated with an increased prevalence of AP. It can be concluded that patients with AS can be more prone to develop AP. However, AS does not reduce the success rate of endodontic treatment, because there was no significant difference between the AS and control groups in terms of RCT teeth with AP.

**Key words:** ankylosing spondylitis, apical periodontitis, endodontics

**Słowa kluczowe:** zeszywniające zapalenie stawów kręgosłupa, zapalenie tkanek okołowierzchołkowych, endodoncja



## Introduction

Ankylosing spondylitis (AS) is a chronic inflammatory autoimmune condition with a prevalence of 0.1–1.4% in the general population.<sup>1</sup> It generally affects patients under the age of 40 and has a higher incidence in males.<sup>2</sup> Ankylosing spondylitis is characterized by enthesitis, spondylitis and sacroilitis,<sup>3</sup> and the underlying mechanism triggering the inflammatory process is believed to be autoimmune or autoinflammatory in nature. Increased levels of interleukin 2 (IL-2), interleukin 6 (IL-6) and tumor necrosis factor alpha (TNF- $\alpha$ ) have been reported in patients with AS.<sup>4</sup> Additionally, significant elevation in the level of C-reactive protein (CRP) is present in AS patients.<sup>4</sup>

Apical periodontitis (AP) is the inflammation of the apical periodontium. This usually occurs following a bacterial invasion of the root canal system.<sup>5</sup> Similarly to AS, increased levels of cytokines and inflammatory mediators have been observed in the case of AP.<sup>6</sup> Additionally, Sirin et al. reported that the level of CRP increases with the severity of AP.<sup>7</sup> Many similarities in the pathogenesis of both AS and AP might suggest a relationship between them. However, there have been no studies evaluating the possible association between AS and AP. Previous studies have shown that there is a link between AS and periodontal disease.<sup>8,9</sup> It has been concluded that patients with AS have a significantly higher risk of periodontal diseases than those without AS.<sup>9</sup> Since AP and periodontitis share similar destructive inflammatory reactions and microbiota, it is possible that there is an association between AP and AS. Therefore, the present study aimed to investigate the possible association between AP and AS. The null hypothesis was that there would be no difference between the AS and control groups in terms of the prevalence of AP.

## Material and methods

Fifty patients diagnosed with AS, receiving treatment at the Rheumatology Clinic in Erzurum, Turkey, were included in the experimental group. None of the patients were suffering from any other systemic disease, and all the patients included in the experimental group were on anti-TNF- $\alpha$  therapy. Another 50 age- and gender-matched individuals without any history of systemic disease were included in the study as the control group. Ethical approval for the pair-matched cross-sectional study was obtained from the Ethics Committee of Atatürk University in Erzurum, Turkey (decision No. 9 as of November 1, 2018) and written informed consent was obtained from all the participants. The study was conducted between January 2, 2018 and January 12, 2018.

Patients with a complete medical and dental history, including panoramic radiographs of the maxilla and mandible, in the age range of 18–65 years, were included. Patients with fewer than 10 teeth present were excluded.

Two examiners who were blinded to the groups evaluated the panoramic radiographs in order to diagnose teeth with AP (Fig. 1,2). Both researchers studied the radiographs simultaneously. If both agreed on the diagnosis of AP, their findings were further confirmed clinically using the pulp vitality, percussion and palpation tests. The following information was recorded for all participants: the smoking habit, the number of teeth present, the number of teeth with AP, the number of root canal-treated (RCT) teeth, and the number of RCT teeth with AP. There were no differences between the researchers in terms of diagnosing AP radiographically.



Fig. 1. Panoramic radiograph of a patient included in the control group



Fig. 2. Panoramic radiograph of a patient included in the experimental group

Due to the cross-sectional nature of the study, patients who had undergone primary root canal treatment were included. Therefore, the cause of endodontic treatment and the time elapsed since the completion of the treatment could not be recorded.

The inflammatory size measurement was performed using the periapical index (PAI). Teeth with normal periapical structure or with small changes in bone structure were categorized as healthy (PAI 1 and PAI 2). Teeth with a widened periodontal ligament, periodontitis with a well-defined radiolucent area and/or severe periodontitis with exacerbating features were categorized as teeth with periapical pathology (PAI3, PAI4 and PAI5).<sup>10</sup> The periapical status of multi-rooted teeth was determined by the highest PAI score of all roots.<sup>11</sup>

The sample size was based on the data of the study's evaluated association between periapical rarefying osteitis and AP,<sup>12</sup> with an effect size of 0.1, an error of alpha equal to 0.05 and a power of 0.8. The IBM SPSS Statistics for Windows, v. 20 software (IBM Corp., Armonk, USA) was used for the statistical analyses at a significance level of 5% ( $p = 0.05$ ). The  $\chi^2$  test was used to determine the possible association between AS and AP. Student's  $t$ -test was used to compare the age variable between the groups.

## Results

A total of 100 participants with 2,588 teeth were examined. There were 1,283 teeth in the AS group and 1,305 in the control group. The number of teeth with AP in the AS group was 37 (2.9%), whereas in the control group it was 17 (1.3%). There was a significant association between teeth with AP and AS, as the prevalence of teeth with AP was

significantly lower in the control group (1.3%) than in the AS group (2.9%) ( $OR$  (odds ratio) = 2.250;  $p = 0.005$ ) (Table 1).

There were 34 (2.7%) and 38 (2.9%) RCT teeth in the AS and control groups, respectively. There was no statistically significant difference between the groups in terms of the number of RCT teeth ( $OR = 0.908$ ;  $p = 0.686$ ). In the AS group, the number of RCT teeth with AP was 13 (1.0%), whereas in the control group, the number of RCT teeth with AP was 7 (0.5%). The difference between the groups was not statistically significant ( $OR = 1.898$ ;  $p = 0.166$ ).

Table 1. Distribution of the analyzed variables in the patients with ankylosing spondylitis (AS) and in the control group

Variable	AS (50 patients, 1,283 teeth)	Control (50 patients, 1,305 teeth)	$p$ -value	$OR$
Age	37.98 ± 9.06	37.60 ± 9.70	0.840	–
Gender				
female	13	13	–	–
male	37	37		
Smoking habit				
present	22 (44.0)	22 (44.0)	1.000	1.000
absent	28 (56.0)	28 (56.0)		
Teeth with AP				
present	37 (2.9)	17 (1.3)	0.005*	2.250*
absent	1,246 (97.1)	1,288 (98.7)		
RCT teeth				
present	34 (2.7)	38 (2.9)	0.686	0.908
absent	1,249 (97.3)	1,267 (97.1)		
RCT teeth with AP				
present	13 (1.0)	7 (0.5)	0.166	1.898
absent	1,270 (99.0)	1,298 (99.5)		

Data presented as mean ± standard deviation ( $M \pm SD$ ), number ( $n$ ) or number (percentage) ( $n$  (%)).

$OR$  – odds ratio; AP – apical periodontitis; RCT – root canal-treated; \* statistically significant.

There was no significant difference between the groups regarding the smoking habit ( $p = 1.000$ ). The mean age of patients in the AS and control groups was  $37.98 \pm 9.06$  and  $37.60 \pm 9.70$  years, respectively ( $p = 0.840$ ).

## Discussion

Apical periodontitis is associated with increased levels of cytokines and inflammatory mediators, such as immunoglobulin A (IgA), immunoglobulin G (IgG), immunoglobulin M (IgM), interleukin 1 (IL-1), IL-2, IL-6, and CRP.<sup>6</sup> Interleukin 2 and IL-6 are normally secreted by T cells, and IL-2 plays an important role in immune regulation.<sup>13</sup> Interleukin 6 may act both as an anti-inflammatory cytokine by acting in muscles, and as a pro-inflammatory cytokine by signaling in macrophages or monocytes.<sup>14</sup> Elevated levels of TNF- $\alpha$  have also been observed in the process of AP development, which is related to the development of periapical granuloma and radicular cysts.<sup>15</sup> As mentioned previously, elevated levels of IL-2, IL-6, TNF- $\alpha$ , and CRP have also been reported in patients with AS.<sup>4</sup> It has been asserted that IL-2 can interfere with various signs and symptoms of AS,<sup>16</sup> and TNF- $\alpha$  and IL-6 could possibly reflect the parameters of disease activity in patients with AS.<sup>4</sup> All these similarities in the pathogenesis of AP and AS could explain the higher prevalence of AP in the patients with AS.

According to the results of the present study, there was no statistically significant difference between the groups in terms of RCT teeth with AP. It can be suggested that the presence of AS does not restrict the healing response of patients with regard to root canal treatment, and does not reduce the success rate of endodontic treatment. In the present study, patients on anti-TNF- $\alpha$  therapy were included in the experimental group. It has been reported that patients undergoing such therapy are associated with faster healing of AP as compared to the control group.<sup>17</sup> The increased level of TNF- $\alpha$  in the AS patients would have been reduced by anti-TNF- $\alpha$  therapy, and this might have resulted in unchanged healing outcomes, similar to those of the control group patients. However, we must take into account several immunologic factors that are related to the process of AS. Additionally, the mean time elapsed since the completion of root canal treatment was unknown. This is a limitation of the cross-sectional design. Moreover, due to the cross-sectional nature of the research, it is impossible to establish a true cause-and-effect relationship.

Previous studies have evaluated the association between AP and such systemic diseases as diabetes mellitus,<sup>11</sup> end-stage renal disease<sup>18</sup> and coronary artery disease.<sup>19</sup> These studies analyzed the number of patients with at least 1 AP lesion, but the total number of teeth with AP was not taken into account. However, in the present study, the total number of teeth with AP was considered. In this way, a larger sample size was analyzed in order to evaluate


the prevalence of AP in the patients with AS. Additionally, in the present study, the presence of AP was confirmed with a radiographic evaluation and a clinical examination.


## Conclusions

Within the limitations of the present study, AS is significantly associated with an increased prevalence of AP. It can be concluded that patients with AS may be more prone to developing AP. However, AS does not reduce the success rate of endodontic treatment, as there was no significant difference between the AS and control groups in terms of RCT teeth with AP. Further studies involving the prospective design are needed to confirm the relationship between AS and AP.

### ORCID iDs

Ertuğrul Karataş  <https://orcid.org/0000-0002-8145-8763>

Ayhan Kul  <https://orcid.org/0000-0003-1313-9469>

Ebru Tepecik  <https://orcid.org/0000-0002-2964-3726>

### References

- Braun J, Bollow M, Remlinger G, et al. Prevalence of spondylarthropathies in HLA-B27 positive and negative blood donors. *Arthritis Rheum.* 1998;41(1):58–67.
- Reveille JD, Weisman MH. The epidemiology of back pain, axial spondyloarthritis and HLA-B27 in the United States. *Am J Med Sci.* 2013;345(6):431–436.
- Braun J, Sieper J. Ankylosing spondylitis. *Lancet.* 2007;369(9570):1379–1390.
- Bal A, Unlu E, Bahar G, Aydog E, Eksioğlu E, Yorgancıoğlu R. Comparison of serum IL-1 beta, sIL-2R, IL-6, and TNF-alpha levels with disease activity parameters in ankylosing spondylitis. *Clin Rheumatol.* 2007;26(2):211–215.
- Márton IJ, Kiss C. Overlapping protective and destructive regulatory pathways in apical periodontitis. *J Endod.* 2014;40(2):155–163.
- Gomes MS, Blattner TC, Sant'Ana Filho M, et al. Can apical periodontitis modify systemic levels of inflammatory markers? A systematic review and meta-analysis. *J Endod.* 2013;39(10):1205–1217.
- Sirin DA, Özcelik F, Uzun C, Ersahan S, Yesilbas S. Association between C-reactive protein, neutrophil to lymphocyte ratio and the burden of apical periodontitis: A case-control study. *Acta Odontol Scand.* 2019;77(2):142–149.
- Keller JJ, Kang JH, Lin HC. Association between ankylosing spondylitis and chronic periodontitis: A population-based study. *Arthritis Rheum.* 2013;65(1):167–173.
- Pischon N, Pischon T, Gülmez E, et al. Periodontal disease in patients with ankylosing spondylitis. *Ann Rheum Dis.* 2010;69(1):34–38.
- Orstavik D, Kerekes K, Eriksen HM. The periapical index: A scoring system for radiographic assessment of apical periodontitis. *Endod Dent Traumatol.* 1986;2(1):20–34.
- López-López J, Jané-Salas E, Estrugo-Devesa A, Velasco-Ortega E, Martín-González J, Segura-Egea JJ. Periapical and endodontic status of type 2 diabetic patients in Catalonia, Spain: A cross-sectional study. *J Endod.* 2011;37(5):598–601.
- Jalali P, Glickman GN, Schneiderman ED, Schweitzer JL. Prevalence of periapical rarefying osteitis in patients with rheumatoid arthritis. *J Endod.* 2017;43(7):1093–1096.
- Cantrell DA, Smith KA. The interleukin-2 T-cell system: A new cell growth model. *Science.* 1984;224(4655):1312–1316.
- Brandt C, Pedersen BK. The role of exercise-induced myokines in muscle homeostasis and the defense against chronic diseases. *J Biomed Biotechnol.* 2010;2010:520258.

15. Santos SCLT, Couto LA, Fonseca JM, et al. Participation of osteoclastogenic factors in immunopathogenesis of human chronic periapical lesions. *J Oral Pathol Med.* 2017;46(9):846–852.
16. Liu HC, Hsieh KH. Elevated serum interleukin-2 receptor; increased in vitro immunoglobulin synthesis and lack of response to testosterone-enhanced in vitro interleukin-2 production in ankylosing spondylitis. *Zhonghua Min Guo Wei Sheng Wu Ji Mian Yi Xue Za Zhi.* 1987;20(1):1–8.
17. Cotti E, Mezzena S, Schirru E, et al. Healing of apical periodontitis in patients with inflammatory bowel diseases and under anti-tumor necrosis factor alpha therapy. *J Endod.* 2018;44(12):1777–1782.
18. Khalighinejad N, Aminoshariae A, Kulild JC, Sahly K, Mickel A. Association of end-stage renal disease with radiographically and clinically diagnosed apical periodontitis: A hospital-based study. *J Endod.* 2017;43(9):1438–1441.
19. Costa TH, de Figueiredo Neto JA, de Oliveira AE, Lopes e Maia Mde F, de Almeida AL. Association between chronic apical periodontitis and coronary artery disease. *J Endod.* 2014;40(2):164–167.



# Effect of the combined zirconium dioxide surface treatment on the shear bond strength of a veneering ceramic to zirconium dioxide

## Wpływ kondycjonowania powierzchni dwutlenku cyrkonu na zdolność wiązania ceramiki licowanej z dwutlenkiem cyrkonu

Maha Kareem Jabbar<sup>A–D</sup>, Suha Fadhil Dulaimi<sup>A–F</sup>

Department of Prosthodontic Technologies, College of Health and Medical Technologies, Middle Technical University, Baghdad, Iraq

A – research concept and design; B – collection and/or assembly of data; C – data analysis and interpretation; D – writing the article; E – critical revision of the article; F – final approval of the article

Dental and Medical Problems, ISSN 1644-387X (print), ISSN 2300-9020 (online)

Dent Med Probl. 2020;57(2):177–183

### Address for correspondence

Suha Fadhil Dulaimi  
Email: suha.f.dulaimi@gmail.com

### Funding sources

None declared

### Conflict of interest

None declared

Received on August 24, 2019  
Reviewed on December 14, 2019  
Accepted on January 9, 2020

Published online on June 19, 2020

### Cite as

Jabbar MK, Dulaimi SF. Effect of the combined zirconium dioxide surface treatment on the shear bond strength of a veneering ceramic to zirconium dioxide. *Dent Med Probl.* 2020;57(2):177–183. doi:10.17219/dmp/116409

### DOI

10.17219/dmp/116409

### Copyright

© 2020 by Wrocław Medical University  
This is an article distributed under the terms of the  
Creative Commons Attribution 3.0 Unported License (CC BY 3.0)  
(<https://creativecommons.org/licenses/by/3.0/>).

## Abstract

**Background.** Yttrium-stabilized tetragonal zirconia polycrystal (Y-TZP) is used as a core material in all-ceramic restorations. The delamination and chipping of a veneering ceramic are the most common complications in the case of zirconia-based restorations.

**Objectives.** The aim of the study was to investigate the effect of the combined treatment of the zirconium dioxide (ZrO<sub>2</sub>) surface (airborne-particle abrasion with liner application) on the shear bond strength (SBS) of a veneering ceramic.

**Material and methods.** Thirty pre-sintered ZrO<sub>2</sub> cuboidal specimens (VITA YZ<sup>®</sup> HT) were sub-divided into 3 groups: group C consisted of 10 specimens without treatment at the sintering stage; group SZ<sub>1</sub> consisted of 10 specimens treated with airborne-particle abrasion (50-micrometer particles of aluminum oxide – Al<sub>2</sub>O<sub>3</sub>; Korox<sup>®</sup> 50), and then coated with a 0.1-millimeter liner (IPS e.max<sup>®</sup> Ceram ZirLiner) after sintering; group SZ<sub>2</sub> consisted of 10 specimens treated with airborne-particle abrasion (50-micrometer particles of Al<sub>2</sub>O<sub>3</sub>), and then coated with a 0.2-millimeter liner after sintering. Ceramic veneers (IPS e.max Ceram Dentin) were then applied using the layering technique. After that, the SBS tests were conducted.

**Results.** The results showed that the combined treatment of the ZrO<sub>2</sub> surface significantly affected SBS ( $p < 0.01$ ). The highest mean value was shown in group C (12.441 ± 2.284 MPa), followed by group SZ<sub>2</sub> (7.889 ± 0.794 MPa), whereas the lowest mean value was observed in group SZ<sub>1</sub> (5.580 ± 0.843 MPa).

**Conclusions.** The combined treatment of the pre-sintered ZrO<sub>2</sub> surface significantly reduced the SBS of a veneering ceramic. However, the combined surface treatment with a liner thickness of 0.2 mm significantly enhanced the SBS of a veneering ceramic compared to the same combined treatment but with a liner thickness of 0.1 mm.

**Key words:** zirconium dioxide, ceramics, aluminum oxide

**Słowa kluczowe:** dwutlenek cyrkonu, ceramiki, tlenek glinu

## Introduction

In restorative dentistry, metal-ceramic restorations have been used in fixed prosthodontic treatment for many years for preparing single crowns and fixed partial dentures. However, an increasing esthetic demand from patients and clinicians has led to a search for metal-free prosthodontic restorations.<sup>1</sup>

As a result, various all-ceramic restorations have become available, such as lithium disilicate, infiltrated ceramics and – more recently – zirconium dioxide ( $ZrO_2$ ; yttrium-stabilized tetragonal zirconia polycrystal – Y-TZP),<sup>2</sup> as they have great esthetic potential due to their improved optical properties, e.g., translucence, and the transmission and diffusion of light.<sup>3</sup>

The brittleness of these materials has led to an increased application of  $ZrO_2$ -based ceramics, due to the fact that  $ZrO_2$  exhibits mechanical properties that are most effective for producing restorations in the posterior oral region.<sup>4</sup>

The polycrystalline nature of Y-TZP reduces esthetic quality. Opaque  $ZrO_2$  cores require the use of ceramic coatings with a high content of silica ( $SiO_2$ ), such as feldspar, in order to enhance the esthetic properties of restorations.<sup>5,6</sup>

Despite a high resistance to fracture exhibited by  $ZrO_2$ -based restorations, the fracture of a veneer poses a problem. Clinical investigations have shown a greater percentage of failure (like chipping or delamination) of a veneering ceramic in restorations with  $ZrO_2$  cores as compared to metal-ceramic restorations. Long-term clinical studies have concluded that bonding at the  $ZrO_2$  – ceramic interface is weaker and adhesion is influenced by many factors, including improper design,<sup>7</sup> a mismatch in the coefficient of thermal expansion (CTE),<sup>8,9</sup> an improper technique of applying a ceramic veneer, and repeated firing cycles.<sup>1</sup> Other influencing factors comprise the rapid cooling of a ceramic veneer, which causes excessive residual tension within it, generating micro-fissures or leading to the debonding of a ceramic veneer in the presence of masticatory force.<sup>10</sup> Delamination (adhesive failure) is more frequent than cases of chipping (cohesive failure). The reasons for that are poor interfacial adhesion and a great variation in mechanical properties between  $ZrO_2$  and a veneering ceramic.<sup>11–13</sup>

Various kinds of surface treatment and surface conditioning have been investigated to prevent the failure of a veneering ceramic.<sup>14–16</sup> Each surface treatment technique refers to a single type of  $ZrO_2$  surface treatment. To date, no technique has been recommended for optimal bonding between  $ZrO_2$  and a ceramic veneer.

The objective of this study was to evaluate the effect of the combined treatment of the pre-sintered  $ZrO_2$  surface on the shear bond strength (SBS) of a veneering ceramic. The null hypothesis tested was that the combined surface treatment of pre-sintered  $ZrO_2$  has no effect on the SBS of a veneering ceramic.

## Material and methods

### Specimen preparation

Zirconium dioxide blanks (partially sintered Y-TZP, VITA YZ<sup>®</sup> HT; VITA Zahnfabrik H. Rauter GmbH & Co. KG, Bad Säckingen, Germany) were used to prepare 30 cuboidal specimens (3.687 mm in height, 19.664 mm in length and width) using a milling machine.<sup>17</sup> Next, the specimens were randomly divided into 3 groups. Each group contained 10 specimens according to the applied  $ZrO_2$  surface treatment. Group C contained 10  $ZrO_2$  specimens without treatment as a control group. Group SZ<sub>1</sub> contained 10  $ZrO_2$  specimens which were treated with airborne-particle abrasion and the application of a 0.1-millimeter-thick liner. Finally, Group SZ<sub>2</sub> contained 10  $ZrO_2$  specimens which were treated with airborne-particle abrasion and the application of a 0.2-millimeter-thick liner.

### Group C

Ten  $ZrO_2$  specimens were left without treatment after sintering (the control group). The  $ZrO_2$  specimens were sintered in a furnace (VITA ZYRCOMAT<sup>®</sup> 6000 MS; VITA Zahnfabrik H. Rauter GmbH & Co. KG) according to the cycle recommended by the manufacturer (a high-speed sintering temperature of 1,450° for 80 min).

During sintering, the milled  $ZrO_2$  specimens were subjected to volumetric shrinkage by about 20% based on the fact that the shrinkage factor for this type of  $ZrO_2$  is 1.229. Following sintering, the dimensions of the specimens – approx.  $3 \pm 0.1$  mm in height, and  $16 \pm 0.1$  mm in length and width – were checked with a digital caliper.<sup>18</sup> After sintering, the specimens were cleaned ultrasonically in distilled water in a digital ultrasonic cleaner (White-Sonic<sup>®</sup>; Whitepeaks Dental Solutions GmbH & Co. KG, Wesel, Germany) for 5 min to remove any surface residue, and then air-dried.

### Group SZ<sub>1</sub>

Ten  $ZrO_2$  specimens were treated with airborne-particle abrasion (50-micrometer particles of aluminum oxide –  $Al_2O_3$ ) (Korox<sup>®</sup> 50; Renfert GmbH, Hilzingen, Germany) before sintering, and then coated with a liner (IPS e.max<sup>®</sup> Ceram ZirLiner; Ivoclar Vivadent AG, Schaan, Liechtenstein) of a 0.1-millimeter thickness after sintering. According to the manufacturer, ZirLiner contains a glass ceramic and fluorapatite crystals ( $Ca_5(PO_4)_3F$ ).

Airborne-particle abrasion was carried out before sintering. The working surfaces of the  $ZrO_2$  specimens were abraded in the perpendicular direction (a 90° angle with the surface), with a crosswise motion of the nozzle at an air pressure of 0.5 bar for 15 s and a fixed distance of 10 mm between the nozzle and the surface of the specimen,

with 50-micrometer  $\text{Al}_2\text{O}_3$  particles using a sandblasting device (EasyBlast<sup>®</sup>; BEGO, Bremen, Germany).<sup>19</sup> Next, all the specimens were ultrasonically cleaned in distilled water for 5 min, and then air-dried. After that, sintering was carried out in a  $\text{ZrO}_2$  sintering furnace (VITA ZYRCOMAT 6000 MS; VITA Zahnfabrik H. Rauter GmbH & Co. KG) according to the manufacturer's instructions.

For the standardization of the liner thickness (0.1 mm and 0.2 mm), a custom-made mold was fabricated. The mold consisted of a rigid base with 2 stainless steel metal straps: the 1<sup>st</sup> strap had a thickness of 0.1 mm and in its center there was a hole of a diameter of 4.5 mm; the 2<sup>nd</sup> strap had a thickness of 0.2 mm and the same 4.5-millimeter-diameter hole in the center. Through this hole, the standardization of the liner thickness was done on the surfaces of the  $\text{ZrO}_2$  specimens. The liner was mixed with respective liquid (IPS e.max Ceram ZirLiner Build-Up Liquid allround; Ivoclar Vivadent AG). For standardization, the same amounts of powder and liquid were mixed for all specimens. For each specimen, 1 mg of powder was mixed with 2 drops of liquid to obtain the desired creamy consistency according to the manufacturer's instructions.<sup>17</sup>

Next, the liner was applied to the prepared surface using a brush; the brush was vibrated to achieve an even, greenish-color effect. Then, the liner was left to dry for 5 min.

When dry, the specimen was fired in a calibrated porcelain furnace (P3000; Ivoclar Vivadent AG) according to the manufacturer's instructions.

After firing, the thickness of each specimen was measured with a digital caliper with an accuracy of 0.02 mm in 3 different locations (the left end, the mid-point and the right end) and corrected with diamond rotary cutting instruments until the desired thickness of 3.1 mm ( $\text{ZrO}_2$  + liner) was achieved.

## Group SZ<sub>2</sub>

Ten  $\text{ZrO}_2$  specimens were treated with airborne-particle abrasion (50-micrometer particles of  $\text{Al}_2\text{O}_3$ ) before sintering, and then coated with a 0.2-millimeter liner thickness after sintering. Airborne-particle abrasion was done before sintering, and the same procedure was performed as in group SZ<sub>1</sub>. Next, the liner was applied according to the procedure mentioned for group SZ<sub>1</sub>, except that the 0.2-millimeter strap was used in the custom-made mold.

## Build-up of a ceramic veneer on the zirconium dioxide specimens

In order to build up a ceramic veneer on the  $\text{ZrO}_2$  surface, a custom-made acrylic resin split cylindrical mold was fabricated.<sup>20</sup> The mold had 2 diameters (an outer diameter of 12.5 mm and an inner diameter of 4.5 mm) and was divided into 2 equal split parts with pins in the edge, through which the 2 parts of the mold were secured in position.

The mold was placed above the liner layer in the center of each specimen. The ceramic powder (IPS e.max Ceram Dentin A2; Ivoclar Vivadent AG) was mixed with an appropriate amount of respective liquid (IPS e.max Ceram Build-Up Liquid; Ivoclar Vivadent AG) according to the manufacturer's instructions. Then, the ceramic was added incrementally to the mold on the prepared  $\text{ZrO}_2$  surface using the layering technique, condensing the ceramic material layer by layer. After each increment of the ceramic was placed, the excess moisture was removed with an absorbent paper tissue and the veneering procedure continued until the veneering ceramic measured 4 mm in thickness. The firing of the ceramic was performed according to the manufacturer's instructions. Due to the volumetric shrinkage which took place during the firing of the porcelain, additional porcelain was added following the abovementioned technique and was fired under the same conditions to achieve the desired dimensions of the ceramic (4.5 mm in diameter and 4 mm in length).<sup>18</sup> After completing firing, the dimensions of the veneering ceramic were checked with a digital caliper, and then adjusted if needed using a straight headpiece. To evaluate SBS, each specimen was embedded in a silicon mold using cold-cured acrylic.<sup>21</sup>

## Shear bond strength testing

Each specimen was attached to a universal testing machine (WDW-50; Laryee Technology Co., Ltd., Beijing, China). Load was applied to the specimen using a stainless steel chisel-shaped piston at a constant crosshead speed of 1 mm/min until failure. The specimen was regarded to be failed when the ceramic veneer was detached from  $\text{ZrO}_2$ . The testing machine was automatically connected to computer software, which displayed the failure load force in newtons. The maximum force was recorded and SBS was calculated in megapascals by dividing the load force by the area of the bonded surface.

$$\text{SBS [MPa]} = \text{force [N]} / \text{bonded area [mm}^2\text{]} \quad (1)$$

where:

SBS – shear bond strength.

## Scanning electron microscopy and energy-dispersive X-ray spectroscopy analyses

One failed specimen was selected from each group and cleaned in an ultrasonic cleaning bath for 5 min, and then air-dried. The interfacial surface was sputter-coated with gold. Next, the specimen was mounted on an aluminum holder and analyzed with secondary electrons. Images were observed under a field-emission scanning electron microscope (SEM) (Inspect S50; FEI Europe B.V., Eindhoven, the Netherlands) and photographs were taken at a magnification of  $\times 200$  with an accelerating voltage of 20 KV to examine surface morphology.



The elemental composition of the same specimen at the fractured interfacial surface was qualitatively analyzed using energy-dispersive X-ray spectroscopy (EDS) and the weight percentage of each traced element was measured (XFlash<sup>®</sup> 6/10; Bruker Optik GmbH, Ettlingen, Germany). The mode of failure was examined under SEM at a magnification of  $\times 29$ ; it was classified as:

- cohesive within the veneering ceramic;
- adhesive at the  $ZrO_2$ -ceramic interface;
- or mixed.

The data was statistically analyzed using IBM SPSS Statistics for Windows, v. 21 (IBM Corp., Armonk, USA). The one-way analysis of variance (ANOVA) and the least significant difference (LSD) tests were applied to determine the significance of the differences between the groups. A  $p$ -value of  $\leq 0.05$  was considered statistically significant.

## Results

The one-way ANOVA test showed that there was a highly significant difference ( $p < 0.01$ ) in the mean value of SBS between the studied groups, as shown in Table 1. The highest mean value was shown in group C ( $12.441 \pm 2.284$  MPa), followed by group  $SZ_2$  ( $7.889 \pm 0.794$  MPa), whereas the lowest mean value was observed in group  $SZ_1$  ( $5.580 \pm 0.843$  MPa).

A further analysis of the data from the 3 groups was performed using the LSD test to examine the source of the differences between the tested groups. The LSD test showed a highly significant difference between group C and groups  $SZ_1$  and  $SZ_2$ . Likewise, the LSD test showed a highly significant difference between group  $SZ_1$  and group  $SZ_2$ .

The results for the failure modes after SBS testing are summarized in Table 2. The predominant mode of failure for groups  $SZ_1$  and  $SZ_2$  was cohesive, whereas mixed failure occurred in all groups in a low percentage. Adhesive failure was observed in group C in a high percentage, as shown in Fig. 1.

**Table 1.** Mean distribution of the shear bond strength (SBS) test among the tested groups

Group	n (N = 30)	M $\pm$ SD [MPa]	SE [MPa]	Range [MPa]		p-value
				min	max	
C	10	12.441 $\pm$ 2.284	0.722	9.52	15.97	
$SZ_1$	10	5.580 $\pm$ 0.843	0.267	4.27	6.54	0.0003*
$SZ_2$	10	7.889 $\pm$ 0.794	0.251	7.02	9.43	

Group C – control group (no treatment); group  $SZ_1$  – airborne-particle abrasion + liner application (1 mm in thickness); group  $SZ_2$  – airborne-particle abrasion + liner application (2 mm in thickness); M – mean; SD – standard deviation; SE – standard error; \* statistically highly significant ( $p < 0.01$ ); ANOVA.

**Table 2.** Modes of failure

Group	Adhesive failure n (%)	Cohesive failure n (%)	Mixed failure n (%)
C	5 (50)	2 (20)	3 (30)
$SZ_1$	1 (10)	9 (90)	0 (0)
$SZ_2$	1 (10)	7 (70)	2 (20)

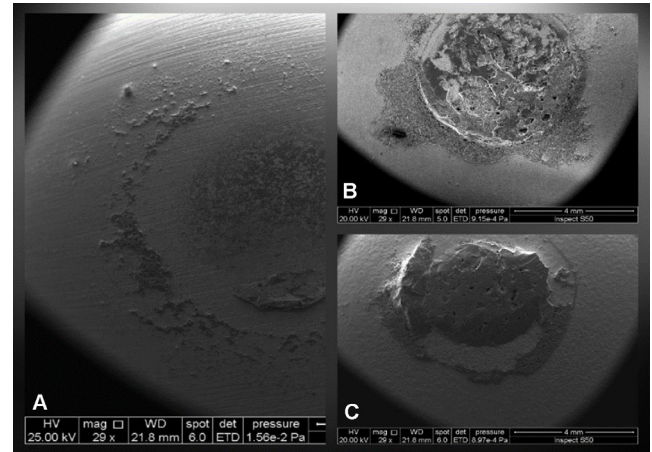


**Fig. 1.** Modes of failure

A – adhesive failure; B – cohesive failure; C – mixed failure; magnification  $\times 29$ .

## Surface morphology (SEM observation)

The SEM images of the specimens from group C revealed numerous scratch lines on the  $ZrO_2$  surface with a thin layer of a veneering ceramic. These numerous scratch lines were produced by the milling machine

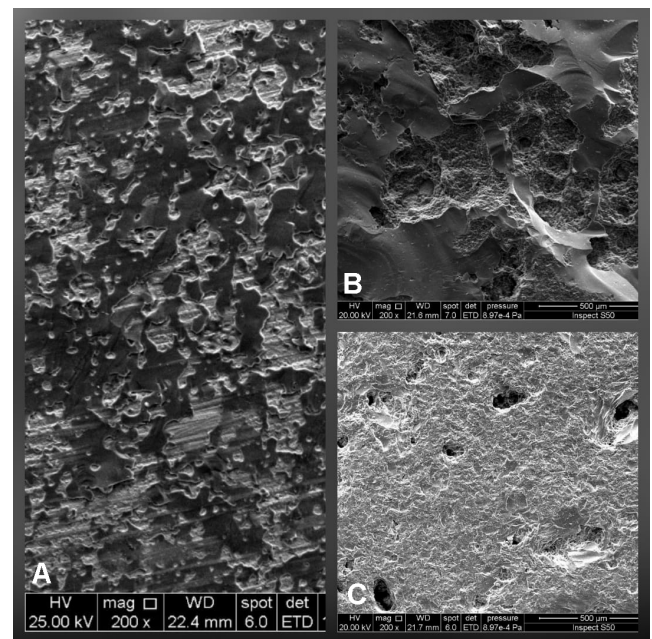


**Fig. 2.** Scanning electron microscope (SEM) images

A – group C; B – group  $SZ_1$ ; C – group  $SZ_2$ ; magnification  $\times 200$ .

during the preparation of the specimens (Fig. 2A). The images for group SZ<sub>1</sub> showed a rugged porous layer with areas of a veneering ceramic (Fig. 2B), whereas the SEM images for group SZ<sub>2</sub> revealed pronounced irregularities and rough texture, characterized by peaks and valleys (Fig. 2C).

## Energy-dispersive X-ray spectroscopy

The chemical analyses within EDS were performed on the surface of the failed specimens after SBS testing. For group C, the elemental analysis showed the presence of Zr in the ceramic veneer layer and the elements characteristic of the veneering layer (mainly Si) in the ZrO<sub>2</sub> layer. The area of mutual diffusion between Zr and Si tended to increase. The EDS line-scan profile analysis showed the transition of the elements Na, Al, In, and P at the bonded interface of the Y-TZP specimens (Fig. 3).

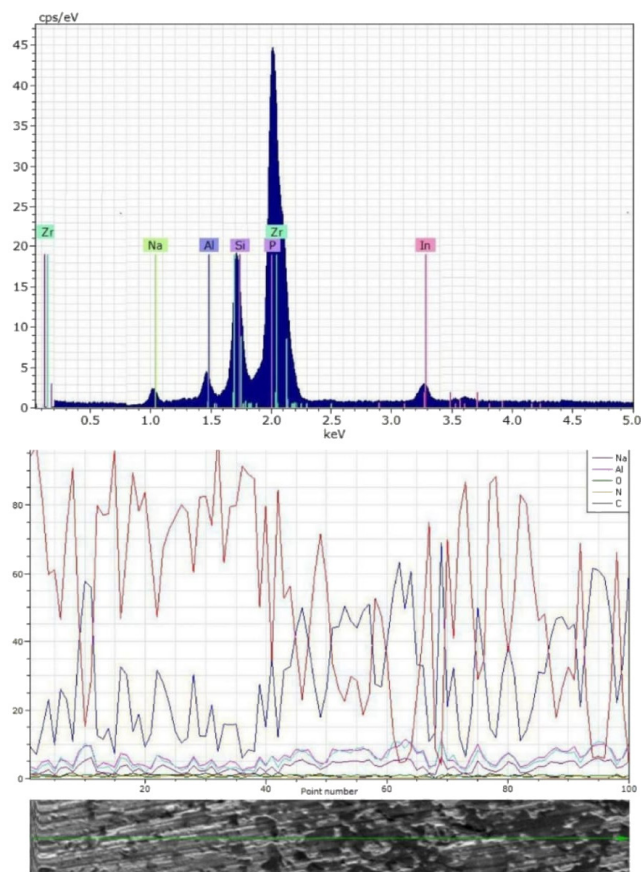


Fig. 3. Energy-dispersive X-ray spectroscopy (EDS) and line-scan profile analyses for group C

The EDS analysis for groups SZ<sub>1</sub> and SZ<sub>2</sub> revealed that the remaining layers and the diffused particles on the surfaces contained SiO<sub>2</sub>, Na, Al, K, and Ca, derived from the veneering ceramic and the liner material (Fig. 4,5).

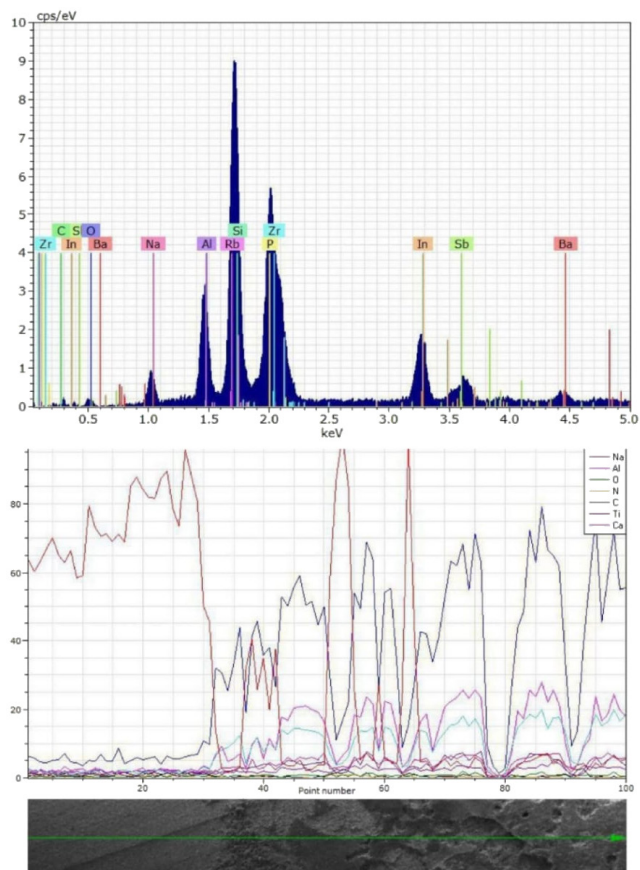


Fig. 4. EDS and line-scan profile analyses for group SZ<sub>1</sub>

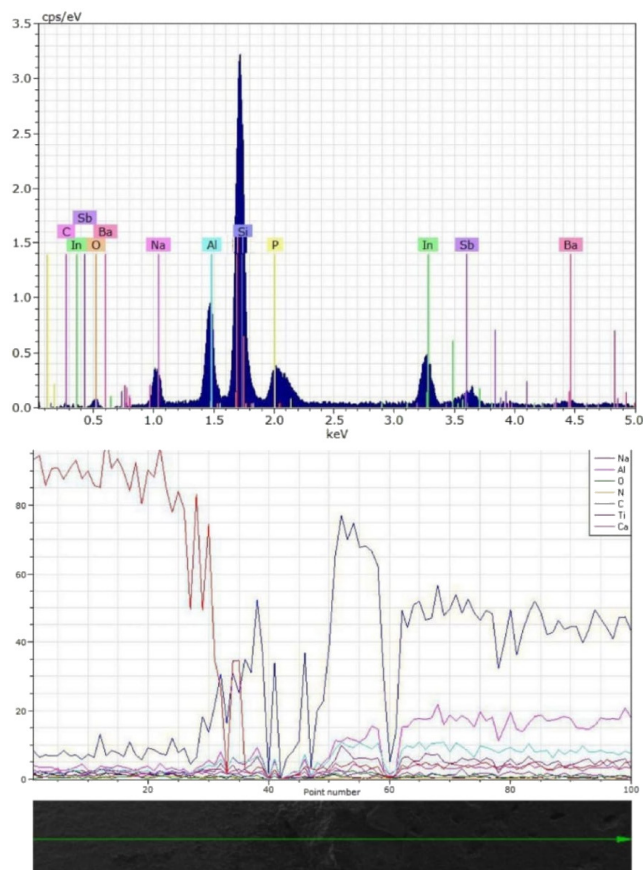


Fig. 5. EDS and line-scan profile analyses for Group SZ<sub>2</sub>

## Discussion

Many factors may affect the SBS of a veneering ceramic to ZrO<sub>2</sub>, such as the preparation of the surface, which may influence mechanical retention, the formation of flaws and structure defects at the ZrO<sub>2</sub>-ceramic interface as well as the wetting properties and the volumetric shrinkage of the veneer.<sup>22</sup> In addition, SBS may be affected by the residual stress generated by a mismatch in CTE.

The coefficients of thermal expansion for ZrO<sub>2</sub> and a veneering ceramic must closely match to obtain a strong interfacial bond. In the current study, the CTE of ZrO<sub>2</sub> ( $10.5 \times 10^{-6} \text{ K}^{-1}$ ) was slightly higher than that of the veneering ceramic ( $9.5 \times 10^{-6} \text{ K}^{-1}$ ). In case when the CTE of ZrO<sub>2</sub> is slightly higher than that of a veneering ceramic, beneficial residual compressive stress is created.<sup>23-25</sup> An excessive difference in CTE may cause damage to a ceramic during cooling.

The ZrO<sub>2</sub> specimens were veneered using the layering technique. This technique is most widely used for applying veneering ceramics to the ZrO<sub>2</sub> surface.<sup>26</sup>

The airborne-particle abrasion of the ZrO<sub>2</sub> specimens at the pre-sintering stage using 50-micrometer AL<sub>2</sub>O<sub>3</sub> particles might be a favorable method of the surface treatment, as after sintering, the entire group treated at the pre-sintering stage showed a complete transformation of the monoclinic phase back to the tetragonal one, thus not subjecting ZrO<sub>2</sub> to early degradation.<sup>19</sup> The objective of treating the ZrO<sub>2</sub> surface with airborne-particle abrasion is to create roughness and increase surface energy, and in consequence, to improve the strength of the bond with a veneering ceramic.

Liners are applied on the ZrO<sub>2</sub> surface mainly to mask its opaque white appearance before the application of a veneering ceramic and to enhance wettability, enabling the fabrication of lifelike restorations.<sup>27,28</sup> ZirLiner is a ceramic liner; the manufacturer suggests that it enhances bonding with ZrO<sub>2</sub> and masks the opaque white color of ZrO<sub>2</sub>. In a previous study, the application of ZirLiner alone did not improve the bonding of a ceramic veneer to the ZrO<sub>2</sub> surface.<sup>16</sup>

The results of this study rejected the null hypothesis, as the combined surface treatment of ZrO<sub>2</sub> resulted in a significant reduction ( $p < 0.01$ ) in the SBS between the ZrO<sub>2</sub> surface and a veneering ceramic.

The highest mean SBS value appeared in group C (12.441 ± 2.284 MPa), followed by group SZ<sub>2</sub>, and then SZ<sub>1</sub>. The comparison between the groups using the one-way ANOVA showed highly significant differences with  $p < 0.01$ . The SEM images showed the bonded interface area and fracture surfaces with numerous porous defects for group SZ<sub>1</sub> (Fig. 2B). The formation of porosity and micro-gaps at the interface was a factor that reduced adhesion in the specimens through mechanical retention, which is comparable with the findings reported in the literature,<sup>6,12</sup> where such formation occurred as well.

The comparison between group SZ<sub>2</sub> and group C showed a highly significant difference, which may be due to the fact that the liquid used for mixing the liner powder contained water. Tholey et al. provided an explanation for this; they found that ZrO<sub>2</sub> grains suffered from faceting (degradation) at the interface when adding a liner and a ceramic that was mixed with distilled water or liquid containing water at high firing temperatures.<sup>13</sup> It is assumed that tensile stress was generated in ZrO<sub>2</sub> crystals due to the diffusion of water molecules, leading to lattice contraction and causing the transformation of the tetragonal phase to the monoclinic phase. This water-induced transformation could have an influence on ceramic failure in the clinical setting; however, the real effect is still unclear.<sup>9</sup>

The LSD test, performed to make comparisons between groups SZ<sub>1</sub> and SZ<sub>2</sub>, showed a highly significant difference ( $p < 0.01$ ) between the groups. Since the same roughening was used under the same conditions for both treated groups and nearly the same rough surface was obtained for both groups, the difference in SBS might be related to the different liner thicknesses applied. When the comparison between the SEM images for both groups was made, it turned out that the application of a 0.1-millimeter liner thickness yielded numerous porous defects (Fig. 2B). This indicated that the liner did not penetrate the irregular surface formed by sandblasting. However, applying a 0.2-millimeter liner thickness to the interface area (Fig. 2C) showed a reduction in the number and size of pores and defects. This indicates that the application of an increased liner thickness improves the wettability of the rough ZrO<sub>2</sub> surface produced by means of sandblasting.

In the present study, the analysis of the failure modes showed that the majority of the specimens exhibited combined failure or cohesive failure at a high percentage, whereas adhesive failure occurred at a low percentage, except for group C, which showed an adhesive mode of failure of 50%. This group revealed a high SBS value, whereas lower SBS values were recorded when failure occurred cohesively within a weak veneer material. The results of this study concur with those of Ereifej et al.<sup>29</sup> They stated that the samples which failed cohesively within a veneer presented low SBS values, whereas those having a mixed cohesive/adhesive fracture pattern or a cohesive fracture within the core showed higher SBS values.<sup>29</sup>

The SEM observation for group C revealed that the residual veneer layer which remained on the surface of the ZrO<sub>2</sub> substructure was thin with a partial exposure of the ZrO<sub>2</sub> surface, indicating that the crack extended along the ZrO<sub>2</sub>-ceramic interface (Fig. 2A). Thus, it can be concluded that the strength of the bond between ZrO<sub>2</sub> and the veneering ceramic was higher than the cohesive strength of the veneering ceramic. It means that the weakest link was not the interface, but the veneering ceramic itself.

It was also reported that the development and propagation of delamination was related to the mismatches in the elastic modulus and fracture toughness of ZrO<sub>2</sub> and porcelain.

A higher fracture toughness of ZrO<sub>2</sub> might induce a deflection of crack propagation from within the porcelain to along the core–veneer interface.<sup>30</sup> On the other hand, the results for groups SZ<sub>1</sub> and SZ<sub>2</sub> showed that the bond failure was predominantly cohesive or mixed. This may be due to performing sandblasting before sintering, which is illustrated by the shift of the failure modes, from mixed to cohesive.<sup>18</sup>

One of the limitations of this study was that the specimen design did not represent the clinical geometry of a ZrO<sub>2</sub> ceramic restoration. The study provided design that allowed for the SBS testing procedure.

In addition, the oral environment was not simulated with thermocycling, so further research is required to investigate its effect together with the combined surface treatment.


## Conclusions

Within the limitations of the present in vitro study, both kinds of combined surface treatment studied significantly reduced the SBS of a veneering ceramic in comparison with the control group without treatment. The combined surface treatment of pre-sintered ZrO<sub>2</sub> using airborne-particle abrasion and liner application (0.2-millimeter thickness) significantly enhanced the SBS of a veneering ceramic to ZrO<sub>2</sub> as compared to the same combined treatment but with a liner thickness of 0.1 mm.

According to the results of the present study, creating the mechanical retention (scratch lines) of the ZrO<sub>2</sub> surface with a milling machine, as in the control group without air-abrasion and liner application, may be recommended for future research.

## ORCID iDs

Maha Kareem Jabbar  <https://orcid.org/0000-0002-2043-4813>

Suha Fadhill Dulaimi  <https://orcid.org/0000-0002-5898-3500>

## References

- Aboushelib MN, de Jager N, Kleverlaan CJ, Feilzer AJ. Microtensile bond strength of different components of core veneered all-ceramic restorations. *Dent Mater.* 2005;21(10):984–991.
- Tinschert J, Natt G, Mautsch W, Augthun M, Spiekermann H. Fracture resistance of lithium disilicate-, alumina-, and zirconia-based three-unit fixed partial dentures: A laboratory study. *Int J Prosthodont.* 2001;14(3):231–238.
- Vidotti HA, Pereira JR, Insaurralde E, Pompéia Fraga de Almeida AL, do Valle AL. Thermo and mechanical cycling and veneering method do not influence Y-TZP core/veneer interface bond strength. *J Dent.* 2013;41(4):307–312.
- Martínez-Galeano G, Bautista-Lora A, Pacheco-Muñoz LF, Garzón-Rayó H. Liner effect on the bond strength of feldspathic ceramic to zirconia using a slow cooling protocol. *Rev Fac Odontol Univ Antioq.* 2015;27(1):63–75.
- Guess PC, Schultheis S, Bonfante EA, Coelho PG, Ferencz JL, Silva NR. All-ceramic systems: Laboratory and clinical performance. *Dent Clin North Am.* 2011;55(2):333–352.
- Dündar M, Ozcan M, Gökçe B, Cömlekoğlu E, Leite F, Valandro LF. Comparison of two bond strength testing methodologies for bilayered all-ceramics. *Dent Mater.* 2007;23(5):630–636.
- Marchack BW, Futatsuki Y, Marchack CB, White SN. Customization of milled zirconia copings for all-ceramic crowns: A clinical report. *J Prosthet Dent.* 2008;99(3):169–173.
- Fischer J, Stawarczyk B, Tomic M, Strub JR, Hämmerle CH. Effect of thermal misfit between different veneering ceramics and zirconia frameworks on in vitro fracture load of single crowns. *Dent Mater J.* 2007;26(6):766–772.
- Daou EE. Bonding mechanism of porcelain to frameworks: Similarities and dissimilarities between metal and zirconia. *Br J Med Res.* 2016;16(3):1–16.
- Swain MV. Unstable cracking (chipping) of veneering porcelain on all-ceramic dental crowns and fixed partial dentures. *Acta Biomater.* 2009;5(5):1668–1677.
- Ozkurt Z, Kazazoglu E, Unal A. In vitro evaluation of shear bond strength of veneering ceramics to zirconia. *Dent Mater J.* 2010;29(2):138–146.
- Guess PC, Kulis A, Witkowski S, Wolkewitz M, Zhang Y, Strub JR. Shear bond strengths between different zirconia cores and veneering ceramics and their susceptibility to thermocycling. *Dent Mater.* 2008;24(11):1556–1567.
- Tholey MJ, Swain MV, Thiel N. SEM observations of porcelain Y-TZP interface. *Dent Mater.* 2009;25(7):857–862.
- Alghazzawi TF, Janowski GM. Effect of liner and porcelain application on zirconia surface structure and composition. *Int J Oral Sci.* 2016;8(3):164–171.
- Wang G, Zhang S, Bian C, Kong H. Interface toughness of a zirconia–veneer system and the effect of a liner application. *J Prosthet Dent.* 2014;112(3):576–583.
- Jabbar MK, Dulaimi SF. Effect of liner thickness and sandblasting of zirconia on the shear bond strength of veneering ceramic. *JODR.* 2018;5(2):40–51.
- Kareem IH, Al-Azzawi HJ. Effect of zirconia surface treatments on the shear bond strength of veneering ceramic. *J Bagh Coll Dent.* 2014;26(3):13–17.
- He M, Zhang Z, Zheng D, Ding N, Liu Y. Effect of sandblasting on surface roughness of zirconia-based ceramics and shear bond strength of veneering porcelain. *Dent Mater J.* 2014;33(6):778–785.
- Ebeid K, Willie S, Salah T, Wahsh M, Zohdy M, Kern M. Evaluation of surface treatments of monolithic zirconia in different sintering stages. *J Prosthodont Res.* 2018;62(2):210–217.
- Saka M, Yuzugullu B. Bond strength of veneer ceramic and zirconia cores with different surface modifications after microwave sintering. *J Adv Prosthodont.* 2013;5(4):485–493.
- Kirmali O, Akin H, Ozdemir AK. Shear bond strength of veneering ceramic to zirconia core after different surface treatments. *Photomed Laser Surg.* 2013;31(6):261–268.
- Aboushelib MN, Kleverlaan CJ, Feilzer AJ. Microtensile bond strength of different component of core veneered all-ceramic restorations. Part II: Zirconia veneering ceramics. *Dent Mater.* 2006;22(9):857–863.
- Craig RG, Powers JM, Wataha JC. *Dental Materials: Properties and Manipulation.* 8<sup>th</sup> ed. St. Louis, USA: Mosby; 2004:578–580.
- Aboushelib MN, Kleverlaan CJ, Feilzer AJ. Effect of zirconia type on its bond strength with different veneer ceramics. *J Prosthodont.* 2008;17(5):401–408.
- Alsarani M, De Souza G, Rizkalla A, El-Mowafy O. Influence of crown design and material on chipping-resistance of all-ceramic molars crowns: An in vitro study. *Dent Med Probl.* 2018;55(1):35–42.
- Gaspariç L, Schaperl Z, Mehuliç K. Shear bond strength in zirconia veneered ceramics using two different surface treatments prior veneering. *Coll Antropol.* 2013;37(1):121–125.
- Liu RY, Zhang YK, Zhou SY, et al. The effect of liner thickness on the color of Y-TZP based all-ceramic restorations. *Key Eng Mater.* 2013;544:380–383.
- Lee HS, Kwon TY. The application of a novel ceramic liner improves bonding between zirconia and veneering porcelain. *Materials (Basel).* 2017;10(9):1023.
- Ereifej N, Rodrigues FP, Silikas N, Watts DC. Experimental and FE shear-bonding strength at core/veneer interfaces in bilayered ceramics. *Dent Mater.* 2011;27(6):590–597.
- Liu D, Matinlinna JP, Pow EHN. Insights into porcelain to zirconia bonding. *J Adhes Sci Technol.* 2012;26(8–9):1249–1265.



# Influence of porcelain firing on changes in the marginal fit of metal-ceramic fixed partial dental prostheses fabricated with laser sintering: An in vivo study

## Wpływ spiekania ceramiki na zmiany integracji brzeżnej mostów metalowo-ceramicznych wykonywanych laserową synteryzacją – badanie in vivo

Qusay Khaznadar Nassif<sup>1,A–F</sup>, Fendi Fendi Alshaarani<sup>2,A–F</sup>

<sup>1</sup> Department of Fixed Prosthodontics, Faculty of Dentistry, Damascus University, Syria

<sup>2</sup> Department of Fixed Prosthodontics, Faculty of Dentistry, Al-Hawash Private University, Homs, Syria

A – research concept and design; B – collection and/or assembly of data; C – data analysis and interpretation; D – writing the article; E – critical revision of the article; F – final approval of the article

Dental and Medical Problems, ISSN 1644-387X (print), ISSN 2300-9020 (online)

*Dent Med Probl.* 2020;57(2):185–190

### Address for correspondence

Qusay Khaznadar Nassif  
E-mail: qusaynassif@gmail.com

### Funding sources

None declared

### Conflict of interest

None declared

### Acknowledgements

The paper has been reviewed and verified by Prof. Loai Aljerf (ORCID: <https://orcid.org/0000-0002-1132-9659>).

Received on September 14, 2019

Reviewed on October 15, 2019

Accepted on November 14, 2019

Published online on June 30, 2020

### Cite as

Nassif QK, Alshaarani FF. Influence of porcelain firing on changes in the marginal fit of metal-ceramic fixed partial dental prostheses fabricated with laser sintering: An in vivo study. *Dent Med Probl.* 2020;57(2):185–190. doi:10.17219/dmp/114196

### DOI

10.17219/dmp/114196

### Copyright

© 2020 by Wrocław Medical University

This is an article distributed under the terms of the

Creative Commons Attribution 3.0 Unported License (CC BY 3.0)

(<https://creativecommons.org/licenses/by/3.0/>).

## Abstract

**Background.** Marginal fit is the most important criterion in the evaluation of the clinical acceptability of fixed restorations. Due to cement solubility and plaque retention, marginal gaps are potentially harmful to both the teeth and the periodontal tissues.

**Objectives.** The aim of the study was to investigate the accuracy of the fit of dental metal-ceramic bridges manufactured with the use of direct metal laser sintering (DMLS), and to explore the effects of porcelain firing on the marginal, axial and occlusal fit of metal-ceramic frameworks.

**Material and methods.** The study involved 10 patients with 3-unit metal-ceramic restorations produced using the DMLS technique. Using the silicone replica technique, we examined the marginal, axial and occlusal fit of the dental bridges before and after ceramic firing. The Shapiro–Wilks normality test and Student's paired *t*-test were implemented to analyze the mean differences in the marginal, axial and occlusal fit of the restorations before and after ceramic firing. A 95% confidence interval (*CI*) and discrepancy values at the level of 1% and 0.1% ( $p > 0.05$ ) were applied.

**Results.** All the mean values of the measurements of marginal (156.08  $\mu\text{m}$ ), axial (95.75  $\mu\text{m}$ ) and occlusal (252.83  $\mu\text{m}$ ) gaps were lower before ceramic veneering than after ceramic veneering, when the mean value for the marginal gap was 178.17  $\mu\text{m}$ , for the axial gap – 106.75  $\mu\text{m}$  and for the occlusal gap – 266.00  $\mu\text{m}$ .

**Conclusions.** Porcelain firing caused no statistically significant differences in the discrepancy values of marginal, axial and occlusal fit. For clinical application, further improvement of the DMLS system is highly recommended. Marginal gaps in DLSM bridges significantly exceed the permissible inaccuracy values of 100–120  $\mu\text{m}$  for prosthetic restorations.

**Key words:** laser, fitting, prosthesis, in vivo study, porcelain

**Słowa kluczowe:** laser, dopasowanie, proteza, badanie in vivo, ceramika

## Introduction

Dental porcelain fused to metal bridges is considered the best choice in prosthetic dentistry, especially in the posterior area of the jaws, due to a high tolerance of these materials to stress.<sup>1,2</sup> The clinical survival of these bridges is largely dependent on the distance between the internal surface of the restoration and the external surface of the abutment.<sup>3,4</sup> When the marginal gap is larger than the clinically acceptable limit, it eventually can cause cement dissolution, followed by secondary caries or periodontal inflammation.<sup>4,5</sup>

The lost-wax technique is considered a conventional method to fabricate metal bridges.<sup>6</sup> The manual phases of the casting process may result in distortions in the metal framework.<sup>4,7,8</sup> Some of these complications could be avoided by using the computer-aided design and computer-aided manufacturing (CAD-CAM) technologies,<sup>9,10</sup> or the laser sintering method (an additive manufacturing technique used in fixed prosthodontics)<sup>11,12</sup> or casting with 3D-printed patterns.<sup>13</sup> The laser sintering technology uses a high-power laser beam transformed by galvano mirrors to aggregate metal powder layer by layer, making three-dimensional (3D) complex patterns. The beam is guided by the information taken from the 3D design generated by CAD software.<sup>14,15</sup> Laser sintering has been modified for dental use; there are several types of it, among them direct metal laser sintering (DMLS).<sup>16,17</sup>

The fit of dental metal-ceramic bridges depends on the accuracy of the manufacturing technique and subsequent production procedures.<sup>18–20</sup> Some studies have referred to the effect of the progress of porcelain firing on the fit of dental bridges.<sup>21,22</sup> Similarly, marginal gaps can be increased after cementation.<sup>23,24</sup>

Studies evaluating the effect of ceramic firing on the fit of modern metal-ceramic devices reported that the marginal gap values were influenced by ceramic firing cycles.<sup>19,20,25,26</sup> At the same time, other studies reported that ceramic firing had no statistically significant effect on the internal and marginal discrepancy values.<sup>17–27</sup>

The aim of this *in vivo* study was to compare the marginal, axial and occlusal fit of metal frameworks produced by means of the DMLS method before and after the application of porcelain. The hypothesis was that the marginal, axial and occlusal gaps would be increased after ceramic application.

## Material and methods

The study involved 10 metal-ceramic fixed partial dentures (FPDs) obtained from 10 patients (7 men and 3 women) who visited the Department of Fixed Prosthodontics at the Faculty of Dentistry of Damascus University in Syria in May 2017. Each individual had lost a first

molar. The exclusion criteria were gingival recession, chronic or acute periodontitis, poor oral health care, and a high rate of generalized caries.

This study was carried out in accordance with the Declaration of Helsinki, good clinical practice and the International Organization for Standardization standard 14155. The protocol (EC ref. No. 1574, 18/04/2017) was approved by the institutional ethics committee at the Faculty of Dentistry of Damascus University, Syria.

The molar and premolar teeth that were the abutments in this study had adequate periodontal support for a 3-unit bridge, without any mobility, and showed a clinically acceptable length after preparation. The molar and premolar abutments were prepared in accordance with the requirements of metal-ceramic prosthodontics.<sup>28</sup> A circumferential chamfer margin (1 mm in width) was created, and an occlusal reduction of 1.3–2.0 mm was performed. After preparing the molar and premolar abutments, impressions were made using additive silicone (Elite HD+® Light Body Normal Set dental silicone; Zhermack SpA, Badia Polesine, Italy) and poured into a type V dental stone. Temporary bridges were fabricated with acrylic resin and cemented with eugenol-free temporary cement. The models were scanned with a 3D dental scanner (imes-icore GmbH, Eiterfeld, Germany) and the obtained data was sent to CAD software. Frameworks for dental bridges were designed with a thickness of 0.6 mm and a cement gap of 50 µm. The 3D design for the frameworks was saved as standard triangle language (STL) files for the production of Co-Cr bridges (Fig. 1) with the MYSINT100® laser sintering machine (SISMA SpA, Piovene Rocchette, Italy). All the frameworks were treated in the N 7/H dental furnace (Nabertherm GmbH, Lilienthal, Germany) for annealing after laser sintering. Then, they were trimmed, polished, steam-cleaned, and dried. After that, measurements were taken using the silicone replica technique.<sup>29</sup> A light-viscosity silicone material was put inside the frameworks, which were placed on the prepared abutments with finger pressure for 3 min (Fig. 2). After the silicone material hardened, the frameworks were removed from the prepared abutments. A medium-viscosity silicone material was inserted into the frameworks covered with the 1<sup>st</sup> silicon layer. After the silicone material hardened, the 2 layers of silicon were separated from the metal frameworks. Each silicone material model contained 2 abutments – one for a premolar and the other for a molar.

Each premolar abutment was sectioned first buccolingually, and then mesiodistally at the center of each surface, resulting in 4 surfaces: I – the distal surface; J – the buccal surface; K – the mesial surface; and L – the lingual surface. Each surface had 3 points for measurement (1 – occlusal; 2 – axial; and 3 – marginal), so 12 measurement points for each premolar abutment were analyzed with the BX41 light microscope (Olympus Optical Co., Ltd., Tokyo, Japan).



Fig. 1. Co-Cr bridges produced using the direct metal laser sintering (DMLS) method



Fig. 2. Silicone replica technique sample before ceramic firing

Each molar abutment was sectioned first buccolingually, then mesiodistally, and then buccomesially to linguodistally and linguomesially to bucodistally at the center of each surface, resulting in 8 surfaces: A – the distal surface;

B – the distobuccal surface; C – the buccal surface; D – the buccomesial surface; E – the mesial surface; F – the mesiolingual surface; G – the lingual surface; and H – the linguodistal surface (Fig. 3). Each surface had 3 points for measurement (1 – occlusal; 2 – axial; and 3 – marginal) (Fig. 4), so 24 measurement points for each molar abutment were analyzed with the Olympus BX41 light microscope.

After the measurements were taken, the frameworks were veneered with porcelain (VMK Master® feldspar veneering; VITA Zahnfabrik H. Rauter GmbH & Co. KG, Bad Säckingen, Germany) in a dental ceramic furnace (Programat® P300/G2; Ivoclar Vivadent AG, Ellwangen, Germany) according to the manufacturer's instructions.<sup>20</sup> All the measurements at the 36 (24 + 12) predefined points on each bridge were repeated after ceramic veneering (Fig. 5). In total, 240 marginal, 240 axial and 240 occlusal discrepancy values were recorded.

Initially, the normal distribution of the data was confirmed using the Shapiro–Wilk test. The data was normally distributed ( $p > 0.05$ ), so corresponding parameter tests were used. Student's paired *t*-test was used to study the mean differences in marginal, axial and occlusal accuracy before and after ceramic firing. The level of statistical significance was set at 0.05.

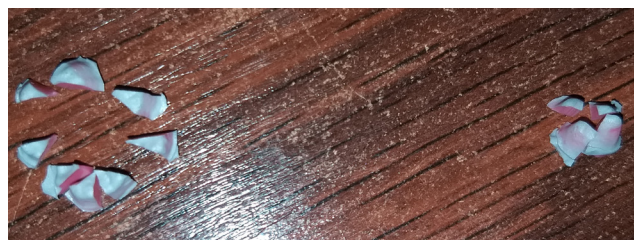


Fig. 3. Molar silicone replica divided into 8 parts and the premolar silicone replica divided into 4 parts

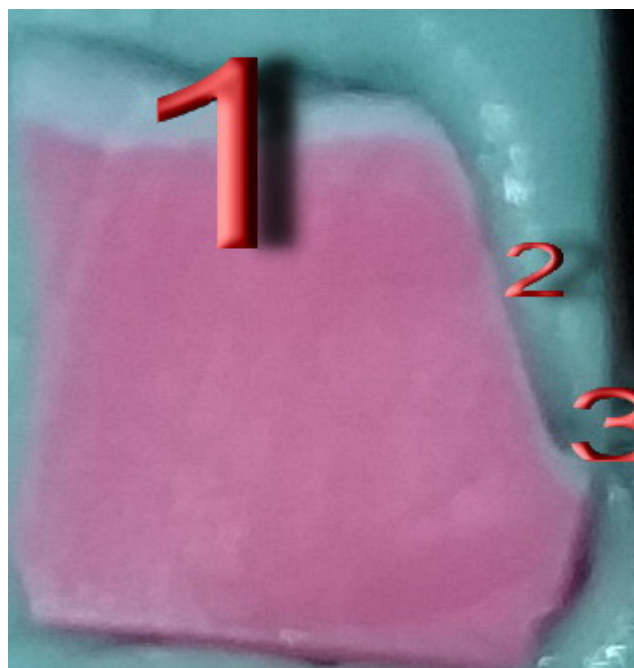


Fig. 4. Silicone replica technique sample, ready for the light microscope measurement of the occlusal (1), axial (2) and marginal (3) fit





Fig. 5. Silicone replica technique sample after ceramic firing

## Results

The mean values of marginal (156.08  $\mu\text{m}$ ), axial (95.75  $\mu\text{m}$ ) and occlusal (252.83  $\mu\text{m}$ ) accuracy in DMLS bridges before ceramic firing were better than those after ceramic firing (178.17  $\mu\text{m}$ , 106.75  $\mu\text{m}$  and 266.00  $\mu\text{m}$ , respectively). The comparison of the 2 phases of measurement showed that the largest values were observed in the case of the occlusal gap, whereas the axial walls were the smallest. The marginal gap was larger than the clinically acceptable range. Table 1 shows the descriptive analysis before and after ceramic firing, at 95% confidence interval (CI).

The Shapiro–Wilk test indicated that the study groups had a normal distribution ( $p > 0.05$ ). Student's  $t$ -test was therefore used to study the mean differences in marginal, axial and occlusal accuracy before and after ceramic firing; the results, presented in Table 2, indicated that there were no statistically differences between the 2 sets of measurements at the framework marginal ( $p = 0.197$ ), axial ( $p = 0.215$ ) or occlusal ( $p = 0.242$ ) regions.

## Discussion

The aim of this in vivo study was to examine the adaptation accuracy of dental metal-ceramic 3-unit bridges manufactured using DMLS, and to investigate the effects of porcelain firing on the marginal, axial and occlusal fitting of metal-ceramic bridges. The null hypothesis was that the ceramic firing process has no effect on the marginal, axial and occlusal adaptation of metal-ceramic bridges.

Metal-ceramic bridges are still the best choice in posterior prosthodontic treatment due to several advantages they have, especially their proven clinical effectiveness over the long term. There are some limitations for using these devices, such as many manual steps involved in their manufacture and large marginal gaps, which are an important factor affecting the durability of metal-ceramic bridges.<sup>5,6</sup> Ensuring a small marginal gap and good marginal fit (a significant criterion for achieving long-term clinical success) as well as the use of the new CAD-laser sintering technique to produce metal-ceramic frameworks have become prerequisites to avoid the disadvantages of the traditional method.<sup>11,30</sup>

There are many ways to measure the thickness of the cement film in the marginal area, as numerous studies have indicated,<sup>29</sup> but in an in vivo study, the silicone replica technique is the best to facilitate studying the marginal, axial and occlusal fit of fixed bridges.<sup>29</sup>

The CAD-DMLS technique makes use of scanners that have a precision of 20–40  $\mu\text{m}$ .<sup>31,32</sup> In the CAD-DMLS technique, stone model scanning and CAD software are used to define the finishing line of preparation, the path of bridge insertion and the 3D framework design. The thickness of the framework, the cement gap and the pontic design can be standardized with this technique,<sup>10</sup> and by using a CAD-DMLS machine that produces about 90 units per run, 450 units of crowns and bridges can be produced in 1 day.<sup>33</sup>

Table 1. Accuracy values for DMLS bridges for the specific locations measured at 2 stages (before and after ceramic firing)

Accuracy	Stage	N	M $\pm$ SD [ $\mu\text{m}$ ]	95% CI	
				upper bound	lower bound
Marginal	before porcelain firing	10	156.08 $\pm$ 43.25	187.02	125.14
	after porcelain firing	10	178.17 $\pm$ 57.47	219.28	137.05
Axial	before porcelain firing	10	95.75 $\pm$ 43.28	126.71	64.79
	after porcelain firing	10	106.75 $\pm$ 32.04	129.67	83.83
Occlusal	before porcelain firing	10	252.83 $\pm$ 105.37	328.21	177.45
	after porcelain firing	10	266.00 $\pm$ 87.53	328.62	203.38

M – mean; SD – standard deviation; CI – confidence interval.

Table 2. Results of Student's  $t$ -test performed before and after the ceramic firing of DMLS bridges

Accuracy	t-value	p-value	M $\pm$ SD	95% CI	
				upper bound	lower bound
Marginal	–1.394	0.197	–22.08 $\pm$ 50.11	–57.93	13.76
Axial	–1.335	0.215	–11.00 $\pm$ 26.05	–29.64	7.64
Occlusal	–1.252	0.242	–13.17 $\pm$ 33.25	–36.96	10.62

Some researchers have compared the DMLS technique with the casting method for internal and marginal fit, and have stated that the gaps in the case of DMLS frameworks are larger than the originally reported acceptable marginal fit values (125–150  $\mu\text{m}$ ).<sup>34,35</sup> In the current study, our descriptive analysis of the 2 stages – before and after ceramic firing – showed that the mean values of the marginal (156.08  $\mu\text{m}$ ), axial (95.75  $\mu\text{m}$ ) and occlusal (252.83  $\mu\text{m}$ ) fit before ceramic firing (i.e., after the production of the framework and before ceramic veneering) were better than those after ceramic veneering (178.17  $\mu\text{m}$ , 106.75  $\mu\text{m}$  and 266.00  $\mu\text{m}$ , respectively) (Table 1). The results of Student's *t*-test revealed no statistically significant differences between the 2 stages of measurement of the marginal ( $p = 0.197$ ), axial ( $p = 0.215$ ) and occlusal ( $p = 0.242$ ) regions (Table 2).

The null hypothesis was not rejected, since porcelain firing had no significant effects on the marginal, axial and occlusal adaptation of metal-ceramic bridges produced by means of DMLS. This result coincides with those of some other researchers,<sup>17,27</sup> but contradicts Kaleli and Saraç and Önöral et al., which conducted in vitro studies.<sup>25,26</sup> The current study differs from previous studies in that it studied the marginal application of bridges consisting of 3 parts; and it was an in vivo study.


In our study, all the measurements before and after ceramic firing indicated that the mean value of marginal discrepancy was higher than the clinically acceptable range, which might be due to many difficulties related to clinical work. Clinical studies cannot be controlled like in vitro studies, and the authors doubt if the latter are able to match clinical realities.

## Conclusions

Repeated firing had no significant influence on the marginal, axial or occlusal accuracy of metal frameworks produced using the DMLS method. For clinical application, however, further improvement of the DMLS system is urgently recommended. The marginal gaps in DLSM bridges significantly exceeded the permissible inaccuracy values of 100–120  $\mu\text{m}$  for prosthetic restorations.

### ORCID iDs

Qusay Khaznadar Nassif  <https://orcid.org/0000-0002-8563-4533>

Fendi Fendi Alshaarani  <https://orcid.org/0000-0003-3609-067X>

### References

- Lüthy H, Filser F, Loeffel O, Schumacher M, Gauckler LJ, Hammerle CHF. Strength and reliability of four-unit all ceramic posterior bridges. *Dent Mater.* 2005;21(10):930–937.
- Pjetursson BE, Sailer I, Makarov NA, Zwahlen M, Thoma DS. All-ceramic or metal-ceramic tooth-supported fixed dental prostheses (FDPs)? A systematic review of the survival and complication rates. Part II: Multiple-unit FDPs. *Dent Mater.* 2015;31(6):624–639.
- Sulaiman F, Chai J, Jameson LM, Wozniak WT. A comparison of the marginal fit of In-Ceram, IPS Empress and Procera crowns. *Int J Prosthodont.* 1997;10(5):478–484.
- Willer J, Rossbach A, Weber HP. Computer-assisted milling of dental restorations using a new CAD/CAM data acquisition system. *J Prosthet Dent.* 1998;80(3):346–353.
- Yeo IS, Yang JH, Lee JB. In vitro marginal fit of three all-ceramic crown systems. *J Prosthet Dent.* 2003;90(5):459–464.
- Kokubo Y, Tsumita M, Kano T, Sakurai S, Fukushima S. Clinical marginal and internal gaps of zirconia all-ceramic crowns. *J Prosthodont Res.* 2011;55(1):40–43.
- O'Brien WJ. *Dental Materials and Their Selection.* 4th ed. Hanover Park, IL: Quintessence Publishing; 2008:243–252.
- Naylor WP. *Introduction to Metal-Ceramic Technology.* 2nd ed. Hanover Park, IL: Quintessence Publishing; 2009:83–107.
- Strub JR, Rekow ED, Witkowski S. Computer-aided design and fabrication of dental restorations: Current systems and future possibilities. *J Am Dent Assoc.* 2006;137(9):1289–1296.
- Örtorp A, Jönsson D, Mouhsen A, Vult von Steyern P. The fit of cobalt-chromium three-unit fixed dental prostheses fabricated with four different techniques: A comparative in vitro study. *Dent Mater.* 2011;27(4):356–363.
- Azari A, Nikzad S. The evolution of rapid prototyping in dentistry: A review. *Rapid Prototyping J.* 2009;15(3):216–225.
- Sun J, Zhang FQ. The application of rapid prototyping in prosthodontics. *J Prosthodont.* 2012;21(8):641–644.
- Dikova T, Vasilev T, Dzhendov D, Ivanova E. Investigation the fitting accuracy of cast and SLM Co-Cr dental bridges using CAD software. *J of IMAB.* 2017;23(3):1688–1696.
- Kruth JP, Mercelis P, Van Vaerenbergh J, van Vaerenbergh J, Froyen L, Rombouts M. Binding mechanisms in selective laser sintering and selective laser melting. *Rapid Prototyping J.* 2005;11(1):26–36.
- Harish V, Mohamed Ali SA, Jagadesan N, et al. Evaluation of internal and marginal fit of two metal ceramic system – in vitro study. *J Clin Diag Res.* 2014;8(12):ZC53–ZC66.
- Kotila J, Syvänen T, Hänninen J, Latikka M, Nyrihilä O. Direct metal laser sintering – new possibilities in biomedical part manufacturing. *Mater Sci Forum.* 2007;534–536:461–464.
- Zeng L, Zhang Y, Liu Z, Wei B. Effects of repeated firing on the marginal accuracy of Co-Cr copings fabricated by selective laser melting. *J Prosthet Dent.* 2015;113(2):135–139.
- Nawafleh NA, Mack F, Evans J, Mackay J, Hatamleh MM. Accuracy and reliability of methods to measure marginal adaptation of crowns and FDPs: A literature review. *J Prosthodont.* 2013;22(5):419–428.
- Aljerf L. Effect of thermal-cured hydraulic cement admixtures on the mechanical properties of concrete. *Interceram.* 2015;64(8):346–356.
- Aljerf L. Reduction of gas emission resulting from thermal ceramic manufacturing processes through development of industrial conditions. *Sci J King Faisal Univ.* 2016;17(1):1–10.
- Gemalmaz D, Alkumru HN. Marginal fit changes during porcelain cycles. *J Prosthet Dent.* 1995;73(1):49–54.
- Shokry TE, Attia M, Mosleh I, Elhosary M, Hamza T, Shen C. Effect of metal selection and porcelain firing on the marginal accuracy of titanium-based metal ceramic restorations. *J Prosthet Dent.* 2010;103(1):45–52.
- Wolfart S, Wegner SM, Al-Halabi A, Kern M. Clinical evaluation of marginal fit of a new experimental all-ceramic system before and after cementation. *Int J Prosthodont.* 2003;16(6):587–592.
- Okutan M, Heydecke G, Butz F. Fracture load and marginal fit of shrinkage-free ZrSiO<sub>4</sub> all-ceramic crowns after chewing simulation. *J Oral Rehabil.* 2006;33(11):827–832.
- Kaleli N, Saraç D. Influence of porcelain firing and cementation on the marginal adaptation of metal-ceramic restorations prepared by different methods. *J Prosthet Dent.* 2017;117(5):656–661.
- Önöral Ö, Ulusoy M, Seker E, Etikan İ. Influence of repeated firings on marginal, axial, axio-occlusal, and occlusal fit of metal-ceramic restorations fabricated with different techniques. *J Prosthet Dent.* 2018;120(3):415–420.
- Kocaağaoğlu H, Albayrak H, Kilinc HI, Gümüş HÖ. Effect of repeated ceramic firings on the marginal and internal adaptation of metal-ceramic restorations fabricated with different CAD-CAM technologies. *J Prosthet Dent.* 2017;118(5):672–677.

28. Naumann M, Ernst J, Reich S, Weißhaupt P, Beuer F. Galvano- vs. metal-ceramic crowns: Up to 5-year results of a randomized split-mouth study. *Clin Oral Investig*. 2011;15(5):657–660.
29. Rahme HY, Tehini GE, Adib SM, Ardo AS, Rifai KT. In vitro evaluation of the “replica technique” in the measurement of the fit of Procera crowns. *J Contemp Dent Pract*. 2008;9(2):25–32.
30. Revilla-León M, Özcan M. Additive manufacturing technologies used for 3D metal printing in dentistry. *Curr Oral Health Rep*. 2017;4(3):201–208.
31. Sinirlioglu MC. Rapid manufacturing of dental and medical parts via LaserCUSING® technology using titanium and CoCr powder materials. US–Turkey Workshop On Rapid Technologies, Istanbul, Turkey, September 24, 2009:89–92.
32. Chua CK, Leong KF, Lim CS. *Rapid prototyping: Principles and Applications*. 3<sup>rd</sup> ed. Singapore: World Scientific Publishing; 2010:199–299.
33. Laser sintering-versatile production of tooling inserts, prototype parts and end products from metal powder. *International Powder Metallurgy Directory (IPMD)*. January 12, 2011. <http://www.ipmd.net/articles/articles/001087.html>. Accessed on April 1, 2011.
34. Kokubo Y, Ohkubo C, Tsumita M, Miyashita A, Vult von Steyern P, Fukushima S. Clinical marginal and internal gaps of Procera AllCeram crowns. *J Oral Rehabil*. 2005;32(7):526–530.
35. Tara MA, Eschbach S, Bohlsen F, Kern M. Clinical outcome of metal-ceramic crowns fabricated with laser-sintering technology. *Int J Prosthodont*. 2011;24(1):46–48.

# In vivo evaluation of the impact of various border molding materials and techniques on the retention of complete maxillary dentures

## Ocena in vivo wpływu różnych materiałów i technik uszczelnienia brzeżnego na utrzymanie protez całkowitych w szczęce

Tameem Khuder Jassim<sup>A-F</sup>, Ali Ehsan Kareem<sup>A-F</sup>, Mohamed Adnan Alloaibi<sup>A-F</sup>

Department of Prosthodontics, College of Dentistry, Mustansiriyah University, Baghdad, Iraq

A – research concept and design; B – collection and/or assembly of data; C – data analysis and interpretation; D – writing the article; E – critical revision of the article; F – final approval of the article

Dental and Medical Problems, ISSN 1644-387X (print), ISSN 2300-9020 (online)

*Dent Med Probl.* 2020;57(2):191–196

### Address for correspondence

Tameem Khuder Jassim  
E-mail: drtameemkh@gmail.com  
tameem.kh@uomustansiriyah.edu.iq

### Funding sources

None declared

### Conflict of interest

None declared

Received on September 13, 2019

Reviewed on November 3, 2019

Accepted on December 5, 2019

Published online on June 30, 2020

### Cite as

Jassim TK, Kareem AE, Alloaibi MA. In vivo evaluation of the impact of various border molding materials and techniques on the retention of complete maxillary dentures. *Dent Med Probl.* 2020;57(2):191–196. doi:10.17219/dmp/115104

### DOI

10.17219/dmp/115104

### Copyright

© 2020 by Wrocław Medical University

This is an article distributed under the terms of the

Creative Commons Attribution 3.0 Unported License (CC BY 3.0)

(<https://creativecommons.org/licenses/by/3.0/>).

## Abstract

**Background.** Different techniques and impression materials are employed in the process of fabricating complete denture (CD) bases.

**Objectives.** The aim of this study was to determine differences in the denture base retention for acrylic maxillary CDs when using 2 different techniques and impression materials. Specifically, the green stick compound impression material was used for the sectional border molding technique and this was compared to using the addition vinyl silicone impression material with the single-step technique.

**Material and methods.** A crossover study was conducted on 10 participants who were completely edentulous in the upper arch (6 men and 4 women), aged 43–70 years. The participants' trays were split into 2 treatment groups: the P-group; and the Z-group. Addition vinyl silicone was used for single-step border molding in the P-group, followed by light-body final-wash impression. For the Z-group, the green stick compound was used for sectional border molding, followed by a final wash using a zinc oxide-eugenol material. To quantify the retention force of the denture base in kilograms-force, a digital force gauge was used.

**Results.** The measurements indicated significantly higher mean retention values ( $p = 0.000$ ) in the P-group ( $4.02 \pm 1.66$  kgf) as compared to the Z-group ( $1.48 \pm 0.90$  kgf).

**Conclusions.** The results suggest the superiority of using the single-step border molding technique in the upper arch with the addition vinyl silicone material owing to the enhanced base retention of the acrylic denture base.

**Key words:** complete denture, dental impression technique, prosthesis retention

**Słowa kluczowe:** proteza całkowita, technika wycisku stomatologicznego, utrzymanie protezy

## Introduction

Dental disease is a condition that continues to heavily affect the older portion of the population; it is likely to cause such individuals to lose most of their natural teeth.<sup>1</sup> This condition can lead to complete edentulism, brought about by the loss of the individual's entire set of original teeth along with the resorption of the alveolar bone. The impact of such a loss is immense – it influences chewing, phonation and other stomatognathic functions, at the same time resulting in adverse social consequences. Furthermore, from a clinical standpoint, one systematic review which assessed the association between oral function and dentition determined that the possession of less than 20 teeth, of which 9 or 10 pairs are in contact, is linked to a diminished masticatory ability and efficiency.<sup>2</sup>

One of the main aims of prosthetic dentistry is to improve the performance of removable prostheses in terms of their retention, stability and denture support.<sup>3</sup> This can be achieved through the use of individual trays and impression materials of a higher accuracy, as recommended in various studies.<sup>4,5</sup> Making impressions is one of the most significant stages of denture fabrication. Boucher laid out 5 primary objectives of complete denture (CD) impressions: retention; stability; support; esthetic value; and the preservation of the alveolar ridge.<sup>6</sup> In CD prosthodontics, the accuracy of the final impression stage is of crucial importance in obtaining a CD. It involves an initial step of determining the vestibule with the use of the border molding technique, and then making the impression of the target edentulous arch.<sup>7</sup>

One can describe border molding as “the shaping of impression material along the border areas of an impression tray by functional or manual manipulation of the soft tissue adjacent to the borders to duplicate the contour and size of the vestibule”<sup>8</sup>[p.e17] It can also be described as the means of establishing the prosthesis extension through manual or functional tissue control, leading to shaping the border region of the material used in an impression.<sup>8</sup>

When utilising a low-fusing impression compound, one study estimated that 17 insertions by several dentists would be needed to perform border molding in the same patient.<sup>9</sup> Although the produced impressions were of high precision, the use of a low-fusing impression compound in border molding was time-consuming and laborious, particularly for new students. It is preferable that the chosen border molding material should be one that establishes contact with the whole vestibular sulcus area in its plastic state, and in a single insertion.<sup>9</sup> A material that enables the synchronized molding of all borders provides the following benefits: fewer insertions of trays for border molding are needed; and the concurrent formation of all borders prevents faults in one section from impacting the contours in another section.<sup>10</sup>

When employing the sectional technique, the material of choice is a low-fusing impression compound.<sup>11</sup> On the other hand, polyether with the addition of silicone of various viscosity is used in the single-step border molding technique.<sup>12,13</sup> When evaluated using the OHIP-Edent (Oral Health Impact Profile for edentulous patients) scale, which assesses the quality of dentures and the masticatory ability, the use of the conventional technique (with a low-fusing material) for forming dental prostheses does not provide as satisfactory results in terms of clinical performance as the more streamlined technique (using silicone). Furthermore, the adjustment time is not any longer in the case of the streamlined technique; rather, the involved time and financial cost are decreased in comparison with the conventional technique. This makes the streamlined technique ideal for the formation of CDs.<sup>14</sup> The streamlined technique involves the use of silicone in place of a low-fusing compound, and the advent of a silicone elastomer constitutes significant development in the formation of denture impressions.<sup>15</sup> Silicone is not only easy to mold, but it also offers high levels of precision and dimensional stability. As a substitute for a low-fusing compound, heavy-body putty silicone is frequently selected for border molding, as it is both viscous and kneadable, has a homogenous texture, and is slow-setting. Thus, it allows the silicone to be kneaded along the entire border of a tray and to be formed in one attempt.<sup>13</sup>

The aim of this study was to compare the use of the green stick compound as a low-fusing material together with zinc oxide-eugenol impression paste with the use of addition silicone (polyvinyl siloxane) and light-body addition silicone to determine the retention of the acrylic complete upper denture base.

## Material and methods

Ten completely edentulous participants were randomly selected for the study. All the participants had visited the clinic for prosthodontic restoration through new upper CDs. The exclusion criteria comprised a fibrous ridge, ridge resorption, tissue undercut, bony exostoses, and tori. The ethical standards outlined in the 1964 Declaration of Helsinki were followed for all methodologies that involved human subjects (approval No. PD/1666/1). All participants were fully informed about all the methodologies used in the study, and consent was attained from all participants following their approval.

A suitable stock tray was chosen together with the red thermoplastic compound impression material (Hoffmann Dental Manufaktur GmbH, Berlin, Germany) for the formation of the primary impressions of the upper arch. The primary impressions were then poured with dental plaster for the formation of the primary casts. These primary casts allowed for the subsequent formation of a custom impression tray for each patient using light-cured acrylic resin.

The trays of the participants were split into 2 groups based on the material used for the final impression. The P-group had border moldings formed of the addition vinyl silicone impression material (Bisico Bielefelder Dentsilicone GmbH & Co. KG, Bielefeld, Germany) with the final impressions made with a light-body material cartridge (Aquasil® Ultra Smart Wetting® Impression Material; Dentsply Sirona, York, USA) (Fig. 1A,1B). The Z-group had border moldings formed of the green stick compound impression material (Hoffmann Dental Manufaktur GmbH) with a zinc oxide-eugenol material (SS White® Impression Paste; Prima Dental Group, Gloucester, UK) used for the final impressions (Fig. 1C,1D). All materials were used as outlined in the manufacturers' guidelines. The border of the denture base was properly shaped, as it was placed in the mouth and molded in accordance with the lip and cheek muscles for each participant.

A master cast was generated by pouring all impressions with type III dental stone (Elite Rock®/sandy brown; Zhermack S.p.A., Badia Polesino, Italy). An orthodontic self-curing acrylic resin material (Orthocryl®; DENTAU-RUM GmbH & Co. KG, Ispringen, Germany) was used for the acrylic denture base of each master cast. Next, a 0.9-gauge, stainless steel U-shaped wire was embedded inside the acrylic denture base material at the palatal rugae area, at the anterior end of the acrylic (Fig. 2). The master cast was then cured for 20 min in the Ivomat® curing machine (MAJOR MINI 2000; Ivoclar Vivadent S.r.l., Casalecchio di Reno, Italy) containing water heated to 40–46°C with the pressure maintained at 30 psi, as outlined in the manufacturer's instructions. Two denture bases – one for each border molding and impression group – were formed for each participant. The participants were then seated upright with their head secured onto a head rest prior to the insertion of the denture base into their mouth. The retention force of each denture base was measured in kilograms-force (kgf) using

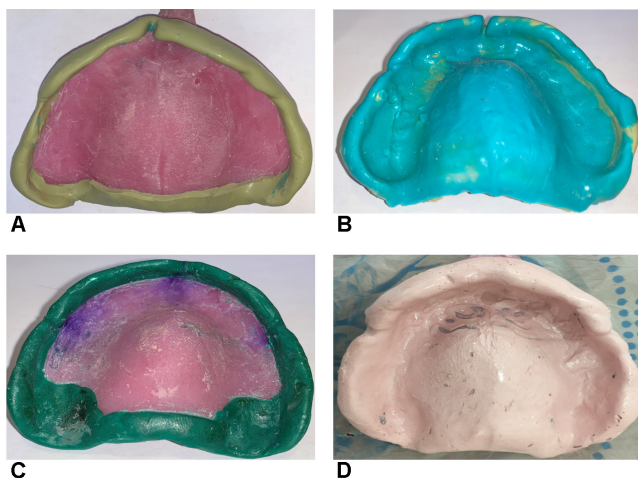


Fig. 1. Final impression using the addition vinyl silicone material and a light-body final impression material with the single-step technique (A,B), and using the green stick compound material and zinc oxide-eugenol paste with the sectional technique (C,D)

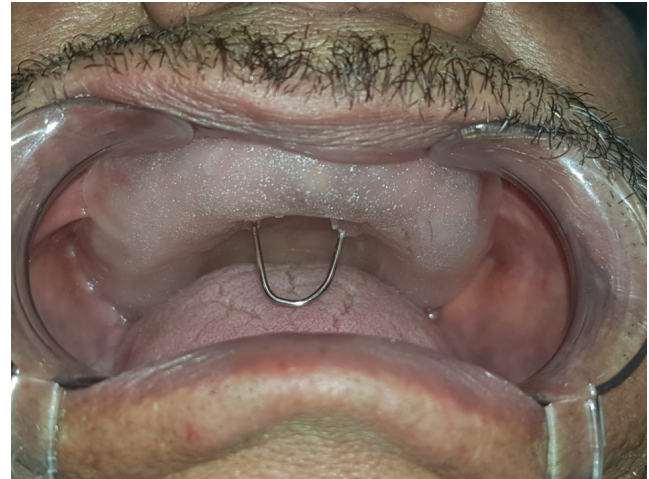


Fig. 2. Stainless steel U-shaped wire embedded inside the self-cured acrylic resin material at the palatal rugae area in the anterior palate

a specifically designed digital force gauge. To link the U-shaped loop in the denture base with the force gauge, a hook was used between them (Fig. 3). Next, downward pulling force was applied to each denture until it was displaced from the mouth (Fig. 4). This step was repeated 4 additional times for a total of 5 runs. To eliminate the bias caused by variations in the technique, all clinical and laboratory procedures were carried out by the same individual.

The IBM SPSS Statistics for Windows software, v. 20 (IBM Corp., Armonk, USA) was used to analyze all the generated data. To assess the degree of normality of the data, the Shapiro–Wilk test was used. This was followed by the analysis of the demographic data (age and gender) for differences using the  $\chi^2$  test, with a  $p$ -value of  $<0.05$  indicating statistical significance. Finally, the difference between the mean values obtained for the quantified retention force for each treatment group was analyzed using the Mann–Whitney test, with a  $p$ -value of  $<0.05$  indicating statistical significance.



Fig. 3. Digital force gauge used to measure the retention force of the denture base in kilograms-force



Fig. 4. Pulling force applied downward until the denture was displaced

## Results

This study used a crossover clinical design to quantify the retention force for each participant's denture base when using 2 types of impression materials and 2 different border molding methods. Six men and 4 women ( $N = 10$ ), aged 43–70 years, took part in the study. The analysis of age and gender indicated no significant differences between the participants for these variables. The mean values (kgf) of the measured retention force with regard to the treatment groups and particular patients are illustrated in Fig. 5. Table 1 lists the mean values (kgf) of the quantified retention force for each treatment group. The data indicates that the retention values for the P-group – with addition vinyl silicon impression border molding material with a light-body final impression – were significantly greater than those for the Z-group, with green stick impression compound material for border molding with a zinc oxide-eugenol final impression.

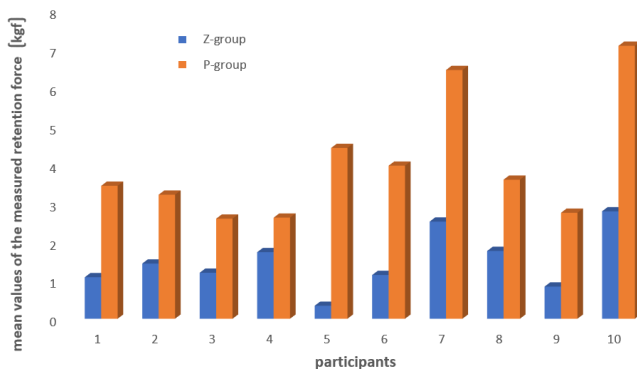


Fig. 5. Mean values of the measured retention force with regard to the treatment groups and particular patients

Table 1. Comparison of the mean values of the measured retention force with regard to the treatment groups

Treatment group	N	Retention force [kgf]	p-value
P-group	10	4.02 ± 1.66	0.000*
Z-group	10	1.48 ± 0.90	

\* statistically significant ( $p < 0.05$ ); Mann–Whitney test.

## Discussion

The CD retention, stability and occlusal vertical dimension are all important, since inadequate retention and stability may significantly affect chewing, and may subsequently increase the patient's complaints.<sup>16</sup> Despite the fact that CD patients adapt well to their dentures in the mouth after some time of usage,<sup>17</sup> it is important to obtain a CD with good retention by ensuring the close adaptation of the denture base to the mucosal bearing tissues.<sup>18</sup>

The CD retention may be influenced by various physical factors, including the denture and the mucosa adhesion, saliva cohesion, salivary consistency, and salivary flow.<sup>19</sup> Furthermore, the type of impression material used and the selected border molding technique both highly impact the retention force of a CD.

Materials frequently used as impression materials are polyethers, polysulfides, hydrocolloids, and addition silicones. Based on the indications of the manufacturer, several of these materials are packaged in cartridges for ease of auto-mixing, which consequently decreases the consumption of time. Moreover, such packaging reduces waste and ensures that the material is free of bubbles when mixed, thereby enhancing the precision of casts. It also decreases the required effort and manipulation time, which is especially beneficial to new students, who may be working with the elderly – as is typically the case when rehabilitating CD patients.<sup>9</sup> Formerly, zinc oxide-eugenol impression paste, impression plaster and impression compound material were the materials most commonly used. They were not only challenging with respect to manipulation, but they would usually alter or fracture if withdrawn from a deep undercut.<sup>20</sup> Considering that the age of the participants in this study was between 43 and 70 years, then based on the findings, there should be a review of the daily clinical use of zinc oxide as a final impression material, following the green stick compound for the formation of CD impressions. The findings indicate that there is a significant advantage of changing to the new technique using addition vinyl silicon for border molding, followed by a light-body material for final impressions employing the single-step technique. This would help to alleviate the patient's burden and reduce the time spent in the clinic.

Another noteworthy point is the impact of gender on the CD retention, as women are reported to show greater degrees of resorption than men.<sup>21</sup> In the case of women,

the growth and development of osteoclasts take more time as a result of a deficiency in estrogen levels; this, in turn, leads to increased bone resorption, which places female patients at a higher risk of more extensive ridge resorption.<sup>22</sup> The finding of this study, however, was not statistically significant with respect to the difference between genders, although only 4 women were included in the study. Our results are further supported by research conducted by Khuder et al., who determined that no association existed between advanced bone resorption and the patients' age and gender.<sup>23</sup>

In the present study, the mean retention force for the denture base material on insertion was decreased when the green stick for border molding and a zinc oxide material for the final impression were used. The observed mean retention values were significantly greater when the addition vinyl silicon border molding material and a light-body final impression material were employed. The findings of this study are supported by the research of Pachar et al., where the green stick compound with light-body final impressions yielded the lowest mean CD retention value.<sup>19</sup> That said, in that study, the mean retention value for green stick border molding was greater than the value attained in this study, with 4.59 kgf in the former compared to 1.48 kgf in the latter. This discrepancy can be explained by the variation in the final impression material used in the 2 studies; Pachar et al.<sup>19</sup> used light-body addition silicone and this study used a zinc-oxide impression material. These findings are also supported by a study performed by Gupta et al.,<sup>24</sup> who reported retention values for the green stick material of 1.50 kgf, which is in keeping with the results of this study (1.48 kgf). In contrast, their result attained for light-body polyvinyl siloxane used as an impression material was lower (1.95 kgf) than that attained in this study (4.02 kgf). This discrepancy, however, could be attributed to the use of different border molding materials, with heavy-body addition silicone (putty) used in Gupta et al.'s study<sup>24</sup> and addition vinyl silicone used in this study.

Another study, conducted by Tasleem et al., reported contrasting findings, where 2 groups of edentulous patients were only found to differ in the time taken to complete the impression technique; no significant differences were noted with respect to the border molding material employed.<sup>25</sup> However, the clinical significance of the findings of Tasleem et al. is questionable, as although their study was a cross-sectional study, it was based on a questionnaire and the assessment of the retention force was dependent on the patients' perspective.<sup>25</sup>

The findings of the present study also contradict those of Qanungo et al., who determined that the sectional technique was more retentive than the single-step border molding technique.<sup>26</sup> Again, this discrepancy may be attributed to the nature of the impression material used. In their study, irreversible hydrocolloid was used as the primary impression material, whereas in the present study, an impression compound was used as the primary impression material.


Finally, only 1 form of polyvinyl siloxane impression material was assessed in this study, even though various different forms are available on the market. This is due to a high cost of polyvinyl siloxane materials. This study did not evaluate the time involved in completing the impression procedure. Furthermore, the study did not consider the retention force of the denture base for the lower arch. Our study concentrated solely on assessing the denture base retention force for the upper arch, so further research is proposed for assessing these other factors.


## Conclusions

After taking into account the limitations of this study, it was concluded that the use of the addition vinyl silicone material together with a light-body final impression material and the single-step technique resulted in superior retention in the acrylic denture base over the denture base formed with the use of the green stick and zinc-oxide eugenol as the final impression material using the sectional technique.

### ORCID iDs

Tameem Khuder Jassim  <https://orcid.org/0000-0002-7630-599X>

Ali Ehsan Kareem  <https://orcid.org/0000-0001-9897-0053>

Mohamed Adnan Alloaibi  <https://orcid.org/0000-0002-3646-9914>

### References

- Allen PF, McMillan AS. A longitudinal study of quality of life outcomes in older adults requesting implant prostheses and complete removable dentures. *Clin Oral Implants Res.* 2003;14(2):173–179.
- Gotfredsen K, Walls AWG. What dentition assures oral function? *Clin Oral Implants Res.* 2007;18(Suppl 3):34–45.
- Papadiochou S, Emmanouil I, Papadiochos I. Denture adhesives: A systematic review. *J Prosthet Dent.* 2015;113(5):391–397.e2.
- Rao S, Chowdhary R, Mahoorkar S. A systematic review of impression technique for conventional complete denture. *J Indian Prosthodont Soc.* 2010;10(2):105–111.
- Petrie CS, Walker MP, Williams K. A survey of U.S. prosthodontists and dental schools on the current materials and methods for final impressions for complete denture prosthodontics. *J Prosthodont.* 2005;14(4):253–262.
- Boucher CO. Complete denture impressions based upon the anatomy of the mouth. *J Am Dent Assoc.* 1944;31(17):1174–1181.
- Davis DM. Developing an analogue/substitute for the maxillary denture-bearing area. In: Zarb GA, Bolender CL, Eckert SE, et al., eds. *Prosthodontic Treatment for Edentulous Patients: Complete Dentures and Implant-Supported Prostheses.* 12<sup>th</sup> ed. St. Louis, USA: Mosby; 2004:211–231.
- The glossary of prosthodontic terms: Ninth edition. *J Prosthet Dent.* 2017;117(5S):e1–e105.
- Woelfel JB, Hickey JC, Berg T Jr. Contour variations in one patient's impressions made by seven dentists. *J Am Dent Assoc.* 1963;67:1–9.
- Smith DE, Toolson LB, Bolender CL, Lord JL. One-step border molding of complete denture impressions using a polyether impression material. *J Prosthet Dent.* 1979;41(3):347–351.
- Friedman S. Edentulous impression procedures for maximum retention and stability. *J Prosthet Dent.* 1957;7(1):14–26.
- Chaffee NR, Cooper LF, Felton DA. A technique for border molding edentulous impressions using vinyl polysiloxane material. *J Prosthodont.* 1999;8(2):129–134.



13. Solomon EGR. Single stage silicone border molded closed mouth impression technique – part II. *J Indian Prosthodont Soc.* 2011;11(3):183.
14. Ye Y, Sun J. Simplified complete denture: A systematic review of the literature. *J Prosthodont.* 2017;26(4):267–274.
15. Marxkors R. Die Funktionsabformung. *Dtsch Zahnärztl Z.* 1970;25:58–63.
16. Medeiros Ribeiro JA, Bastos Machado de Resende CM, Correia Lopes AL, Mestriner W Jr, Roncalli AG, Farias-Neto A, da Fonte Porto Carreiro A. Evaluation of complete denture quality and masticatory efficiency in denture wearers. *Int J Prosthodont.* 2012;25(6):625–630.
17. Raftu G, Sin EC, Leon A, Caraiane A, Buştiuc SG. The clinical and statistical study on the quality of complete acrylic dentures. *Rom J Oral Rehabil.* 2019;11(1):116–120.
18. Giglio JJ, Lace WP, Arden H. Factors affecting retention and stability of complete dentures. *J Prosthet Dent.* 1962;12(5):848–856.
19. Pachar RB, Singla Y, Kumar P. Evaluation and comparison of the effect of different border molding materials on complete denture retention: An in vivo study. *J Contemp Dent Pract.* 2018;19(8):982–987.
20. Anusavice KJ, Shen C, Rawls HR, eds. *Phillips' Science of Dental Materials.* 11<sup>th</sup> ed. St. Louis, USA: Saunders; 2003:177–178.
21. Jayaram B, Shenoy KK. Analysis of mandibular ridge resorption in completely edentulous patients using digital panoramic radiography. *J Dent Med Sci.* 2017;16:66–73.
22. Nishimura I, Hosokawa R, Kaplan ML, Atwood DA. Animal model for evaluating the effect of systemic estrogen deficiency on residual ridge resorption. *J Prosthet Dent.* 1995;73(3):304–310.
23. Khuder T, Yunus N, Sulaiman E, Ibrahim N, Khalid T, Masood M. Association between occlusal force distribution in implant overdenture prostheses and residual ridge resorption. *J Oral Rehabil.* 2017;44(5):398–404.
24. Gupta R, Luthra RP, Mehta S. Comparative analysis of two border molding techniques and materials on maxillary complete denture retention – an in-vivo study. *J Adv Med Dent Scie Res.* 2015;3(4):109–112.
25. Tasleem R, Bin Saeed MH, Javed MU. Comparison of complete denture fabricated by two different border molding materials, in terms of patients' satisfaction. *J Ayub Med Coll Abbottabad.* 2013;25(3–4):78–80.
26. Qanungo A, Aras MA, Chitre V, Coutinho I, Rajagopal P, Mysore A. Comparative evaluation of border molding using two different techniques in maxillary edentulous arches: A clinical study. *J Indian Prosthodont Soc.* 2016;16(4):340–345.

# Clinical outcomes of lithium disilicate glass-ceramic crowns fabricated with CAD/CAM technology: A systematic review

## Ocena kliniczna koron szklano-ceramicznych z dwukrzemianu litu wytwarzanych w technologii CAD/CAM – systematyczny przegląd piśmiennictwa

Ahmed Aziz<sup>1,A–E</sup>, Omar El-Mowafy<sup>2,A–C,E,F</sup>, Saira Paredes<sup>3,A–C,E,F</sup>

<sup>1</sup> Department of Preventive and Restorative Dentistry, College of Dental Medicine, University of Sharjah, UAE

<sup>2</sup> Department of Restorative Dentistry, Faculty of Dentistry, University of Toronto, Canada

<sup>3</sup> Private practice, Toronto, Canada

A – research concept and design; B – collection and/or assembly of data; C – data analysis and interpretation;

D – writing the article; E – critical revision of the article; F – final approval of the article

Dental and Medical Problems, ISSN 1644-387X (print), ISSN 2300-9020 (online)

*Dent Med Probl.* 2020;57(2):197–206

### Address for correspondence

Ahmed Aziz

Email: a.aziz@sharjah.ac.ae

### Funding sources

None declared

### Conflict of interest

None declared

Received on October 29, 2019

Reviewed on November 26, 2019

Accepted on December 19, 2019

Published online on June 30, 2020

### Cite as

Aziz A, El-Mowafy O, Paredes S. Clinical outcomes of lithium disilicate glass-ceramic crowns fabricated with CAD/CAM technology: A systematic review. *Dent Med Probl.* 2020;57(2):197–206. doi:10.17219/dmp/115522

### DOI

10.17219/dmp/115522

### Copyright

© 2020 by Wrocław Medical University

This is an article distributed under the terms of the

Creative Commons Attribution 3.0 Unported License (CC BY 3.0)

(<https://creativecommons.org/licenses/by/3.0/>).

### Abstract

The use of ceramic materials and the computer-aided design/computer-aided manufacturing (CAD/CAM) technology for the fabrication of complete-coverage restorations has significantly increased in the last decade. The aim of this study was to evaluate the survival rate of anterior and posterior monolithic and bilayered lithium disilicate glass-ceramic (LDGC) CAD/CAM crowns, and to identify the types of complications associated with the main clinical outcomes reported in clinical trials. MEDLINE/PubMed, Embase, Scopus, Web of Science, Cochrane Library, and ClinicalTrials.gov were searched by 2 independent reviewers for clinical studies published between 2006 and 2019, following the Preferred Reporting Items for Systematic Reviews and Meta-Analyses (PRISMA) statement. The electronic search was supplemented by a hand search. Quality assessment for the included studies was performed. Qualitative and quantitative data was extracted from each study. Out of 219 studies, 6 studies that evaluated LDGC CAD/CAM crowns were identified and used for data extraction. The included studies had 154 participants, who received 204 crowns.

The short- to medium-term survival and success rates were high. Biological complications occurred more frequently than technical complications. No esthetic complications were reported. This review indicated that the medium-term survival rate of LDGC CAD/CAM crowns was high. Further multicenter studies with longer follow-ups and larger sample sizes are needed in order to augment the data already in existence.

**Key words:** survival, glass-ceramic, prosthodontics, dental porcelain, computer-aided design/computer-aided manufacturing

**Słowa kluczowe:** przetrwanie, szklano-ceramiczne, protetyka stomatologiczna, ceramika stomatologiczna, komputerowo wspomagane projektowanie i produkcja

## Introduction

The advance of digital dentistry and a high demand for metal-free restorations have led to rapid evolution in processing technologies as well as to the development of newer restorative materials. Several clinical studies have demonstrated that all-ceramic crowns, particularly lithium disilicate glass-ceramic (LDGC), may be a potentially promising alternative to metal-based crowns.<sup>1–9</sup>

Lithium disilicate glass-ceramic materials are available as pressable (IPS® e.max Press; Ivoclar Vivadent AG, Schaan, Liechtenstein) and machinable for the computer-aided design/computer-aided manufacturing (CAD/CAM) processing technology (IPS e.max CAD; Ivoclar Vivadent). Since it was introduced in 2006, the latter has become widely used because of its excellent performance both *in vitro* and *in vivo*.<sup>10,11</sup> Due to its improved translucency and good mechanical properties, IPS e.max CAD can be used as a core material with the layering technique or as a fully anatomical restoration.<sup>12,13</sup> Lithium disilicate glass-ceramic monolithic blocks have become the material of choice for chairside systems due to their high strength and greater translucency as compared to other ceramic blocks.<sup>14</sup> However, the use of LDGC crowns in the bilayered arrangement has not gained popularity due to a weak link between the core and the veneering porcelain, which caused pre-mature failure. IPS e.max CAD demonstrates excellent biomechanical characteristics, as it exhibits a flexural strength of 360 MPa after complete crystallization.<sup>15</sup> A significant increase in the strength of the restoration takes place when an adhesive cement is used rather than a conventional one, as concluded in an *in-vitro* study done in 2006.<sup>16</sup>

The blocks are manufactured by the continuous pressure casting of transparent glass ingots to obtain a defect-free block without pores or pigments. The blocks are made available for milling in the CAD/CAM machine in a partially crystallized, 'soft' state to minimize the damage to the material caused by the wear of the milling diamond burs.<sup>17</sup> IPS e.max CAD blocks are composed of 0.2–1.0-micrometer lithium metasilicate

crystals ( $\text{Li}_2\text{SiO}_3$ ) (40.0% by volume); blocks in this state appear blue-violet. These crystals give the material favorable processing properties, a moderately high strength and a high edge stability. After milling, the restoration undergoes a 2-stage firing process for <20 min in order to complete the crystallization process, during which lithium disilicate crystals ( $\text{Li}_2\text{Si}_2\text{O}_5$ ) are formed, giving the restoration its final shade and the desired high strength. The resulting ceramic is composed of fine grains of size 1.5  $\mu\text{m}$  and 70.0% of crystals by volume.

Due to its reliable performance, the LDGC material is indicated for several types of dental restorations, such as inlays, onlays, veneers, crowns, and implant-supported crowns.<sup>11</sup> Several clinical studies have reported the clinical performance and survival rate of LDGC CAD/CAM crowns.<sup>1–9</sup> A systematic review needs to be conducted in order to combine the findings from these studies and to establish overall conclusions about their clinical performance. Therefore, the aim of this systematic review was to evaluate the survival rate of anterior and posterior monolithic and bilayered LDGC crowns manufactured with CAD/CAM systems as well as to identify the types of clinical complications reported in clinical trials.

## Material and methods

This review was conducted in accordance with the Preferred Reporting Items for Systematic Reviews and Meta-Analyses (PRISMA) statement.<sup>18</sup>

### Eligibility criteria

A PICOS question was used to identify studies in this review: P (population) – patients who received ceramic crowns; I (intervention) – crowns made of glass ceramic; C (comparison) – not applicable in this study; O (outcomes) – survival rate and type of complication; S (study type) – randomized controlled trials (RCTs) and clinical follow-up studies. The inclusion and exclusion criteria are listed in Table 1.

Table 1. Inclusion and exclusion criteria

Criteria	Description
Inclusion criteria	– clinical studies including RCTs, prospective and retrospective cohort studies
	– articles published in peer-reviewed journals
	– studies that included patients examined clinically with a minimum follow-up of 2 years
Exclusion criteria	– studies that report on the clinical performance of tooth-supported crowns
	– <i>in vitro</i> studies, reviews, case reports, and studies not published as full articles
	– studies with a follow-up of <12 months
	– studies based on chart reviews and interviews
	– studies that report on the clinical performance of different all-ceramic materials, such as zirconia
	– studies that report on the clinical performance of implant-supported LDGC crowns
	– reports on FPDs

RCT – randomized clinical trial; LDGC – lithium disilicate glass-ceramic; FPD – fixed partial denture.

## Information sources and search strategy

Several electronic databases, including MEDLINE/ PubMed, Embase, Scopus, Web of Science, and Cochrane Library were searched to identify clinical trials performed to evaluate the clinical performance of LGDC crowns fabricated with CAD/CAM systems. The search was carried out from January 2006 (the year in which IPS e.max CAD was introduced) until June 2019, and it was limited to human studies and the English language only. The search was extended to find unpublished and ongoing

clinical trials using ClinicalTrials.gov (www.clinicaltrials.gov). The search strategies defined for the databases described above are listed in Appendix 1. The appropriate search terms for the electronic search were key words, Medical Subject Headings (MeSH) and subject headings. The electronic search was further supplemented by the manual search of 4 different journals: *The International Journal of Prosthodontics*, *Journal of Prosthodontics*, *Journal of Prosthetic Dentistry*, and *Journal of Esthetic and Restorative Dentistry*.

### Appendix 1. Search strategy

#### PubMed

- 1 lithium disilicate.mp. (578)
- 2 Crowns/ (15475)
- 3 Dental Restoration Failure/ (7474)
- 4 dental restoration, permanent/ or inlays/ (22529)
- 5 "glass ceramic\*.mp. [mp=title, abstract, original title, name of substance word, subject heading word, floating sub-heading word, keyword heading word, protocol supplementary concept word, rare disease supplementary concept word, unique identifier, synonyms] (1811)
- 6 "crown\*.mp. [mp=title, abstract, original title, name of substance word, subject heading word, floating sub-heading word, keyword heading word, protocol supplementary concept word, rare disease supplementary concept word, unique identifier, synonyms] (36366)
- 7 (dental adj2 restor\*).mp. [mp=title, abstract, original title, name of substance word, subject heading word, floating sub-heading word, keyword heading word, protocol supplementary concept word, rare disease supplementary concept word, unique identifier, synonyms] (30249)
- 8 "clinical performance".mp. [mp=title, abstract, original title, name of substance word, subject heading word, floating sub-heading word, keyword heading word, protocol supplementary concept word, rare disease supplementary concept word, unique identifier, synonyms] (6738)
- 9 failure.mp. [mp=title, abstract, original title, name of substance word, subject heading word, floating sub-heading word, keyword heading word, protocol supplementary concept word, rare disease supplementary concept word, unique identifier, synonyms] (740680)
- 10 success.mp. [mp=title, abstract, original title, name of substance word, subject heading word, floating sub-heading word, keyword heading word, protocol supplementary concept word, rare disease supplementary concept word, unique identifier, synonyms] (212925)
- 11 survival.mp. [mp=title, abstract, original title, name of substance word, subject heading word, floating sub-heading word, keyword heading word, protocol supplementary concept word, rare disease supplementary concept word, unique identifier, synonyms] (1003959)
- 12 treatment outcome.mp. or exp Treatment Outcome/ (909585)
- 13 exp Dental Porcelain/ (10050)
- 14 Lithium Compounds/ (2759)
- 15 1 or 5 or 13 or 14 (13806)
- 16 3 or 8 or 9 or 10 or 11 or 12 (2470226)
- 17 longevity.mp. (35015)
- 18 "all ceramic".mp. (1712)
- 19 16 or 17 (2495410)
- 20 15 or 18 (14260)
- 21 "CAD CAM".mp. (2268)
- 22 exp Computer-Aided Design/ (16406)
- 23 21 or 22 (16808)
- 24 2 or 4 or 6 or 7 (63551)
- 25 19 and 20 and 24 (1829)
- 26 23 and 25 (401)
- 27 limit 26 to (clinical study or clinical trial, all or clinical trial, phase i or clinical trial, phase ii or clinical trial, phase iii or clinical trial, phase iv or clinical trial or controlled clinical trial or multicenter study or pragmatic clinical trial or randomized controlled trial) (56)

#### Embase

- 1 lithium disilicate.mp. (667)
- 2 "glass ceramic\*.mp. [mp=title, abstract, heading word, drug trade name, original title, device manufacturer, drug manufacturer, device trade name, keyword, floating subheading word, candidate term word] (2087)
- 3 "crown\*.mp. [mp=title, abstract, heading word, drug trade name, original title, device manufacturer, drug manufacturer, device trade name, keyword, floating subheading word, candidate term word] (55906)
- 4 (dental adj2 restor\*).mp. [mp=title, abstract, heading word, drug trade name, original title, device manufacturer, drug manufacturer, device trade name, keyword, floating subheading word, candidate term word] (6613)
- 5 "clinical performance".mp. [mp=title, abstract, heading word, drug trade name, original title, device manufacturer, drug manufacturer, device trade name, keyword, floating subheading word, candidate term word] (9743)
- 6 failure.mp. [mp=title, abstract, heading word, drug trade name, original title, device manufacturer, drug manufacturer, device trade name, keyword, floating subheading word, candidate term word] (1388858)
- 7 success.mp. [mp=title, abstract, heading word, drug trade name, original title, device manufacturer, drug manufacturer, device trade name, keyword, floating subheading word, candidate term word] (354138)
- 8 survival.mp. [mp=title, abstract, heading word, drug trade name, original title, device manufacturer, drug manufacturer, device trade name, keyword, floating subheading word, candidate term word] (1535084)
- 9 treatment outcome.mp. or exp Treatment Outcome/ (1472690)
- 10 CAD CAM.mp. or exp Computer-Aided Design/ (24107)
- 11 exp Dental Porcelain/ (1768)
- 12 longevity.mp. (43666)
- 13 "all ceramic".mp. (1874)
- 14 exp tooth crown/ (20916)
- 15 exp dental restoration/ (59432)
- 16 exp lithium derivative/ (4817)
- 17 1 or 2 or 11 or 13 (5184)
- 18 5 or 6 or 7 or 8 or 9 or 12 (4066948)
- 19 ("emax" or "e.max").mp. [mp=title, abstract, heading word, drug trade name, original title, device manufacturer, drug manufacturer, device trade name, keyword, floating subheading word, candidate term word] (4898)
- 20 17 or 19 (9613)
- 21 16 or 20 (14287)
- 22 3 or 4 or 14 or 15 (110597)
- 23 10 and 18 and 20 and 22 (266)
- 24 limit 23 to (clinical trial or randomized controlled trial or controlled clinical trial or multicenter study or phase 1 clinical trial or phase 2 clinical trial or phase 3 clinical trial or phase 4 clinical trial) (36)

#### Scopus

((TITLE-ABS-KEY ("lithium disilicate") OR TITLE-ABS-KEY ("glass ceramic\*") OR TITLE-ABS-KEY ("dental ceramic\*")) AND ((TITLE-ABS-KEY ("crown\*")) AND ((TITLE-ABS-KEY ("clinical performance") OR TITLE-ABS-KEY ( failure) OR TITLE-ABS-KEY ( success) OR TITLE-ABS-KEY ( longevity) OR TITLE-ABS-KEY ( survival) )) AND (TITLE-ABS-KEY ("CAD CAM")) AND (LIMIT-TO (DOCTYPE, "ar") OR LIMIT-TO (DOCTYPE, "re"))

**Web of Science**

Topic: ("lithium disilicate") OR Topic: ("lithium disilicate") OR Topic: ("glass ceramic\*") OR Topic: ("dental ceramic\*") AND Topic: ("crown\*") AND Topic: ("clinical performance") OR Topic: ("failure") OR Topic: ("success") OR Topic: ("longevity") OR Topic: ("survival") AND Topic: ("CAD CAM")

# 1 14,889

TOPIC: ("lithium disilicate") OR TOPIC: ("glass ceramic\*") OR TOPIC: ("dental ceramic\*")

Indexes=SCI-EXPANDED, SSCI, A&HCI, CPCI-S, CPCI-SSH, ESCI Timespan=All years

# 2 128,987

TOPIC: ("crown\*")

Indexes=SCI-EXPANDED, SSCI, A&HCI, CPCI-S, CPCI-SSH, ESCI Timespan=All years

# 3 2,180,903

TOPIC: ("clinical performance") OR TOPIC: ("failure") OR TOPIC: ("success") OR TOPIC: ("longevity") OR TOPIC: ("survival")

Indexes=SCI-EXPANDED, SSCI, A&HCI, CPCI-S, CPCI-SSH, ESCI Timespan=All years

# 4 5,877

TOPIC: ("CAD CAM")

Indexes=SCI-EXPANDED, SSCI, A&HCI, CPCI-S, CPCI-SSH, ESCI Timespan=All years

# 5 77

#4 AND #3 AND #2 AND #1

Indexes=SCI-EXPANDED, SSCI, A&HCI, CPCI-S, CPCI-SSH, ESCI Timespan=All years

# 7 76

#4 AND #3 AND #2 AND #1

Refined by: DOCUMENT TYPES: ( ARTICLE OR REVIEW )

Indexes=SCI-EXPANDED, SSCI, A&HCI, CPCI-S, CPCI-SSH, ESCI Timespan=All years

**Cochrane Library**

#1 "lithium disilicate":ti,ab,kw (word variations have been searched)

#2 MeSH descriptor: [Crowns] explode all trees

#3 MeSH descriptor: [Dental Restoration Failure] explode all trees

#4 MeSH descriptor: [Dental Restoration, Permanent] explode all trees

#5 MeSH descriptor: [Inlays] explode all trees

#6 "glass ceramic\*":ti,ab,kw

#7 "crown\*":ti,ab,kw

#8 "inlay\*":ti,ab,kw

#9 "onlay\*":ti,ab,kw

#10 "clinical performance":ti,ab,kw

#11 "failure":ti,ab,kw

#12 "success":ti,ab,kw

#13 "survival":ti,ab,kw

#14 "longevity":ti,ab,kw

#15 "treatment outcome\*":ti,ab,kw

#16 MeSH descriptor: [Treatment Outcome] explode all trees

#17 "CAD CAM":ti,ab,kw

#18 MeSH descriptor: [Dental Porcelain] explode all trees

#19 #1 or #6 or #18

#20 #2 or #7 or #8 or #9

#21 #3 or #10 or #11 or #12 or #13 or #14

#22 #17 and #19 and #20 and #21

**Study selection**

The electronic search was conducted systematically by 2 independent investigators at multiple stages. The 1<sup>st</sup> stage involved screening the relevant titles after removing duplicated studies; any disagreements were resolved through a discussion. At the 2<sup>nd</sup> stage, the abstracts of the selected titles were independently analyzed and any disagreements were resolved through a discussion. At the final stage, the full texts of the studies of possible relevance were obtained. The manual search of the references of the

selected articles was performed to supplement the electronic search. The inter-reviewer agreement of 0.86 was calculated using Cohen's kappa coefficient at the title and abstract stages.

**Quality assessment in individual studies**

The quality assessment of the selected studies was carried out according to the methods described by Hayashi et al.<sup>19</sup> Each study was evaluated following 26 criteria and a percentage value was calculated, representing the quality of the study (Appendix 2).

**Appendix 2.** Quality assessment criteria according to the methods described by Hayashi et al.<sup>19</sup>

Item	Question
1	Is the hypothesis / aim / objective of the study clearly described?
2	Is the setting of the study or the source of the subjects described?
3	Is the distribution of the study population by age or gender described?
4	Are the inclusion criteria stated?
5	Are the exclusion criteria stated?
6	Are the kinds of treatment well described?
7	Are the main outcomes to be measured clearly described in the Introduction or Methods section?
8	Is the sample size stated?
9	Was the sample size justified?
10	Was the concurrent control group used?
11	Was random allocation to treatment used?
12	Was the method of random allocation given?
13	Was the blind assessment of the outcome carried out?
14	Was there more than 1 examiner for outcome assessment?
15	Was the examiner calibration carried out?
16	Are the statistical methods described?
17	Is the participation/follow-up rate stated?
18	Was the participation/follow-up rate greater than 80%?
19	Are the non-participants/subjects lost to follow-up described?
20	Are the main findings of the study clearly described?
21	Are the results stated in absolute numbers when feasible (e.g., 10/20, not 50%)?
22	Are confidence intervals given?
23	Are any important adverse events reported?
24	Are any conclusions stated?
25	Was this a prospective study?
26	Was the ethical approval obtained?

**Data collection**

The following qualitative data was extracted from the definitive list: author(s), year of publication, type of study, study setting, number of operators providing the crowns, number of evaluators and their independency, reported follow-up period, assessment criteria used for each study, tooth type (anterior or posterior), type of crown

(monolithic vs layered), and method of fabrication (chair-side vs laboratory). The following quantitative data was extracted: number of patients, drop-out rate, participants' age range, number of crowns, number of crowns made in the university setting vs private practice or both, condition of the restored teeth (vital vs non-vital), location of the crowns (anterior, premolar or molar), type of cement, number of complications, type of complications – biological (caries, pulpal involvement, tooth fracture), technical (framework fracture, chipping, debonding) or esthetic (color mismatch, marginal discoloration) – and success and survival rates.

In this review, success was defined as crowns that were present without core fracture, porcelain fracture, caries, periodontal inflammation, or endodontic signs and symptoms.<sup>20</sup> Survival was defined as crowns having remained in situ, with or without modification during the entire period of observation; these were referred to as “survived

crowns”.<sup>21</sup> After the data had been collected, no meta-analysis was performed due to qualitative differences across the studies and insufficient data.

## Results

### Study selection

The primary electronic search resulted in a total number of 219 studies. After eliminating duplicates, and screening the studies at the title and abstract levels, 12 studies were carried forward for full-text assessment from the electronic search and 1 article from hand searching. Out of these 13 studies, 7 studies were excluded, and the remaining 6 studies were included and used for data extraction. The process of identifying eligible articles is described in Fig. 1.

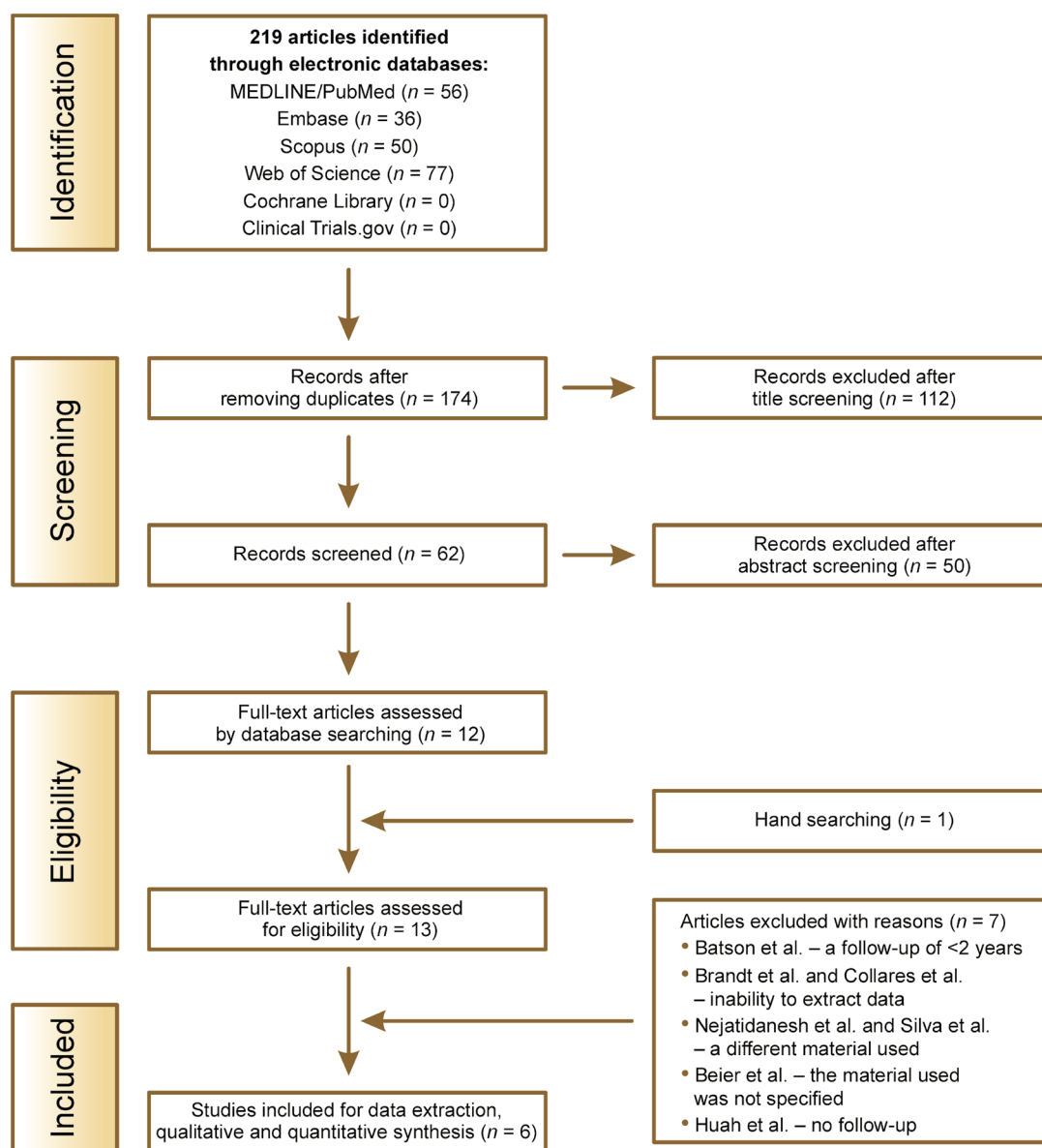


Fig. 1. Flowchart of the study selection process

Appendix 3. Results of the quality assessment of the included studies

Study	Items assessed according to Appendix 2																										Percentage of 'yes' answers [%]
	1	2	3	4	5	6	7	8	9	10	11	12	13	14	15	16	17	18	19	20	21	22	23	24	25	26	
Fasbinder et al. <sup>1</sup> 2010	X	X	-	X	-	X	X	X	-	-	-	-	X	X	-	-	X	X	X	X	X	-	X	X	X	X	65.4
Cortellini and Canale <sup>3</sup> 2012	X	X	X	X	X	X	X	X	-	X	X	X	-	-	-	X	-	-	-	X	X	-	X	X	X	-	65.4
Seydler and Schmitter <sup>4</sup> 2015	X	X	X	X	X	X	X	X	X	X	X	X	-	-	-	X	-	-	-	X	X	-	X	X	X	X	73.1
Akın et al. <sup>8</sup> 2015	X	X	X	X	X	X	X	X	X	X	X	-	-	X	X	X	X	X	-	X	X	-	X	X	X	X	84.6
Rauch et al. <sup>5</sup> 2018	X	X	X	X	X	X	X	X	X	X	X	X	X	X	X	X	X	-	X	X	X	X	X	X	X	X	96.2
Aziz et al. <sup>9</sup> 2019	X	X	X	X	X	X	X	X	X	-	-	-	X	X	X	X	X	-	X	X	X	X	X	X	-	X	80.8

X – answer 'yes'.

Table 2. Characteristics of the included studies

Study	Study design	Setting	Method of fabrication	Type of crown	Tooth type	No. of operators	No. of evaluators	Observation period [months]	Evaluation criteria
Fasbinder et al. <sup>1</sup> 2010	prospective	university	chairside	monolithic	posterior	1	2 independent	24	modified USPHS
Cortellini and Canale <sup>3</sup> 2012	prospective	private practice	laboratory	monolithic	posterior	1	the same operator	42	NR
Seydler and Schmitter <sup>4</sup> 2015	prospective	private practice	chairside	monolithic	posterior	1	the same operator	26	USPHS
Akın et al. <sup>8</sup> 2015	RCT	university	laboratory	layered	anterior	1	1 independent	24	modified USPHS
Rauch et al. <sup>5</sup> 2018	prospective	university/private practice	chairside	monolithic	posterior	4	2 independent	120	modified USPHS
Aziz et al. <sup>9</sup> 2019	retrospective	university	chairside	monolithic	posterior	dental students	2 independent	48	modified CDA

USPHS – United States Public Health Service; CDA – California Dental Association; NR – not reported.

Table 3. Quantitative data extracted from the included studies

Study	No. of patients	Drop-out [%]	Age range [years]	Location of the crowns	No. of crowns	Treated at the university	Treated in private practice
Fasbinder et al. <sup>1</sup> 2010	43/42	2.3	NR	A = 0 P = 20 M = 42	23 39	23 39	0 0
Cortellini and Canale <sup>3</sup> 2012	NR	NR	20–61	NR	23	0	23
Seydler and Schmitter <sup>4</sup> 2015	30	NR	35–58	A = 0 P = 0 M = 30	30	0	30
Akın et al. <sup>8</sup> 2015	15	0	18–64	A = 15 P = 0 M = 0	15	15	0
Rauch et al. <sup>5</sup> 2018	34/26	23.5	26.2–73.8	A = 0 P = 8 M = 26	34	20	14
Aziz et al. <sup>9</sup> 2019	32	0	29–79	A = 0 P = 22 M = 18	40	40	0

A – anterior teeth; P – premolar teeth; M – molar teeth; NR – not reported.

## Results of quality assessment

According to the criteria of quality assessment, the studies in this review involved results ranging from 65.4% to 96.2% (Appendix 3).

## Data collection and the characteristics of the studies

The included studies were published between 2010 and 2019. Five studies evaluated LDGC CAD/CAM crowns prospectively,<sup>1,3–5,8</sup> 1 study was an RCT<sup>8</sup> and 1 – a retrospective study.<sup>9</sup> Of the studies presenting results derived from the same sample, only the most recent study was included.<sup>2,5–7</sup> Five studies reported on the clinical performance of posterior monolithic LDGC CAD/CAM crowns<sup>1,3–5,9</sup> and 1 study, by Akin et al., reported on anterior layered crowns.<sup>8</sup> Four studies used the chairside technique<sup>1,4,5,9</sup> and 2 used the laboratory method of fabrication.<sup>3,8</sup> The characteristics of the studies are presented in Table 2. The quantitative data related to the clinical performance of LDGC CAD/CAM (IPS e.max CAD) crowns are presented in Table 3.

In the included studies, a total of 204 crowns were inserted in 154 patients and evaluated for a period ranging from 2 to 10 years. A total of 9 participants were lost to follow-up from all the studies combined. All the studies reported the number of participants who received LDGC CAD/CAM crowns and the location of the crowns (anterior, premolar or molar) except the study by Cortellini and Canale.<sup>3</sup> Two studies reported the distribution of the crowns in the maxilla or the mandible.<sup>4,9</sup> Using the pooled data, it was found that

there was a total of 14 complications in 204 crowns that had been placed, representing a complication rate of 6.9% (Table 4). Nine crowns were considered as failed and 5 were considered as survived. There were more biological ( $n = 10$ ) than technical complications ( $n = 4$ ). The most common biological failure reported was an endodontic complication ( $n = 5$ ), followed by secondary caries ( $n = 4$ ) and tooth fracture ( $n = 1$ ). In Rauch et al.'s study, the tooth extracted due to an apical infection was counted as an endodontic complication and the tooth fractured due to caries was counted as a recurrent caries complication.<sup>5</sup> Four technical complications were reported – 1 debonding, 1 crown fracture and 2 open margins. The most frequently reported complications occurred in the molar teeth, but it was not possible to determine whether there was any particular predilection for failure in the maxilla vs the mandible, as there was not enough information available to make a definitive conclusion. No esthetic complications such as color mismatch or marginal discoloration were reported.

The survival rate reported by Fasbinder et al.,<sup>1</sup> Cortellini and Canale,<sup>3</sup> and Akin et al.<sup>8</sup> was 100.0%, as no complications were reported over a follow-up period of 2–3.5 years. In Seydler and Schmitter's study, the survival rate was stipulated from the survival curve analysis (93.3%), as they counted the 2 endodontic complications as failed rather than survived crowns after 2 years.<sup>4</sup> Rauch et al. reported a survival rate of 85.3% after 10 years.<sup>5</sup> Except for the studies performed by Rauch et al.<sup>5</sup> and Aziz et al.,<sup>9</sup> none of the others actually reported the overall success rates. The success rates presented in Table 3 were calculated as the percentage of crowns without complications.

Vital	Non-vital	Type of cement	No. of complications	Success rate [%]	Survival rate [%]
NR	NR	Multilink® Automix; Ivoclar Vivadent AG	0	100.0	100.0
NR	NR	experimental cement; Ivoclar Vivadent AG	2	94.9	100.0
NR	NR	Multilink Automix; Ivoclar Vivadent AG, Variolink® Veneer; Ivoclar Vivadent AG	0	100.0	100.0
14	16	Multilink Automix; Ivoclar Vivadent AG	2	93.3	93.3
NR	NR	Variolink II; Ivoclar Vivadent AG	0	100.0	100.0
17	17	Multilink Sprint; Ivoclar Vivadent AG	9	73.5	85.3
7	33	RelyX® Unicem; 3M ESPE, Calibra® Universal; Dentsply Sirona	3	92.5	95.0



**Table 4.** Summary of all complications reported for LDGC computer-aided design/computer-aided manufacturing (CAD/CAM) crowns

Study	Complication	Category of complication	Period [months]	Outcome
Seydler and Schmitter <sup>4</sup> 2015	endodontic complication	biological	12	failed
	endodontic complication	biological	12	failed
Rauch et al. <sup>5</sup> 2018	endodontic complication	biological	at baseline	survived
	endodontic complication	biological	13.2	survived
	recurrent caries	biological	24	failed
	recurrent caries	biological	48	survived
	tooth extraction due to an apical infection	biological	72	failed
	tooth fracture due to recurrent caries	biological	72	failed
	tooth fracture	biological	84	failed
	debonded crown	technical	24	survived
	crown fracture	technical	33.6	failed
	Aziz et al. <sup>9</sup> 2019	recurrent caries	biological	24
open margin		technical	30	failed
open margin		technical	37	failed
Total	14	10 biological 4 technical	–	5 survived 9 failed

## Discussion

The present study aimed at establishing scientific evidence regarding the efficacy of LDGC CAD/CAM crowns. Only published clinical trials were included. Conference abstracts and studies published by the manufacturer were excluded, because it was not possible to extract the required data from them. The sample size was relatively small for all the included studies. However, since they were mostly prospective clinical trials, the known difficulty of recruiting more patients and maintaining a low drop-out rate are always a limitation inherent to this type of study.

There was no significant association between the incidences of failure and the type of cement. This could be explained by a reliable bond that could be achieved with resin cements. The group of crowns cemented with an experimental cement in Fasbinder et al.'s study was excluded from the analysis, since the cement was withdrawn from the market, and therefore, findings with this particular cement would be irrelevant to the main goals of this investigation.<sup>1</sup>

None of the included studies reported any association between the incidence of complications and the tooth type (premolar vs molar). In fact, the location of the crowns (premolars vs molars) was not correlated with failure or success in most investigations with the exception of 1 study, where it was stated that most complications occurred in the molar teeth.<sup>5</sup> Unfortunately, this report did not provide enough data for our investigation to make meaningful conclusions regarding the impact of this factor.<sup>5</sup> Moreover, none of the studies reported

whether there were any differences in the occurrence of complications when comparing the restorations placed in the maxilla vs the mandible. Similarly, there was no evident statement whether the setting in which the crowns were placed (university vs private practice) had an impact on survival. There were no evident differences that could be found regarding the survival of the crowns placed on vital or non-vital teeth. This particular issue was not even reported in the studies included in our review.

None of the included studies compared the clinical outcome of LDGC crowns to the “gold standard”, that being metal-ceramic crowns. In the study by Cortellini and Canale, LDGC CAD/CAM crowns ( $n = 23$ ) were compared to 212 pressed crowns for a period of 42 months.<sup>3</sup> No complication was reported for the CAD/CAM group and only 1 crown fractured in the pressed group after 3 years.<sup>3</sup> In the study conducted by Seydler and Schmitter, the performance of 30 monolithic LDGC CAD/CAM crowns was compared to 30 veneered zirconia crowns.<sup>4</sup> The number of biological complications was similar for both groups; 2 endodontic complications occurred in each. No technical complications such as fracture, chipping or cracks were noted for either group after 2 years of follow-up.<sup>4</sup>

This systematic review demonstrated that biological complications occurred more often than technical complications. The need for endodontic treatment after the cementation of crowns can be attributed to the over-reduction of the natural tooth structure, especially in young patients, in addition to continuous pulpal trauma. The incidence of recurrent secondary caries could not be linked to the status of oral hygiene due to insufficient information, but could be related to an increased marginal gap

in all-ceramic crowns. Akin et al. compared the marginal and internal adaptation of 15 LDGC CAD/CAM crowns to 15 heat-pressed LDGC crowns (IPS. e.max Press, Ivoclar Vivadent AG); there was no statistically significant difference between the 2 fabrication techniques.<sup>8</sup> The median marginal gap for the CAD/CAM group was within the clinically acceptable range (132.2  $\mu\text{m}$ ), but it was reported as low as 71.0  $\mu\text{m}$ . Also, no recurrent caries was detected in their study due to a small sample size and a short observation time of 2 years, which was not sufficient for carious lesions to develop.<sup>8</sup> Caries at the crown margin was reported in 1 study, and occurred in 2 teeth.<sup>5</sup> The mean marginal gap measured in that study was 81.0  $\mu\text{m}$ , but the actual marginal gap in the crowns affected by recurrent caries was not disclosed, and therefore, it was not possible to make any solid conclusions regarding the contribution of the marginal gap to the occurrence of recurrent caries.<sup>5</sup> Although such a marginal gap is considered to be within the clinically acceptable range, it might be concluded that even within this range, secondary caries could be detected if a good oral hygiene level was not maintained.<sup>22</sup> However, LDGC crowns demonstrated similar recurrent caries rate and fewer endodontic problems as compared to metal-ceramic crowns after 5 years, and it could be assumed that the level of oral hygiene was most likely the same in both study populations.<sup>23</sup>

With regard to technical complications, 1 fracture and 1 case of debonding occurred in the same study.<sup>5</sup> The authors reported that the crown fractured due to the insufficient occlusal reduction of the lower second molar, whereas the other crown debonded due to inadequate retention, as the tooth height was <3.0 mm.<sup>5</sup> These technical complications could likely have been avoided had the manufacturer's recommendations been followed carefully. No crown chipping was reported due to the absence of veneering porcelain in monolithic crowns, which is usually associated with this type of complication. Even in the case of the layered crowns evaluated in 1 study, there was no chipping or fracture after 2 years.<sup>8</sup> However, this could be attributed to a short-term follow-up and to the location of the crowns in the anterior region, where the occlusal forces are minimal.<sup>8</sup> Two crowns provided by dental students presented with open margins.<sup>9</sup> No esthetic complications were reported. The color match of LDGC CAD/CAM crowns was rated as being good to excellent in all studies, and the patients were very satisfied with the esthetic appearance of the crowns.

Apart from the clinical findings reported here, this review also showed that there was a limited number of studies with relatively small sample sizes that focused on the clinical performance of LDGC CAD/CAM crowns. There is a need for clinical trials evaluating both fabrication techniques (chairside and laboratory) with larger sample sizes, longer follow-up times and blinded evaluators. This is highly important, as it will considerably enrich the currently available data and will help to identify with more


confidence the clinical performance of LDGC crowns fabricated using both methods of manufacturing. It is also recommended that, in order to provide more useful data, studies should be designed to include the distribution of complications with regard to the tooth type, tooth location, tooth condition (vital or non-vital), study setting (university and/or private practice), and the experience level of the operator(s).


## Conclusions

Based on the findings and within the limitations of this systematic review, it can be concluded that the short- to medium-term survival rate of LDGC CAD/CAM crowns was high (from 93.3% to 100%). Biological complications were the most frequently reported sequelae and mostly occurred in the first 2 years after the cementation of the crowns, regardless of the type of cement used.

### ORCID iDs

Ahmed Aziz  <https://orcid.org/0000-0001-9724-8376>

Omar El-Mowafy  <https://orcid.org/0000-0002-3301-3911>

Saira Paredes  <https://orcid.org/0000-0003-2165-9560>

### References

1. Fasbinder DJ, Dennison JB, Heys D, Neiva G. A clinical evaluation of chairside lithium disilicate CAD/CAM crowns: A two-year report. *J Am Dent Assoc.* 2010;141(Suppl 2):S10–S14.
2. Reich S, Fischer S, Sobotta B, Klapper HU, Gozdowski S. A preliminary study on the short-term efficacy of chairside computer-aided design/computer-assisted manufacturing-generated posterior lithium disilicate crowns. *Int J Prosthodont.* 2010;23(3):214–216.
3. Cortellini D, Canale A. Bonding lithium disilicate ceramic to feather-edge tooth preparations: A minimally invasive treatment concept. *J Adhes Dent.* 2012;14(1):7–10.
4. Seydler B, Schmitter M. Clinical performance of two different CAD/CAM-fabricated ceramic crowns: 2-year results. *J Prosthet Dent.* 2015;114(2):212–216.
5. Rauch A, Reich S, Dalchau L, Schierz O. Clinical survival of chair-side generated monolithic lithium disilicate crowns: 10-year results. *Clin Oral Investig.* 2018;22(4):1763–1769.
6. Reich S, Schierz O. Chair-side generated posterior lithium disilicate crowns after 4 years. *Clin Oral Investig.* 2013;17(7):1765–1772.
7. Rauch A, Reich S, Schierz O. Chair-side generated posterior monolithic lithium disilicate crowns: Clinical survival after 6 years. *Clin Oral Investig.* 2017;21(6):2083–2089.
8. Akin A, Toksavul S, Toman M. Clinical marginal and internal adaptation of maxillary anterior single all-ceramic crowns and 2-year randomized controlled clinical trial. *J Prosthodont.* 2015;24(5):345–350.
9. Aziz A, El-Mowafy O, Tenenbaum HC, Lawrence HP, Shokati B. Clinical performance of chairside lithium disilicate glass-ceramic CAD-CAM crowns. *J Esthet Restor Dent.* 2019;31(6):613–619.
10. Giordano R. Materials for chairside CAD/CAM-produced restorations. *J Am Dent Assoc.* 2006;137(Suppl):145–215.
11. Poticny DJ, Klim J. CAD/CAM in-office technology: Innovations after 25 years for predictable, esthetic outcomes. *J Am Dent Assoc.* 2010;141(Suppl 2):5S–9S.
12. Wolfart S, Eschbach S, Scherrer S, Kern M. Clinical outcome of three-unit lithium-disilicate glass-ceramic fixed dental prostheses: Up to 8 years results. *Dent Mater.* 2009;25(9):e63–e71.
13. Etman MK, Woolford MJ. Three-year clinical evaluation of two ceramic crown systems: A preliminary study. *J Prosthet Dent.* 2010;103(2):80–90.

14. Duret F, Preston JD. CAD/CAM imaging in dentistry. *Curr Opin Dent.* 1991;1(2):150–154.
15. Guess PC, Schultheis S, Bonfante EA, Coelho PG, Ferencz JL, Silva NRFA. All-ceramic systems: Laboratory and clinical performance. *Dent Clin North Am.* 2011;55(2):333–352.
16. Bindl A, Lüthy H, Mörmann WH. Thin-wall ceramic CAD/CAM crown copings: Strength and fracture pattern. *J Oral Rehabil.* 2006;33(7):520–528.
17. Coelho Santos G Jr, Moraes Coelho Santos MJ Jr, Rizkalla AS, Madani DA, El-Mowafy O. Overview of CEREC CAD/CAM chairside system. *Gen Dent.* 2013;61(1):36–40;quiz 41.
18. Moher D, Liberati A, Tetzlaff J, Altman DG; PRISMA Group. Preferred reporting items for systematic reviews and meta-analyses: The PRISMA statement. *PLoS Med.* 2009;6(7):e1000097.
19. Hayashi M, Wilson NHF, Yeung CA, Worthington HV. Systematic review of ceramic inlays. *Clin Oral Investig.* 2003;7(1):8–19.
20. Patel DR, O'Brien T, Petrie A, Petridis H. A systematic review of outcome measurements and quality of studies evaluating fixed tooth-supported restorations. *J Prosthodont.* 2014;23(6):421–433.
21. Pjetursson BE, Sailer I, Zwahlen M, Hämmerle CH. A systematic review of the survival and complication rates of all-ceramic and metal-ceramic reconstructions after an observation period of at least 3 years. Part I: Single crowns. *Clin Oral Implants Res.* 2007;18(Suppl 3):73–85.
22. Matta RE, Schmitt J, Wichmann M, Holst S. Circumferential fit assessment of CAD/CAM single crowns – a pilot investigation on a new virtual analytical protocol. *Quintessence Int.* 2012;43(9):801–809.
23. Sailer I, Makarov NA, Thoma DS, Zwahlen M, Pjetursson BE. All-ceramic or metal-ceramic tooth-supported fixed dental prostheses (FDPs)? A systematic review of the survival and complication rates. Part I: Single crowns (SCs). *Dent Mater.* 2015;31(6):603–623.

# Mirror-image phenomenon in Turkish monozygotic twins: A report of 3 cases

## Fenomen lustrzanych odbić u tureckich monozygotycznych bliźnięt – opis trzech przypadków

Damla Torul<sup>A–F</sup>, Mehmet Melih Omezli<sup>A,C,E,F</sup>

Department of Oral and Maxillofacial Surgery, Faculty of Dentistry, Ordu University, Turkey

A – research concept and design; B – collection and/or assembly of data; C – data analysis and interpretation; D – writing the article; E – critical revision of the article; F – final approval of the article

Dental and Medical Problems, ISSN 1644-387X (print), ISSN 2300-9020 (online)

*Dent Med Probl.* 2020;57(2):207–211

### Address for correspondence

Damla Torul  
E-mail: damlatorul@gmail.com

### Funding sources

None declared

### Conflict of interest

None declared

### Acknowledgements

The authors would like to thank Taha Alpaydin, DDS, from the Department of Orthodontics, Faculty of Dentistry at Ordu University, Turkey, for his valuable help during the preparation of the photographs of the twins.

Received on August 30, 2019  
Reviewed on October 5, 2019  
Accepted on November 15, 2019

Published online on June 30, 2020

### Abstract

Due to the special circumstances and the pre-natal environment in twin gestations, disruptions in the development of the embryo are more frequently observed in twin births as compared to singleton births. Twin research provides an excellent model to explore the etiology of disruptions in craniofacial biology. Mirror imaging (MI) is a special manifestation of twinning, and the elucidation of the etiology of this phenomenon is important to understand the biological mechanisms which underlie congenital defects, like orofacial clefts, and to provide insight into left-right asymmetry.

The aim of this paper was, therefore, to present 3 pairs of Turkish monozygotic (MZ) twins with MI dental features, and to contribute to the knowledge of the MI phenomenon in the literature. We examined 2 male and 1 female MZ twin pairs clinically and radiographically in terms of their MI features. Mirror-image features in dental and other ectodermal structures were detected in all the twins. Understanding the biological mechanisms of MI provides broad insight into preventive measures and treatment protocols. Furthermore, the presence of MI features may lead to the detection of other MI pathologies in twins.

**Key words:** asymmetry, identical twins, mirror image

**Słowa kluczowe:** asymetria, bliźnięta identyczne, lustrzane odbicie

### Cite as

Torul D, Omezli MM. Mirror-image phenomenon in Turkish monozygotic twins: A report of 3 cases. *Dent Med Probl.* 2020;57(2):207–211. doi:10.17219/dmp/114248

### DOI

10.17219/dmp/114248

### Copyright

© 2020 by Wrocław Medical University  
This is an article distributed under the terms of the Creative Commons Attribution 3.0 Unported License (CC BY 3.0) (<https://creativecommons.org/licenses/by/3.0/>).

## Introduction

Over the centuries, twinning and its unique features have been a valuable source for exploring the relative contributions of nature and nurture to various phenotypic traits and pathologies in humans.<sup>1,2</sup> Mirror imaging (MI) is a special manifestation of twinning, also known as reverse asymmetry, in which one member of a twin pair 'mirrors' the other in 1 or more features.<sup>1,3,4</sup> The underlying biological mechanisms of MI are still not clear, but preliminary evidence in the literature suggests that reverse asymmetry may be a reflection of a genetically mediated embryological event. Also, it has been suggested that MI is epigenetically linked to the timing of twinning, and therefore the type of placentation.<sup>4,5</sup> Some aspects of this phenomenon are estimated to occur in 25% of monozygotic (MZ) twins and are typically observed in the tissues derived from the ectoderm; they comprise dentation, hair whorls, dermatoglyphics, eyesight, nevi, handedness, and the cerebral hemispheres.<sup>1,3,6</sup> In the literature, several MI features and pathologies have been reported.<sup>3,6-10</sup>

The aim of this article was to present 3 pairs of Turkish MZ twins with MI dental features, and to contribute information about the MI phenomenon to the literature.

## Case report

Two male and 1 female MZ twin pairs (5, 9 and 10 years old, respectively) were referred to the Department of Oral and Maxillofacial Surgery, Faculty of Dentistry at Ordu University in Turkey for routine examinations. Written informed consent to participate in the study was obtained from the parents of the twins. The zygosity of the twins was determined according to a standard zygosity questionnaire and blood groups.<sup>11</sup> Handedness was measured with a hand preference (HP) inventory based on the Edinburgh Handedness Inventory.<sup>12</sup>



Fig. 1. Front view of twins A<sub>1</sub> and A<sub>2</sub>

Hand use was evaluated during drawing, writing, using scissors, throwing a ball, cutting with a knife, using a spoon, using a toothbrush, using a broom, taking a lid off a box, and dealing cards. The inventory awarded 2 points for each right-handed action, 0 points for left-handed actions, and 1 point for mixed or unclear preference, with the total score ranging from 0 (left-handed) to 20 (right-handed).

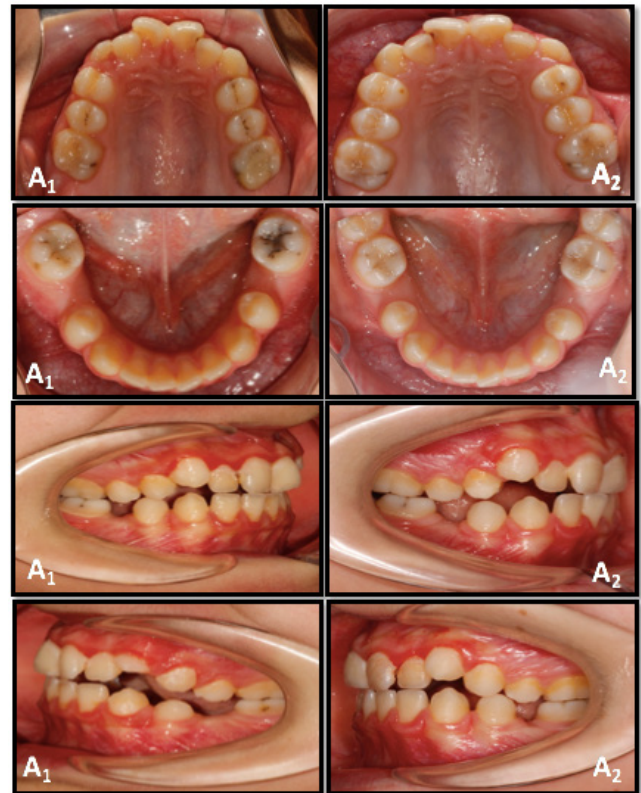


Fig. 2. Intraoral photographs of A<sub>1</sub> and A<sub>2</sub>

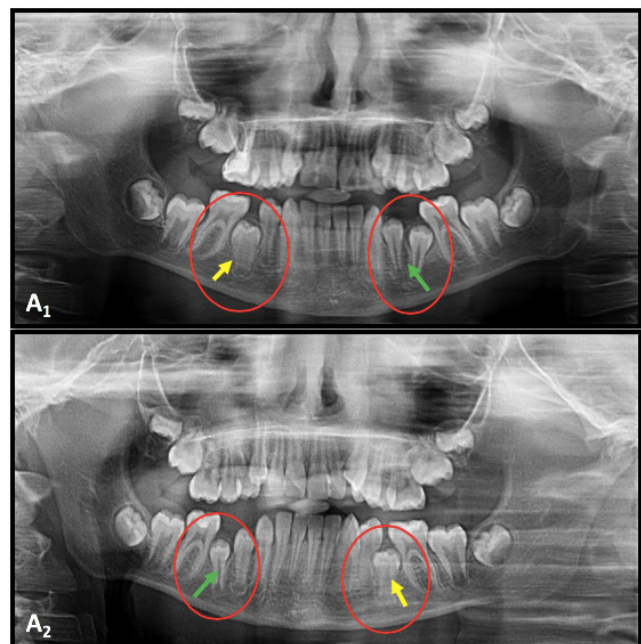


Fig. 3. Panoramic radiographs showing the mirror-image (MI) dental features of A<sub>1</sub> and A<sub>2</sub> (arrows)

The twins’ medical and dental histories were noncontributory. All 3 twin pairs were subjected to clinical and radiographic examinations. Panoramic and lateral cephalometric radiographs were obtained from all 3 pairs.

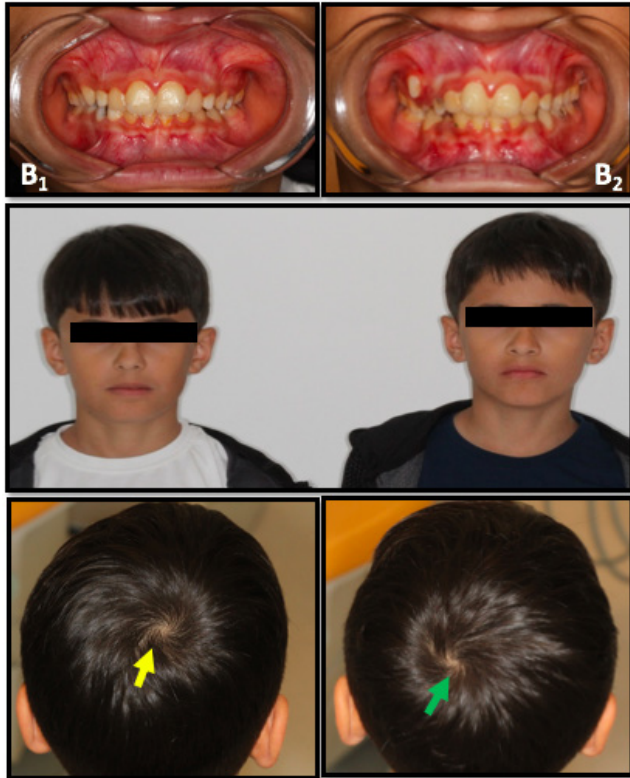


Fig. 4. Front view and hair whorls of twins B<sub>1</sub> and B<sub>2</sub>

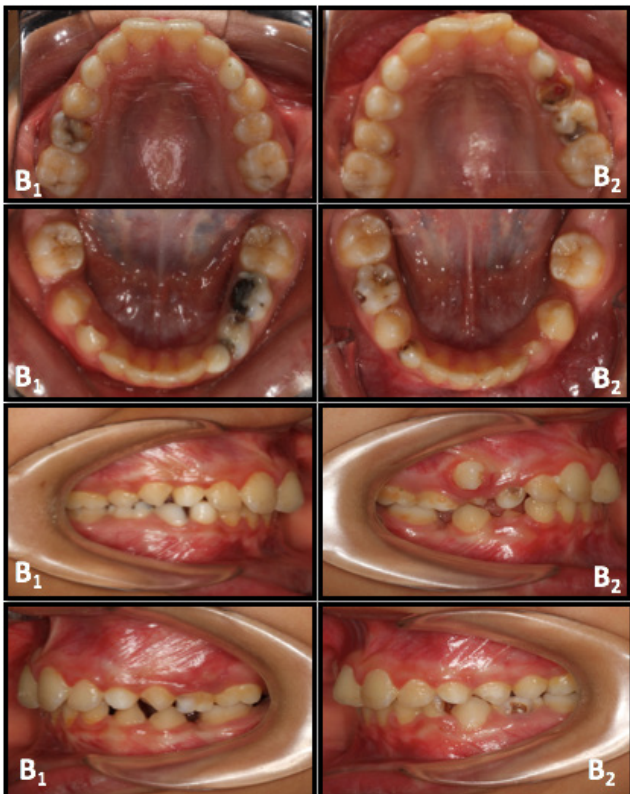


Fig. 5. Intraoral photographs of B<sub>1</sub> and B<sub>2</sub>

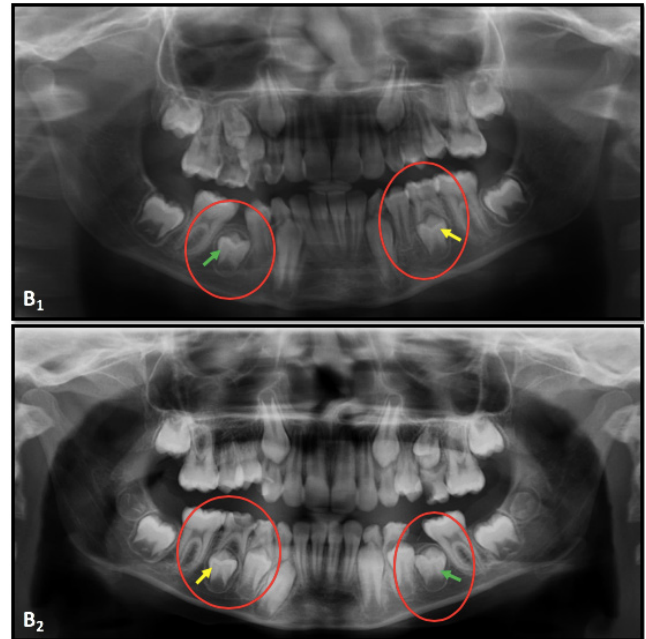


Fig. 6. Panoramic radiographs showing the MI dental features of B<sub>1</sub> and B<sub>2</sub> (arrows)

Clinically, twins A<sub>1</sub> and A<sub>2</sub> were at the mixed dentition stage, with the mandibular premolar teeth showing MI asymmetries (Fig. 1–3). Also, A<sub>1</sub> was right-handed and kicked with his right foot, whereas A<sub>2</sub> was left-handed and kicked with his left foot.

Twins B<sub>1</sub> and B<sub>2</sub> were also at the mixed dentition stage and had MI features in their dentition. The hair whorls of B<sub>1</sub> and B<sub>2</sub> were in opposite directions: one’s clockwise, and the other’s counter-clockwise (Fig. 4–6).

Twins C<sub>1</sub> and C<sub>2</sub> were also at the mixed dentition stage and showed MI features in the eruption pattern of their mandibular central incisor teeth (Fig. 7–9).



Fig. 7. Front view of twins C<sub>1</sub> and C<sub>2</sub>

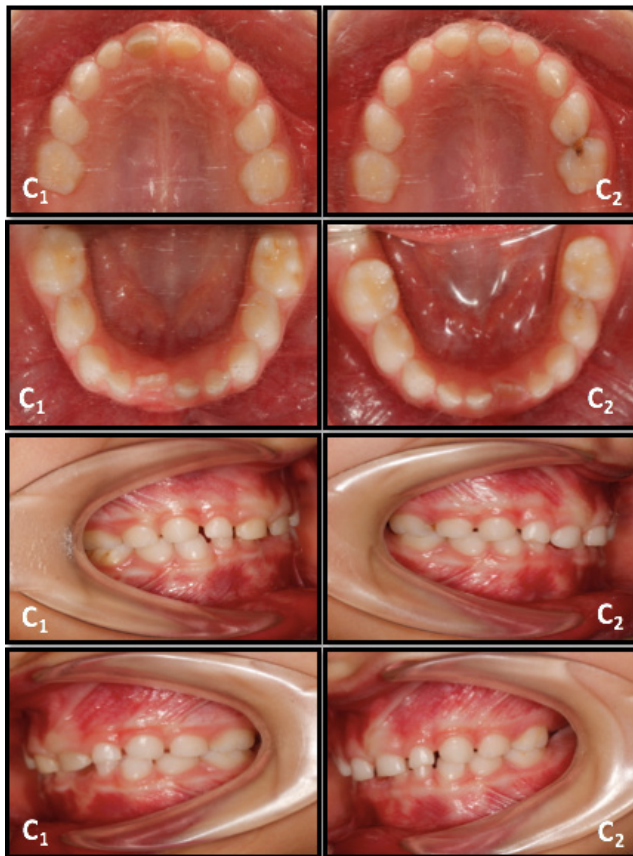


Fig. 8. Intraoral photographs of C<sub>1</sub> and C<sub>2</sub>

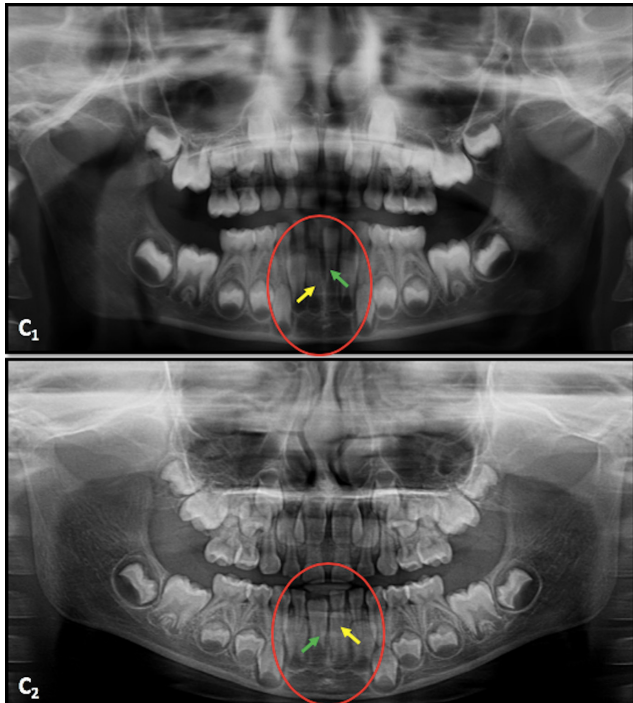


Fig. 9. Panoramic radiographs showing the MI dental features of C<sub>1</sub> and C<sub>2</sub> (arrows)

## Discussion

Mirror imaging – a special manifestation of twinning, also referred to as reverse asymmetry – occurs in MZ twin pairs, who are considered to have identical features.<sup>9</sup>

Rather than an epiphenomenon, MI is considered a biological polarization that describes the role of biochemical, genetic, psychological, and environmental factors in the occurrence of not only reverse asymmetry, but also opposite tendencies in the development of personality, sex orientation as well as psychiatric and pathological conditions.<sup>2,13</sup>

The exact biological pathways of this polarization are still not clearly understood. Mirror-image asymmetries are believed to occur as a result of the blockage of predetermined cells, leading to the establishment of a second reversed morphogenetic gradient.<sup>9</sup> Also, the maldistribution of the homeobox genes which define the anterior-posterior axis and the early molding of the embryo during splinting has been reported to deteriorate regulatory balance.<sup>14</sup> Another explanation of MI is the timing of the cleavage of the zygote, and therefore the type of placentation.<sup>2</sup> Regarding placentation, MZ twins can be grouped as dichorionic/diamniotic (cleavage occurring 1–5 days post-conception, before implantation), dichorionic/monoamniotic (cleavage occurring 6–9 days post-conception, after implantation) and monochorionic/monoamniotic (late cleavage, probably occurring 9–10 days post-conception<sup>2,5</sup>) It has been noted that the basic symmetry of the embryo occurs at around 7–8 days, when the amnion is differentiating.<sup>4</sup> If the zygote divides in late embryogenesis, this may result in asymmetries, and the incomplete redefinition of these asymmetries may lead to discordance for the left-right orientation and different degrees of MI in MZ twin pairs.<sup>4,9</sup> However, according to Badzakova-Trajkov et al., the occurrence of MI asymmetries is largely due to chance.<sup>15</sup>

The MI phenomenon typically affects the tissues derived from the ectodermal layer, which develops early.<sup>1,6</sup> Although situs inversus or heterotaxy syndrome have been reported in internal organs, this phenomenon rarely affects mesodermally derived organs.<sup>14,16</sup> Mirror-image ectodermal features, such as the tooth eruption pattern, eyesight, hair whorls, dermatoglyphics, the laterality disturbances of the cerebral hemispheres, and non-right handedness are frequently observed in MZ twin pairs.<sup>1,3,6</sup> Mirror-image handedness is presumed to be a reflection of variations in cerebral lateralization among twins.<sup>4</sup> Nearly 30% of the reported MZ twin pairs have MI handedness.<sup>5</sup> In the present cases, only twins A<sub>1</sub> and A<sub>2</sub> presented discordant handedness. Also, MI hair whorls were observed in twins B<sub>1</sub> and B<sub>2</sub>.

The bilateral symmetrical development of dentition commences at about 4 weeks in utero and extends until physical maturity at about 21 years post-natally. Thus, dentation provides a good model to explore the fascinating phenomenon of MI.<sup>1,4</sup> Dentition is strictly under genetic control. Thus, MI asymmetries in dental features provide insight into genetic control over phenotypic expression, and also other etiologic factors of the asymmetric developmental mechanisms in MZ twins.<sup>9</sup>

Mirror-image dental fusion, hypodontia, germination, and supplemental teeth have been reported in the literature.<sup>9,10</sup> Song et al. reported a case of twins presenting with hip cysts, who also had an MI crossbite in their dentition.<sup>2</sup> They suggested that, depending on the degree of MI, multiple organ systems can be affected; thus, if one of the MZ twins presents with a medical problem, it may be logical to perform a diagnostic workup on the other twin as well.<sup>2</sup> In all 3 of our cases, MI dental features were detected in the tooth eruption patterns and impaction.


Mirror-imaging pathological conditions have also been noticed in MZ twins. Zhou et al. described a pair of MZ twins who developed MI arachnoid cysts in the temporal fossa.<sup>6</sup> The MI first and second branchial arch syndrome associated with cleft lips and palates was reported in MZ twins by Satoh et al.<sup>7</sup> In another case report, Brent described the surgical management of twins who were afflicted with MI unilateral microtia.<sup>8</sup>

Even when physical characteristics are concordant, MI monozygotic twins can exhibit discordance in psychiatric conditions. Lohr and Bracha reported a twin pair in which one was diagnosed with bipolar disorder and the other with schizophrenia.<sup>17</sup>

In conclusion, the MI phenomenon may cause biological polarization, reflected in twin pairs as reverse asymmetrical physiological features or pathological conditions, in different degrees. Our report on 3 cases of MZ twins with MI dental features contributes to the understanding of the limitations of genetic control over dental phenotypic expression and possible epigenetic origin. We also suggest that twin pairs who show 1 or more MI features should be examined extensively for medical, dental and psychological asymmetry.

### ORCID iDs

Damla Torul  <https://orcid.org/0000-0003-2323-606X>

Mehmet Melih Omezli  <https://orcid.org/0000-0002-6606-6593>

### References

- Hughes TE, Townsend GC, Pinkerton SK, et al. The teeth and faces of twins: Providing insights into dentofacial development and oral health for practising oral health professionals. *Aust Dent J.* 2014;59(Suppl 1):101–116.
- Song J, Song A, Shim A, Kim E, Song M. Mirror-image identical twins presenting in mirror-image hip cysts: A case report and review of the literature. *Rheumatol Curr Res.* 2013;517:001.
- Sommer IE, Ramsey NF, Bouma A, Kahn RS. Cerebral mirror-imaging in a monozygotic twin. *Lancet.* 1999;354(9188):1445–1446.
- Townsend G, Richards L. Twins and twinning, dentists and dentistry. *Aust Dent J.* 1990;35(4):317–327.
- Townsend GC, Richards L, Hughes T, Pinkerton S, Schwerdt W. The value of twins in dental research. *Aust Dent J.* 2003;48(2):82–88.
- Zhou JY, Pu JL, Chen S, Hong Y, Ling CH, Zhang JM. Mirror-image arachnoid cysts in a pair of monozygotic twins: A case report and review of the literature. *Int J Med Sci.* 2011;8(5):402–405.
- Satoh K, Shibata Y, Tokushige H, Onizuka T. A mirror image of the first and second branchial arch syndrome associated with cleft lip and palate in monozygotic twins. *Br J Plast Surg.* 1995;48(8):601–605.
- Brent B. Repair of microtia with sculpted rib cartilage grafts in identical, mirror-image twins: A case study. *Ann Plast Surg.* 2011;66(1):62–64.
- Sperber GH, Machin GA, Bamforth FJ. Mirror-image dental fusion and discordance in monozygotic twins. *Am J Med Genet.* 1994;51(1):41–45.
- Beere D, Hargreaves JA, Sperber GH, Cleaton-Jones P. Mirror image supplemental primary incisor teeth in twins: Case report and review. *Pediatr Dent.* 1990;12(6):390–392.
- Kaprio J, Sarna S, Koskenvuo M, Rantasalo I. The Finnish Twin Registry: formation and compilation, questionnaire study, zygosity determination procedures, and research program. *Prog Clin Biol Res.* 1978;24(Pt B):179–184.
- Bishop DVM. Handedness and specific language impairment: A study of 6-year-old twins. *Dev Psychobiol.* 2005;46(4):362–369.
- Golbin A, Golbin Y, Keith L, Keith D. Mirror imaging in twins: Biological polarization – an evolving hypothesis. *Acta Genet Med Gemellol (Roma).* 1993;42(3–4):237–243.
- Sommer IE, Ramsey NF, Mandl RC, Kahn RS. Language lateralization in monozygotic twin pairs concordant and discordant for handedness. *Brain.* 2002;125(Pt 12):2710–2718.
- Badzakova-Trajkov G, Häberling IS, Corballis MC. Cerebral asymmetries in monozygotic twins: An fMRI study. *Neuropsychologia.* 2010;48(10):3086–3093.
- Thacker D, Gruber PJ, Weinberg PM, Cohen MS. Heterotaxy syndrome with mirror image anomalies in identical twins. *Congenit Heart Dis.* 2009;4(1):50–53.
- Lohr JB, Bracha HS. A monozygotic mirror-image twin pair with discordant psychiatric illnesses: A neuropsychiatric and neurodevelopmental evaluation. *Am J Psychiatry.* 1992;149(8):1091–1095.





# Clinical aspects of pulp stones: A case report series

## Aspekty kliniczne kamieni miazgi – seria przypadków

Krystyna Pietrzycka<sup>A–F</sup>, Halina Pawlicka<sup>B,D,E</sup>

Department of Endodontics, Medical University of Lodz, Poland

A – research concept and design; B – collection and/or assembly of data; C – data analysis and interpretation;  
D – writing the article; E – critical revision of the article; F – final approval of the article

Dental and Medical Problems, ISSN 1644-387X (print), ISSN 2300-9020 (online)

*Dent Med Probl.* 2020;57(2):213–220

### Address for correspondence

Krystyna Pietrzycka  
E-mail: krystyna.pietrzycka@umed.lodz.pl

### Funding sources

None declared

### Conflict of interest

None declared

Received on December 4, 2019

Reviewed on January 24, 2020

Accepted on February 5, 2020

Published online on June 30, 2020

### Abstract

Pulp stones (PSs) are calcified masses that can be found in the pulp cavity of any deciduous or permanent tooth. They can be observed in healthy, diseased, and even unerupted or impacted teeth. Calcifications within the pulp may lead to a poorer outcome of a root canal procedure, as they can block access to the root canals, and hinder their subsequent cleaning and shaping.

The paper describes 4 clinical cases of denticles located in the coronal and radicular pulp. Therapeutic methods of PS removal with different techniques and instruments are discussed. Specialist root canal treatment (RCT) was performed in aseptic conditions with the use of long-shank rose-head burs and an endodontic ultrasonic device under the magnification of a dental operative microscope (OM). During endodontic treatment, all PSs were totally removed, which allowed the further preparation, and finally obturation of the canal system. The use of modern diagnostic and therapeutic methods – three-dimensional (3D) diagnostic radiology, endodontic techniques, such as ultrasounds used during the removal of PSs and the irrigation of the canals, and the thermoplastic methods of canal obturation – can provide good results of treatment of this pathology. The removal of PSs from the pulp cavity is a complex and difficult procedure, requiring skill, dexterity, and appropriate equipment and facilities. The clinical approach introduced in this paper allows endodontists to avoid potential complications like perforation, the unnecessary removal of hard tissues or the weakening of the tooth structure.

**Key words:** root canal treatment, dental operating microscope, pulp stones, denticles, ultrasonic tips

**Słowa kluczowe:** leczenie kanałowe, stomatologiczny mikroskop operacyjny, kamienie miazgi, zębiniaki, końcówki ultradźwiękowe

### Cite as

Pietrzycka K, Pawlicka H. Clinical aspects of pulp stones:  
A case report series. *Dent Med Probl.* 2020;57(2):213–220.  
doi:10.17219/dmp/117944

### DOI

10.17219/dmp/117944

### Copyright

© 2020 by Wrocław Medical University

This is an article distributed under the terms of the

Creative Commons Attribution 3.0 Unported License (CC BY 3.0)

(<https://creativecommons.org/licenses/by/3.0/>).

## Introduction

Pulp stones (PSs) are defined as calcified foci that are observed in the coronal or, less frequently, radicular pulp cavity. They are found in the dental pulp of the teeth in primary and permanent dentition. These calcified structures can be detected in the pulp of healthy, infected, and even impacted teeth.<sup>1</sup> Dental pulp calcifications were mentioned for the first time in 1921 by Norman and Johnson as dental pulp nodules; this term was later modified to denticles. Kronfeld and Boyle classified pulp calcifications histologically into discrete ‘true’ or ‘false’ forms, the former containing irregular dentine and the latter being degenerative pulp calcifications.<sup>2</sup> Other studies have proposed new classifications. Based on their size, PSs have been divided into fine and diffuse mineralization, and based on location – into embedded and free types.<sup>3–5</sup> Pulp stones may be embedded, attached to dentin walls or free within the pulp tissue.<sup>6</sup> The exact etiology of PS formation still remains unclear. Some factors that have been implicated in PS formation include pulp calcification, aging, orthodontic tooth movement, periodontal disease, various systemic diseases, genetic predisposition, bacterial infection, deep caries, restorations, and calcifying nanoparticles.<sup>7–10</sup> Previous studies have reached no consensus regarding the prevalence of PSs, though reports range from 8% to 90%, depending on the study type, design, and radiographic technique employed. Pulp stones may range in size from a macroscopic to microscopic mass, less than 200  $\mu\text{m}$ , beyond radiographic resolution. The histological method of evaluation is reported to yield higher values than the radiographic method.<sup>11,12</sup>

Calcifications within the pulp may lead to a poorer outcome of a root canal procedure, as they can block access to the root canals, and hinder their subsequent cleaning and shaping. The paper describes 4 clinical cases of denticles located in the coronal and radicular pulp, and the therapeutic methods of denticle removal with different techniques and instruments.

## Case reports

### Case 1

A female patient, aged 28, with no relevant medical history, was referred to the dental office for the specialist root canal treatment (RCT) of tooth 27 with a diagnosis of calcifications within the pulp and blocked access to the root canals. The previous week the tooth had been trepanned and the root canal orifices had been detected with blue dye. The clinical examination revealed no pain on percussion, no reaction of the tooth to electrical or thermal stimuli, and physiological mobility. Radiovisio-

graphy (RVG) showed an extensive filling on the occlusal surface, the presence of a PS within the pulp cavity (homogenous radiopaque contrast) and a periapical lesion (Fig. 1A). A diagnosis of chronic apical periodontitis was made and antiseptic RCT was scheduled. After isolating the tooth with a rubber dam, the temporary filling was removed. The presence of an extensive PS blocking the orifice of the palatal canal was confirmed with an operating microscope (OM) (Labomed Prima DNT®; Labo America, Inc., Fremont, USA). The floor of the pulp cavity was discolored due to the application of the Canal Detector® blue dye (CERKAMED, Stalowa Wola, Poland) (Fig. 1B). The pulp cavity was prepared and the denticle was removed with the use of the BUC® 2 ultrasonic tip (Obtura Spartan, Fenton, USA) and the Munce Discovery Burs® (CJM Engineering, Inc., Santa Barbara, USA). Then, the ProTaper® SX rotary file (Dentsply Sirona, Ballaigues, Switzerland) and Gates–Glidden drills (Dentsply Sirona) were applied to prepare the canal orifices. After determining the working length of the 4 canals with an apex locator, they were initially shaped with the rotary PathFiles® (Dentsply Sirona) to size 019. Due to a lack of time, an antibiotic-steroid dental paste (Dexadent®; Chema-Elektromet, Rzeszów, Poland), a cotton pledget and a temporary filling (Cavit®; 3M ESPE, Seefeld, Germany) were applied. At the following appointment, the canals were prepared with the Mtwo® instruments (VDW, Munich, Germany) to size 35/.04 (Fig. 1C). During the preparation, ultrasonically activated irrigation was performed with a 5.25% NaOCl solution (20 mL) and 15% EDTA (10 mL) to remove the smear layer, and isopropyl alcohol (CERKAMED) was administered for a final rinse. Gutta-percha points were fitted and the canals were filled using the method of the gutta-percha continuous wave of condensation with SuperEndo®  $\alpha 2$  and SuperEndo  $\beta$  (B&L Biotech, Inc., Fairfax, USA) as well as AH Plus® (Dentsply Sirona) as a sealer. The canal orifices were secured with a flowable, colored composite material. The pulp chamber and



Fig. 1A. Case 1, tooth 27: Pre-operative X-ray

the cavity were closed with glass-ionomer cement. On RVG, all canals appeared properly filled (Fig. 1D). The patient was referred for prosthetic reconstruction.



Fig. 1B. Case 1, tooth 27: Microscope-captured images of the pulp chamber floor before denticle removal



Fig. 1C. Case 1, tooth 27: Microscope-captured images of the pulp chamber floor after denticle removal



Fig. 1D. Case 1, tooth 27: Post-operative X-ray

## Case 2

A healthy 52-year-old female patient came to the dental office with a referral from a general dental practitioner (GDP) for the specialist RCT of tooth 16 with a diagnosis of calcifications within the pulp and chronic apical periodontitis. The patient made an appointment for the cone-beam computed tomography (CBCT) examination. The clinical examination revealed no pain on percussion, no reaction of the tooth to electrical or thermal stimuli, and physiological mobility. The CBCT scans with sagittal, axial, and coronal views showed an extensive filling on the mesial, distal and occlusal surfaces, the presence of a PS within the pulp cavity (homogenous radiopaque contrast), and a periapical lesion (Fig. 2A–2C). The CBCT analysis detected a denticle in the pulp cavity above the orifice of the palatal canal, severe curvature of the buccal canals and chronic apical periodontitis. A diagnosis of chronic granuloma periodontitis was made and antiseptic RCT was arranged. Endodontic treatment with rubber-dam isolation was started. The tooth was trepanned and the pulp cavity was prepared using a dental OM. After the roof of the pulp chamber was removed with a long-shank rose-head bur for a slow-speed handpiece, the presence of an extensive PS blocking the orifice of the palatal canal was confirmed. The preparation of the pulp cavity and the removal of the denticle were carried out with the use

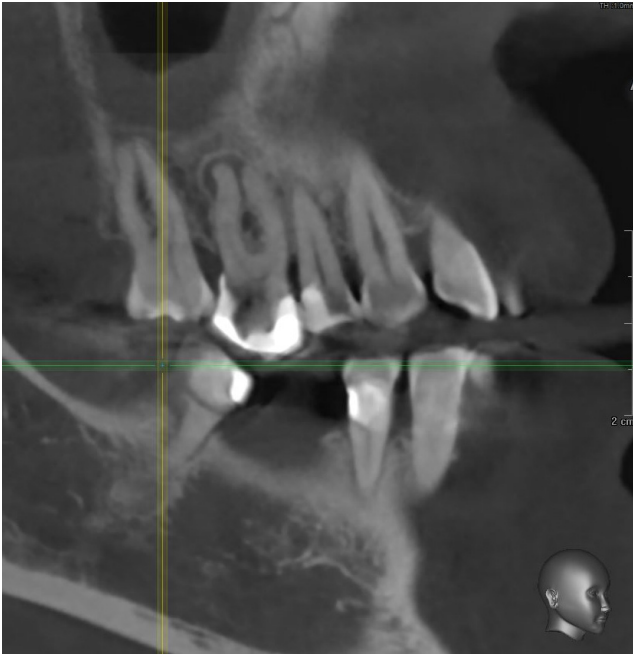


Fig. 2A. Case 2, tooth 16: Cone-beam computed tomography (CBCT) scan with a sagittal view

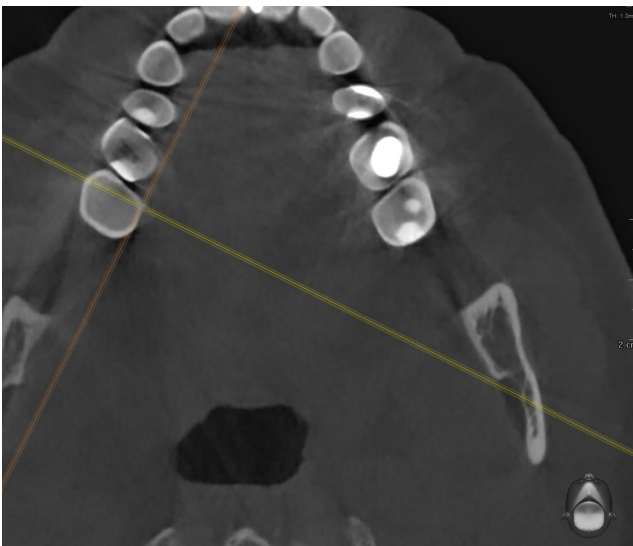


Fig. 2B. Case 2, tooth 16: CBCT scan with an axial view

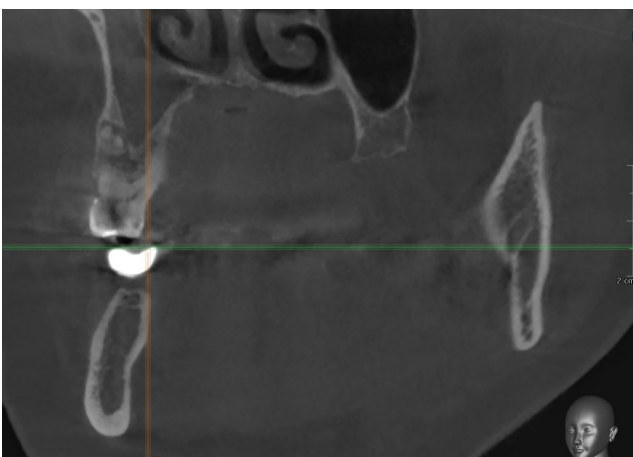


Fig. 2C. Case 2, tooth 16: CBCT scan with a coronal view

of the BUC 2 ultrasonic tip (Obtura Spartan) and Muncce Discovery Burs No. 1 (CJM Engineering, Inc.). Gates–Glidden drills (Dentsply Sirona) were used to prepare the canal orifices. After determining the working length of all canals with an apex locator, they were initially shaped with the C-Pilot® size 06–10 hand files (VDW) to create a glide path. Due to a lack of time, an antibiotic-steroid dental paste (Dexadent; Chema-Elektromet) and a cotton pledget were inserted, and a Cavit temporary filling was applied (3M ESPE). At the following appointment, the canals were shaped with the ProTaper Next NiTi rotary files (Dentsply Sirona); the last file for all buccal canals was PT X2, size 25.06, and for the palatal canal, PT X3 size 30.07. The rinsing and filling protocol was followed as described above. A control X-ray was taken (Fig. 2D) and the patient was referred to her GDP for the final restoration.



Fig. 2D. Case 2, tooth 16: Post-operative X-ray

### Case 3

A generally healthy patient, aged 57, visited the dental office with spontaneous, long-lasting pain radiating to the ear, characteristic of irreversible pulpitis. The clinical examination of tooth 47 revealed pain on vertical percussion, and a prolonged reaction to electric and thermal stimuli. An initial periapical tooth X-ray was taken. Non-homogenous radiopaque contrast in the projection of the pulp chamber and the root canals, indicating their partial

obliteration, were revealed on the X-ray as well as the widening of the periodontal ligament space (Fig. 3A). The tooth was anesthetized with 4% articaine hydrochloride with adrenaline at 1:100,000. Under rubber-dam isolation, the pulp cavity was trepanned and massive bleeding was observed for a few minutes. After gaining access to the pulp chamber, its roof was removed with a surgical drill with extended handles for a slow-speed handpiece and the canal orifices were located by means of a dental OM. When bleeding stopped, the pulp chamber floor was irrigated with a 5.25% NaOCl solution, dried with a cotton pledget, and carefully inspected in order to find color changes that could indicate the way to the canal orifices. The floor of the pulp chamber had a non-homogenous, dark yellow structure varying in shape and size, closing the canal orifices (Fig. 3B). By scouting the pulp cavity floor gently with the C-Pilot instruments (VDW), access to all canal orifices was established. However, shaping the distal canal was problematic due to the obstruction by a PS. For the removal of the radicular pulp stone, 2 Hedström® size 15 files (Kerr Dental, Orange, USA) were used. All canals

were cleaned and shaped to full working length according to an apex locator with the Mtwo rotary files (VDW) to size 35/.04 (Fig. 3C). Due to a lack of time, the canals were filled with calcium hydroxide and a sterile cotton pledget, and a Cavit temporary filling was applied (3M ESPE). At the next appointment, all canals were finally obturated. A rinsing and filling protocol was followed as described in the cases above. At the end of RCT, a control X-ray was taken (Fig. 3D). The canals were filled properly and the patient was referred for final reconstruction.



Fig. 3A. Case 3, tooth 47: Pre-operative X-ray



Fig. 3B. Case 3, tooth 47: Microscope-captured image of the pulp chamber floor before denticle removal



Fig. 3C. Case 3, tooth 47: Microscope-captured image of the pulp chamber floor after denticle removal



Fig. 3D. Case 3, tooth 47: Post-operative X-ray

## Case 4

A 38-year-old, generally healthy patient reported to the dental office because of the hypersensitivity to cold of the maxillary teeth on the right side. Tooth 16 was the most sensitive to a cold stimulus (ethyl chloride). Initial RVG was performed and radiopaque contrast within the pulp chamber was noticed, which could indicate the presence of a denticle (Fig. 4A). Infiltration anesthesia with Citocartin® 100 (Molteni Dental S.r.l., Milan, Italy) was administered and an amalgam filling was removed from the occlusal surface. At the height of the proximal buccal cusp, the entrance to the pulp cavity was visible. After placing a rubber dam, proper access was prepared and the presence of an extensive calcification with the PS features was visible under a dental OM (Fig. 4B). The Start-X® ultrasonic tip No. 3 (Dentsply Sirona) was used to remove the denticle. After removing the PS – which loosely filled the pulp chamber – with an endodontic probe (Fig. 4C), the pulp cavity was prepared using surgical drills with extended handles. Due to a lack of time, an antibiotic-steroid dental paste (Dexadent; Chema-Elektromet), a cotton pledget and a Cavit temporary filling (3M ESPE) were inserted. At the next appointment, 4 canal orifices were detected: palatal; mesio-buccal 1; mesio-buccal 2; and disto-buccal. Gates–Glidden drills (Dentsply Sirona) were applied to prepare the canal orifices. After preparing a glide path with hand instruments, the working length was determined with the use of an apex locator and the Mtwo rotary files were used up to No. 30. During the mechanical preparation, 5% NaOCl and EDTA irrigation solutions were administered with ultrasonic activation. All canals were filled with the thermal method of gutta-percha and AH Plus (Dentsply Sirona) as a sealer. The canal orifices were protected by a flowable, colored composite material and the cavity within the tooth crown was filled with Herculite XRV Ultra® (Kerr Dental). Control RVG was performed (Fig. 4D).



Fig. 4A. Case 4, tooth 16: Pre-operative X-ray

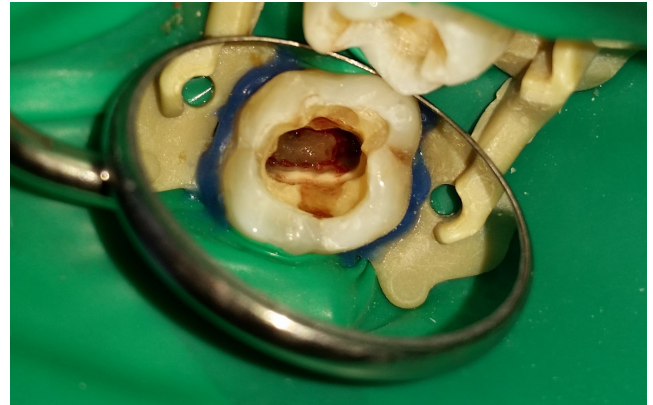


Fig. 4B. Case 4, tooth 16: Microscope-captured images of the pulp chamber floor before denticle removal

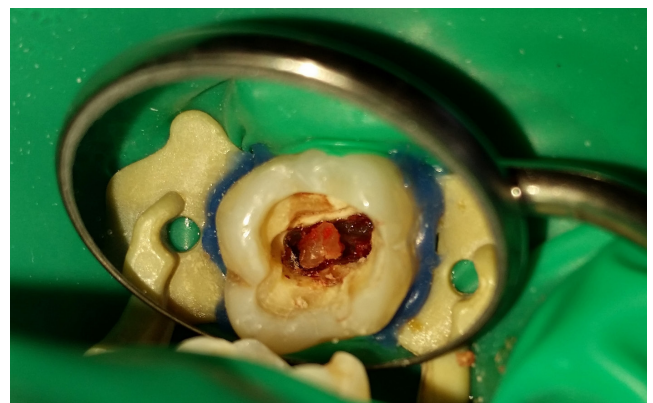


Fig. 4C. Case 4, tooth 16: Microscope-captured images of the pulp chamber floor during denticle removal



Fig. 4D. Case 4, tooth 16: Post-operative X-ray

## Discussion

Denticles are foci of calcification in the dental pulp, located mostly in pulp chambers. Denticles differ in size, ranging from microscopic particles to larger masses that nearly obliterate the pulp chamber and are visible on radiographs as dense, radiopaque masses.<sup>2–6</sup> Although the etiological agents in the formation of pulpal calcifications are not completely understood, the gender and age of the patient, various systemic disorders and long-term irritation, such as deep caries and extensive restorations, have been proposed as possible factors in the formation of PSs.<sup>7–10</sup> The association of PSs and the age of patients has been assessed by researchers in previous studies. No significant correlation with an increasing age was found in the studies by Aslantas et al. and Kannan et al.<sup>13,14</sup> This data is in agreement with the present study.

Many prevalence studies have identified PSs using radiography. Pulpal calcifications appear radiographically as dense, radiopaque masses. When the diameter of a PS is smaller than 200  $\mu\text{m}$ , a diagnosis of denticles cannot be made using dental radiography. The most commonly used radiographic techniques to detect denticles are panoramic radiographs,<sup>15</sup> intraoral periapical radiographs<sup>16</sup> and bitewing radiographs.<sup>11</sup> The CBCT imaging has also been reported to increase predictability in treating calcified canals.<sup>17</sup>

A small number of studies analyzing the location of denticles in the pulp cavity have been published.<sup>15,18,19</sup> According to Syryńska et al., denticles occurred in the pulp chambers of 69.4% of individuals; PSs were found in the canals on only 3.5% of 165 panoramic radiographs.<sup>15</sup> This data corresponds with our study, where a radicular stone was described in only 1 case (case 3). According to the literature, denticles occur more frequently in the maxillary teeth than in the mandibular teeth. The present study is in accordance with this finding.<sup>20,21</sup> Nowadays, CBCT is more common in dental practice, as it is helpful in providing precise three-dimensional (3D) images of anatomic details, which are useful for diagnosis and endodontic treatment planning.<sup>22</sup> The CBCT examination could be an efficient technique in diagnosing and locating denticles and calcified canals. The knowledge of the distribution of PSs can help dental practitioners in clinical endodontic treatment. This diagnostic tool was also applied in case 2. The removal of PSs from the pulp chamber is a difficult, laborious and time-consuming process, which requires not only skill and dexterity, but also the right equipment and magnification devices.<sup>23,24</sup> These conditions were fulfilled while treating the teeth described in this study in all cases. At present, the main methods for dealing with root canal calcification include appropriate pre-operative dental radiography, good magnification (a dental OM), instruments such as small K files or C files, and ultrasonic equipment with endodontic tips.<sup>25</sup> Large PSs can be dissected out of the pulp cavity using long-shank rose-head burs for a slow-speed

handpiece, but ultrasonic instruments with diamond-coated ultrasonic tips make their removal far easier. The power of an ultrasonic device for the endodontic tips should be set according to the manufacturer's recommendations. Ultrasonic tips can be used with or without water cooling. When used in dry conditions, it is recommended to take several breaks for the irrigation of the pulp cavity with a NaOCl or EDTA rinsing solution. Denticles in our study were removed from the pulp chamber with Muncie Discovery Burs and an ultrasonic device with endodontic tips. In our cases, ultrasonic tips were used without water cooling and with profuse NaOCl irrigation during the breaks. A similar procedure was presented by Nanjannawar et al., who reported removing denticles with ultrasonic instruments used with copious sodium hypochlorite irrigation.<sup>26</sup> In their study, long radicular calcifications were finally retrieved from the palatal canals with the help of tweezers.<sup>26</sup> Recently, a new report on the potential of non-instrumental methods to remove pulpal calcifications was published. Chen et al., in an ex vivo study, evaluated the removal of calcifications with the GentleWave® system using the micro-CT imaging as the method of estimation.<sup>27</sup> The researchers concluded that calcifications in the distal canals of the mandibular molars could be partially or completely removed by the multisonic cleaning system without instruments.<sup>27</sup>

Severe pulp space calcification is a challenge in cases of periapical lesions. In cases 1 and 2 of this study, with diagnoses of calcifications and apical periodontitis, denticles were successfully removed with the use of elongated rose-head burs and ultrasonic special tips. Unfortunately, in dealing with calcified root canals, the preparation of an access cavity and the identification of the canal orifices may lead to an excessive loss of the tooth tissue, the risk of fracture, and – in consequence – a high failure rate. The dentist must be familiar with the anatomical clues which are helpful in locating calcified canal orifices: the color of the pulp chamber floor is always darker than the yellowish walls, and the root canal orifices are always located at the junction of the walls and the floor. The orifices of the root canals are located at the terminus of the root developmental fusion lines.<sup>28</sup>

Recently, guided endodontics has become an optional solution for cases with severe pulp space calcification. This modern technology is designed to handle pulp canal calcifications in teeth with straight and thin roots with the use of the CBCT scans to map the degree of obliteration and a printed template that guides the bur to the calcified root canal. Micro-guided endodontics provides a precise, fast and operator-independent technique without the unwanted removal of enamel and dentin.<sup>29,30</sup> Due to the rapid technological progress in dentistry, guided endodontics may become standard in the future and may also be established in endodontic practices.

### ORCID iDs

Krystyna Pietrzycka  <https://orcid.org/0000-0003-4664-0890>  
Halina Pawlicka  <https://orcid.org/0000-0002-0135-0673>



## References

- Langeland K, Rodrigues H, Dowden W. Periodontal disease, bacteria, and pulpal histopathology. *Oral Surg Oral Med Oral Pathol.* 1974;37(2):257–270.
- Kronfeld R, Boyle PE. *Histopathology of the Teeth and Their Surrounding Structures.* 4<sup>th</sup> ed. London, UK: Henry Kimpton; 1955.
- Mahajan P, Monga P, Bahunguna N, Bajaj N. Principles of management of calcified canals. *Indian J Dent Sci.* 2010;2(Suppl):3–5.
- Arys A, Philippart C, Dourov N. Microradiography and light microscopy of mineralization in the pulp of undemineralized human primary molars. *J Oral Pathol Med.* 1993;22(2):49–53.
- Moss-Salentijn L, Klyvert MH. Epithelially induced denticles in the pulps of recently erupted, noncarious human premolars. *J Endod.* 1983;9(12):554–560.
- Goga R, Chandler NP, Oginni AO. Pulp stones: A review. *Int Endod J.* 2008;41(6):457–468.
- Bains SK, Bhatia A, Singh HP, Biswal SS, Kanth S, Nalla S. Prevalence of coronal pulp stones and its relation with systemic disorders in northern Indian central punjabi population. *ISRN Dent.* 2014;2014:617590.
- Edds AC, Walden JE, Scheetz JP, Goldsmith LJ, Drisko CL, Eleazer PD. Pilot study of correlation of pulp stones with cardiovascular disease. *J Endod.* 2005;31(7):504–506.
- Jena D, Balakrishna K, Singh S, Naqvi ZA, Lanje A, Arora N. A retrospective analysis of pulp stones in patients following orthodontic treatment. *J Contemp Dent Pract.* 2018;19(9):1095–1099.
- Zeng J, Yang F, Zhang W, Gong Q, Du Y, Ling J. Association between dental pulp stones and calcifying nanoparticles. *Int J Nanomedicine.* 2011;6:109–118.
- Ranjitkar S, Taylor JA, Townsend GC. A radiographic assessment of the prevalence of pulp stones in Australians. *Aust Dent J.* 2002;47(1):36–40.
- Moss-Salentijn L, Hendricks-Klyvert M. Calcified structures in human dental pulps. *J Endod.* 1988;14(4):184–189.
- Aslantas EE, Buzoglu HD, Karapinar SP, et al. Age-related changes in the alkaline phosphatase activity of healthy and inflamed human dental pulp. *J Endod.* 2016;42(1):131–134.
- Kannan S, Kannepady SK, Muthu K, Jeevan MB, Thapasum A. Radiographic assessment of the prevalence of pulp stones in Malaysians. *J Endod.* 2015;41(3):333–337.
- Syryńska M, Durka-Zajac M, Janiszewska-Olszowska J. Prevalence and location of denticles on panoramic radiographs. *Ann Acad Med Stetin.* 2010;56(2):55–57.
- Gulsahi A, Cebeci AI, Ozden S. A radiographic assessment of the prevalence of pulp stones in a group of Turkish dental patients. *Int Endod J.* 2009;42(8):735–739.
- Patel S, Durack C, Abella F, Shemesh H, Roig M, Lemberg K. Cone beam computed tomography in endodontics – a review. *Int Endod J.* 2015;48(1):3–15.
- Rodakowska E, Ochnio A, Struniawska A. Not to be forgotten: Denticles. Case reports and review of the literature. *Ann Acad Med Stetin.* 2011;57(3):77–81.
- Udoye CI, Sede MA. Prevalence and analysis of factors related to occurrence of pulp stone in adult restorative patients. *Ann Med Health Sci Res.* 2011;1(1):9–14.
- Hsieh CY, Wu YC, Su CC, et al. The prevalence and distribution of radiopaque, calcified pulp stones: A cone-beam computed tomography study in a northern Taiwanese population. *J Dent Sci.* 2018;13(2):138–144.
- Nogueira Leal da Silva EJ, Prado MC, Queiroz PM, et al. Assessing pulp stones by cone-beam computed tomography. *Clin Oral Investig.* 2017;21(7):2327–2333.
- Patel S, Brown J, Pimentel T, Kelly RD, Abella F, Durack C. Cone beam computed tomography in endodontics – a review of the literature. *Int Endod J.* 2019;52(8):1138–1152.
- Olczak K, Kabacińska K, Pawlicka H. Management of pulp canal obliterations. *Czas Stomatol.* 2017;70(5):597–612.
- Pałatyńska-Ulatowska A, Pietrzycka K, Koprowicz A. Denticles of the pulp chamber – diagnostics and management. Case studies. *Pomeranian J Life Sci.* 2019;65(2):29–36.
- Freedman G, Glassman G. Buyers' guide to endodontic equipment. An in-depth look at today's apex locators, obturation systems, and ultrasonic systems. *Dent Today.* 2009;28(4):118,120,122 passim.
- Nanjannawar GS, Vagarali H, Nanjannawar LG, Prathasarathy B, Patil A, Bhandi S. Pulp stone – an endodontic challenge: Successful retrieval of exceptionally long pulp stones measuring 14 and 9.5 mm from the palatal roots of maxillary molars. *J Contemp Dent Pract.* 2012;13(5):719–722.
- Chen B, Szabo D, Shen Y, et al. Removal of calcifications from distal canals of mandibular molars by a non-instrumentational cleaning system: A micro-CT study. *Aust Endod J.* 2019 [Epub]. doi: 10.1111/aej.12376
- Krasner P, Rankow HJ. Anatomy of the pulp-chamber floor. *J Endod.* 2004;30(1):5–16.
- Connert T, Zehnder MS, Amato M, Weiger R, Kühl S, Krastl G. Microguided endodontics: A method to achieve minimally invasive access cavity preparation and root canal location in mandibular incisors using a novel computer-guided technique. *Int Endod J.* 2018;51(2):247–255.
- Moreira Maia L, de Carvalho Machado V, Alves da Silva NRF, et al. Case reports in maxillary posterior teeth by guided endodontic access. *J Endod.* 2019;45(2):214–218.

Dental  
and Medical Problems

